博士論文

論文題目　**Lithium isotope ratios in playas, submarine hydrothermal fluids, and rivers: implication for global lithium cycles at earth surface environment**
（プラヤ，海底熱水，河川におけるリチウム同位体比：地球表層リチウム循環の解明に向けて）

氏　名　　荒岡　大輔

東京大学大学院新領域創成科学研究科

環境学研究系自然環境学専攻

地球海洋環境学分野

平成 25 年度

博士論文

Lithium isotope ratios in playas, submarine

hydrothermal fluids, and rivers: implication for global

lithium cycles at earth surface environment

（プラヤ，海底熱水，河川におけるリチウム同位体比：

地球表層リチウム循環の解明に向けて）

2014 年 3 月修了

指導教員　　教授　川幡穂高

47-117602　荒岡大輔

Contents

Chapter 4   39

Lithium isotopic composition of submarine vent fluids from arc and back-arc hydrothermal systems at western pacific

Chapter 1

Preface　– background and objective –

During my master's program, I undertook researches on past tsunami hazards, such as their timing and recurrence interval, by radiometric dating of coral boulders cast along the shoreline in the southern Ryukyu regions. Especially, I applied U-series (^{230}Th) and radiocarbon (^{14}C) dating to *Porites* coral boulders cast ashore by past tsunamis. Based on my master thesis, two international papers were published (Araoka et al. 2010; Araoka et al. 2013). Araoka et al. (2010) is the first report of high-precision ^{230}Th dating applied to tsunami deposits in Ishigaki Island, southwest Japan and revealed that *Porites* boulders have enormous potential for determining the timing of past tsunamis. Araoka et al. (2013) demonstrated that the southern Ryukyu Islands have repeatedly experienced tsunami events since at least 2400 years ago, with a recurrence interval of ~150–400 years. This study estimated tsunami recurrence intervals from tsunami boulders for the first in the world and demonstrates that it is possible to ascertain the timing, recurrence interval, and magnitude of past tsunamis in a location where few adequate survey sites of sandy tsunami deposits exist.

As described above, major and trace element isotopes are useful not only for paleo-environmental and paleo-climatic studies but also paleo-geohazard studies. Then, many research fields with non-traditional stable isotopes have still remained. In my Ph.D. thesis, I focus on lithium and its isotopes for understanding global lithium cycle in earth surface systems by making good use of my acquired skills about isotope geochemistry throughout my graduate researches.

Lithium, a type of rare metal element established by the Japanese government, is an industrially useful element. It is known that massive lithium ore deposits have been formed in playas and salt crusts by evaporative enrichment. Lithium ore deposits are eccentrically-located on shore, especially more than half of lithium resources are expected to exist in South America. Moreover, three foreign corporations have kept approximately 50 % of the market share of lithium carbonate. Thus, understanding

global lithium cycle on the earth's surface and genesis of lithium ore deposits by the use of lithium isotopes would contribute researches on assessment of lithium resource potential and exploration of lithium ore deposits for stable supply of lithium.

To reveal the genesis of lithium ore deposits, previous studies analyzed the chemical composition of evaporite deposits all over the world (e.g. Lowenstein and Risacher 2009; Risacher and Fritz 2009; Risacher et al. 2003). However, the origin and accumulation mechanism of lithium in playas were not well understood because the contents of lithium and other elements were modified by evaporation and enrichment. In addition, no studies used lithium isotopic ratios to examine the origin of lithium-rich playas.

On the other hand, lithium has draw attention as fluid tracer during geological and geochemical processes such as weathering processes and material cycles in subduction zones because aqueous solubility of lithium is very large (e.g. Tomascak 2004; Tang et al. 2007; Burton and Vigier 2012). In particular, lithium contents and its isotopes are expected as proxies for silicate weathering in recent years (e.g. Kisakurek et al. 2005).

Lithium contents and its isotopes in the open ocean reservoir have changed drastically although these are currently homogeneous (e.g. Misra and Froelich 2012). The lithium contents and its isotopic composition of seawater reflect a balance between input (submarine hydrothermal fluids and rivers) and removal fluxes and their isotopic compositions (Table 1-1 and Fig. 1-1). Input fluxes from submarine hydrothermal systems and rivers to the ocean are important compared to removal fluxes for changes in seawater composition of lithium. This is because that input lithium fluxes and its isotopic compositions are variable while isotopic differences between seawater and removal processes are constant through Cenozoic. In addition, most dissolved lithium in river water (>90 %) is derived from weathering of silicate rocks (Kisakurek et al. 2005). Therefore, understanding global lithium cycle on the earth's surface, especially in

8

submarine hydrothermal and river systems, and changes in lithium seawater chemistry would contribute changes in atmospheric carbon dioxide levels because of consumption of carbon dioxide during silicate weathering.

Table 1-1 Estimates of dissolved lithium input and output fluxes and their isotopic compositions from each reservoir to the ocean (after Misra and Froelich 2012). Global lithium cycles on the earth's surface and major input/output systems to the ocean are illustrated in Fig. 1-1.

Input/output	Lithium flux (10^9 moles/year)	Average δ^7Li (‰)
Inputs		
Hydrothemal vents	13	8.3
Rivers	10	23
Subduction reflux	6	15
Total input	29	15
Outputs		
Alteration of oceanic crust	8	15
Sediment uptake	20	15
Total output	29	15
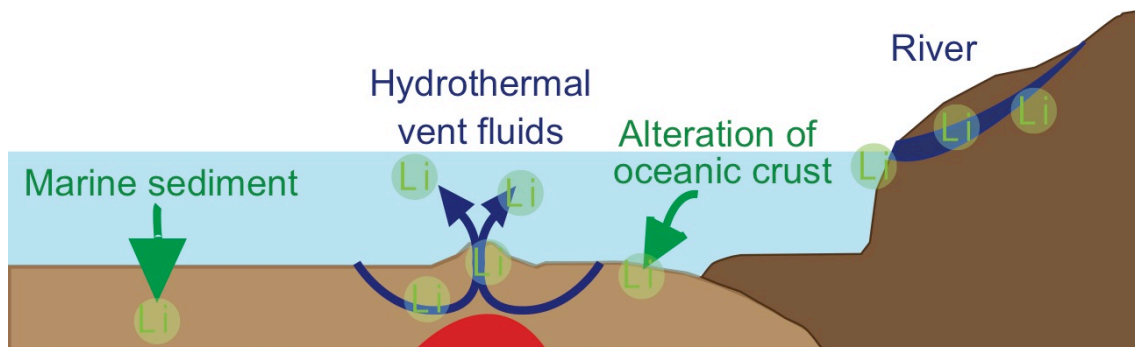
Fig. 1-1 Illustration of global lithium cycles on the earth's surface systems. The Li concentration and its isotopic composition of seawater reflect a balance between input and removal fluxes and their isotopic compositions. The two major sources of Li to seawater are rivers and submarine hydrothemal vent fluids (*blue*) (Misra and Froelich 2012). Subduction reflux of Li from the convergent margins is relatively-minor component of Li input to seawater (Misra and Froelich 2012). The removal of Li from seawater is by incorporation into marine sediments and low-temperature altered oceanic crust via formation of Li-, Mg-, and Fe-bearing marine authigenic alumino silicate clays (*Green*) (Misra and Froelich 2012). The dissolved Li input and output fluxes and their compositions reported in Misra and Froelich (2012) are listed in Table 1-1.

There are some studies on lithium isotopic compositions in submarine hydrothermal fluids and rivers. Most of the lithium isotopic studies have targeted mid ocean ridge (MOR) sites among submarine hydrothermal systems all over the world (e.g. Misra and Froelich 2012). Previous studies suggested that MOR sites are typical hydrothermal systems controlled by seawater-basalt interaction at high-temperature. In contrast, arc and back-arc sites consisted of various tectonic settings are considered to be influenced by subduction zone. However, lithium behavior and its control factor in submarine hydrothermal fluids from arc and back-arc have not been clear. Those in river waters are also insufficient. In particular, few previous studies dealt with space-time distribution in world's major river systems in detail. Moreover, estimates of lithium fluxes from submarine hydrothermal fluids to the ocean may be strongly biased toward data on MOR sites. Similarly, lithium fluxes and its isotopic compositions are roughly estimated on the basis of a small number of data in major river systems (Misra and Froelich 2012).

I therefore focus on lithium isotopes. Lithium has two stable isotopes with atomic masses of 6 and 7. The measured $^7Li/^6Li$ ratios are expressed as permille deviations from the NIST L-SVEC standard: $\delta^7Li = [[^7Li/^6Li]_{sample}/[^7Li/^6Li]_{L\text{-}SVEC\ standard} - 1] \times 1,000$. The large mass difference between the isotopes (15 %) results in large isotopic fractionation during some geochemical and geological processes (Tomascak 2004; Tang et al. 2007; Burton and Vigier 2012). Especially, large isotopic fractionation has been occurred during lithium migration via fluids such as alteration and weathering processes (Tomascak 2004; Tang et al. 2007). Recent advances in lithium isotope geochemistry have shown that lithium isotopic compositions ($^7Li/^6Li$) vary greatly, by up to 80 ‰, in different reservoirs (Fig. 1-2 and 1-3; Tomascak 2004; Tang et al. 2007). Therefore, $^7Li/^6Li$ has great potential as a powerful tool for investigating water–rock interactions.
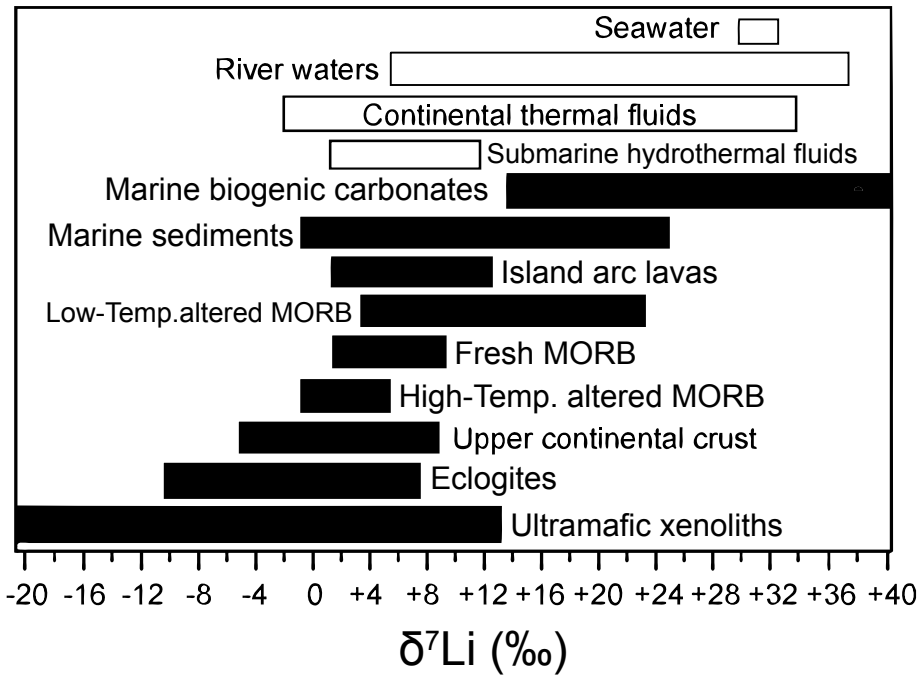
Fig. 1-2 Lithium isotopic compositions of various reservoirs (after Tang et al. 2007). Reservoirs in geosphere are shown as *black bars*, while those in hydrosphere are shown as *white bars*. Some reservoirs are shown in schematic illustrations of lithium isotope systematics in the hydrological cycle and subducttion zone setting (Fig. 1-3).
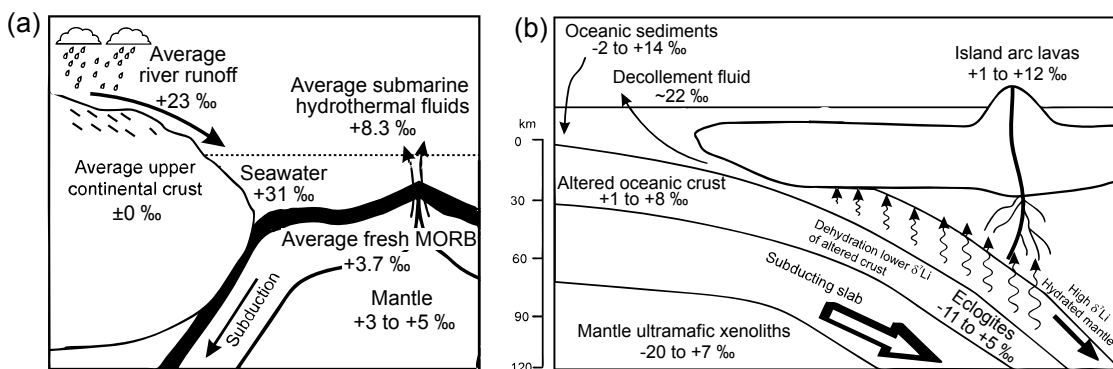
Fig. 1-3 Schematic Illustrations of lithium isotope systematics (a) in the hydrological cycle and (b) subduction-zone setting (modified from Elliott et al. 2004, Zack et al. 2003, and Tang et al. 2007). The range of lithium isotopic compositions of various reservoirs are shown in Fig. 1-2.

It was difficult to measure the lithium isotopic ratios in geological samples because of the lower lithium contents compared to other major elements. However, recent developments in analytical instruments have been made it possible to measure lithium isotopic ratios with a small amount of lithium and high precision.

Therefore, in my Ph.D. thesis, I describe the detailed procedure to analyze lithium isotopic ratios in the samples in the beginning. Then, I discuss the control factor of lithium contents and its isotope ratios in evaporites and lacustrine sediments from playas in Nevada (onshore lithium ore deposits) (Araoka et al. in press), submarine vent fluids from arc and back-arc hydrothermal systems in the western pacific, river and ground waters from Ganges-Brahmaputra-Meghna river systems, as representatives of major systems for global lithium cycles on the earth's surface, based on lithium isotopic analyses together with various elemental and isotopic analyses (Fig. 1-4).
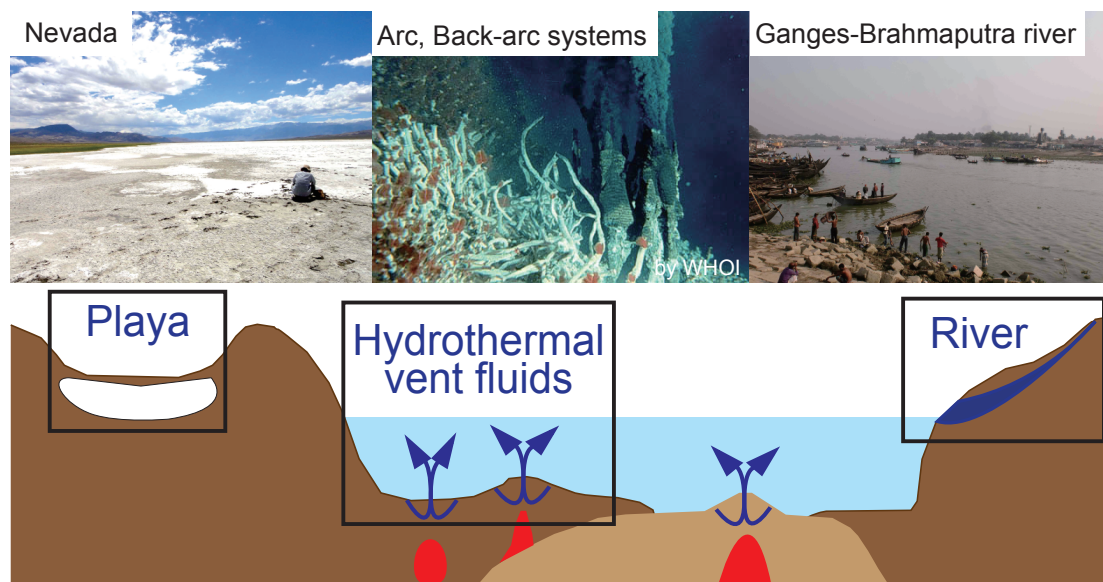
Fig. 1-4 Illustration of valuable systems for Li on the earth's surface. The Li iso-topic systematics in playas in Nevada, in arc/back-arc hydrothermal systems at the western pacific, and in Ganges-Brahmaputra-Meghna river systems are discussed in this thesis, as representatives of two major input systems to the ocean and onshore lithium ore deposit.

Chapter 2

Analytical procedures of lithium and strontium isotopic measurements

2.1. Outline

Lithium and strontium isotopic ratios were analyzed at the Kochi Core Center (KCC), Japan Agency for Marine-Earth Science and Technology (JAMSTEC), Japan. Two-step column separation was conducted for separation of lithium and strontium from other elements in the samples to prevent the interference during mass spectrometry measurements (matrix effect) (Fig. 2-1a). All separate operations were performed in a clean laboratory (cleanliness level better than class 1,000). After column separation, lithium and strontium isotopic ratios were determined by a multi-collector ICP-MS (MC-ICP-MS, Neptune, Thermo Sci. Co., Fig. 2-1b) and a thermal ionization mass spectrometer (TIMS, Triton, Thermo Sci. Co., Fig. 2-1c), respectively. These instruments for high-sensibility and high-precision isotopic measurements allow determination isotopic ratios precisely in trace amount of lithium (20 ng Li) and strontium (80 ng Sr) in the samples. Most analytical protocols in this study are documented previously (Nishio and Nakai 2002; Nishio et al. 2004; Nishio et al. 2010), which modified the analytical procedures of Tomascak et al. (1999) and Jeffcoate et al. (2004). The detailed procedures of column separation and mass spectrometry were described in the following sections.
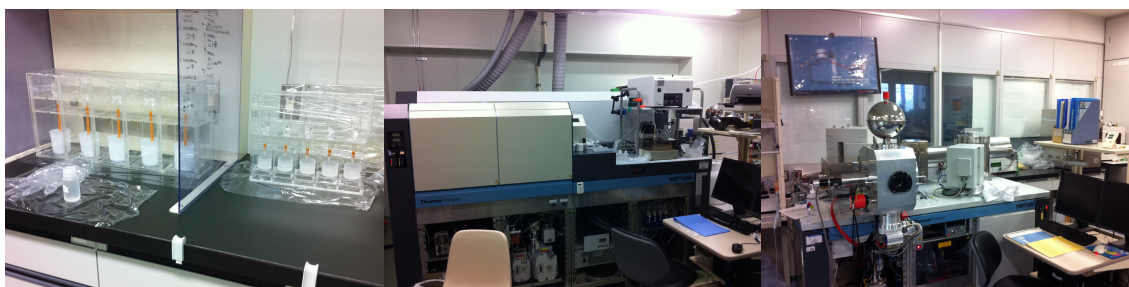
Fig. 2-1 The photographs of (a) two types of column for lithium separation, (b) MC-ICP-MS, Neptune (Thermo Sci. Co.) for lithium isotopic measurement, and (c) TIMS, Triton (Thermo Sci. Co.) for strontium isotopic measurement at the Kochi Core Center, JAMSTEC, Japan.

2.2. Chemical separation for lithium and strontium

2.2.1. Setup for chemical separation

The first-step column separation was carried out using a quartz glass column filled with a height of 12 cm (approximately 6 ml) Bio-Rad AG50W-X8 (200–400 mesh) cation-exchange resin. To keep a stable position of the resin and prevent the resin flowing out of the column, a height of 1cm wet pure-quartz cotton was filled with the bottom of the column. Similarly, the second-step column separation for lithium was carried out using a quartz glass column filled with a height of 2 cm (approximately 0.8 ml) Bio-Rad AG50W-X12 (200–400 mesh) cation-exchange resin together with a height of 1cm wet pure-quartz cotton at the bottom of the column. The second-step column separation for strontium was carried out using a polypropylene column filled with a height of 2 cm (approximately 0.8 ml) Eichrom Sr resin (50–100 μm).

Before column separation, all resins were washed repeatedly. For the resins of first-step and second-step for lithium, firstly, sequential cleaning was conducted once with 6 M EL-grade HCl (Kanto Chemical Co.) and then three times with Milli-Q water. This set of cleaning was repeated three times in total. Secondary, 6 M ultrapure100-grade HCl (Kanto Chemical Co.) was passed through the resins and then Milli-Q water was also passed. Finally, just before sample separation, 6 M TAMAPURE-AA-100-grade HCl (Tama Chemicals Co.), which is the most pure grade in the protocols, was passed through the resins and then Milli-Q water was also passed. This is an important procedure to determine $^7Li/^6Li$ ratios accurately (Nishio and Nakai, 2002), which results in reduction of Li blank less than 10 pg Li (Nishio et al. 2010). The amount of Li blank is far less than that of Li in the analyzed samples (20–1,200 ng Li). After lithium separation, the cation-exchange resins for lithium were reused by series of repeated cleaning described above.

For the resin of second-step for strontium, the resin was washed about 15 times using 0.05 M ultrapure100-grade HNO_3 (Kanto Chemical Co.) before set up the resin to the column. After the set up the resin, 10 ml of 7 M ultrapure100-grade HNO_3 was passed through the resin three times and then 10 ml of warmed (~50 °C) 0.05 M ultrapure100-grade HNO_3 was also passed three times. Finally, 10 ml of 3 M ultrapure100-grade HNO_3 was passed once. During strontium separation, the amount of Sr blank (50 pg Sr) is far less than that of Sr in the analyzed samples (<400 ng Sr) (Nishio et al. 2010). After strontium separation, the Sr resin was discarded and then new cleaned Sr resin was set up to the column.

2.2.2. First-step column separation for lithium and strontium

Solution samples containing with 20–1,200 ng Li and more than 400 ng Sr in that solution were evaporated in the heated (~150 °C) clean evaporator. After complete evaporation, the residual solid were dissolved in 3 ml of 5 wt% TAMAPURE-AA-100-grade HNO_3 (Tama Chemicals Co.) and then the container were put inside an ultrasonic bath for complete dissolution of the residual. Just before the first column separation, 1.5 ml of 100% EL-grade methanol (Kanto Chemical Co.) was added into the samples, yielding 4.5 ml of the solution. The sample solution was loaded into the first-step column, and then 89 ml of 1 M TAMAPURE-AA-100-grade HNO_3:80 % v/v EL-grade methanol was passed through the resin. The loading solution and first 5 ml was discarded and the following 84 ml was collected as the lithium fraction. Continuously, 60 ml of 2 M ultrapure100-grade HCl was passed through the resin. The first 45 ml was discarded and the following 15 ml was collected as the strontium fraction. The lithium and strontium fractions were separated once more by subsequent operations individually.

2.2.3. Second-step column separation for lithium

The lithium fraction obtained by first-step was evaporated and dissolved in 0.2 ml of 0.25 M TAMAPURE-AA-100-grade HCl. Just before the second column separation, 0.5 ml of 0.5 M TAMAPURE-AA-100-grade HCl:80% v/v EL-grade methanol was added. The sample solution was loaded into the second-step column for lithium, and then 2 ml of 0.5 M TAMAPURE-AA-100-grade HCl:80 % v/v EL-grade methanol was passed through the resin and discarded. Subsequently, 32 ml of 1 M TAMAPURE-AA-100-grade HCl:80 % v/v EL-grade methanol was passed and collected as the purified lithium fraction. The purified lithium fraction was evaporated completely. Before isotopic measurements, 2% TAMAPURE-AA-100-grade HNO_3 was added into purified lithium residual for dilution into about 20 ng g^{-1} Li content in the sample solution. The lithium contents of the sample solution have been checked by comparing the beam intensities of the sample solution with those of L-SVEC standard solution containing 20 ng g^{-1} Li. Then, I have been confirmed that the recovery rate of lithium during the two-step column separation was approximately 100 %.

2.2.4. Second-step column separation for strontium

The strontium fraction obtained by first-step was evaporated and dissolved in 2 ml of 3 M ultrapure100-grade HNO_3. The sample solution was loaded into the second-step column for strontium. Then, 6 ml of 3 M ultrapure100-grade HNO_3, 6 ml of 7 M ultrapure100-grade HNO_3, and 2 ml of 3 M ultrapure100-grade HNO_3 were passed through the resin sequentially and discarded. Subsequently, 10 ml of warmed (~50 °C) 0.05 M ultrapure100-grade HNO_3 was passed and collected as the purified strontium fraction. The purified strontium fraction was evaporated completely. Total recovery rate of strontium in this procedure during two-step column separation was about 50 % (Nishio et al. 2010).

2.3. Mass spectrometry

2.3.1. Lithium isotopic measurement

The $^7Li/^6Li$ ratios were measured by MC-ICP-MS with a high-sensitivity skimmer cone (X-cone) and those in the samples were determined by standard-sample bracketing method. The prepared sample solution was introduced into MC-ICP-MS through an Aridus II desolvating nebulizer system (Cetac Technologies) with a microconcentric PTFE nebulizer (100 µl min^{-1}). Before all sample and standard measurements, the beam intensities on m/e 6 and 7 of 2% TAMAPURE-AA-100-grade HNO_3 were monitored as a background for 30 s. Subsequently, after 1 min of initial uptake of sample solution, the beam intensities on m/e 6 and 7 of sample solution were measured repeatedly 30 times every 4 s. The L-SVEC standard solution containing 20 ng g^{-1} Li was measured before and after sample analyses to correct for instrumental mass bias. The ordinal ^7Li intensity of the 20 ng g^{-1} Li standard solution is 20 pA (about 2 V signal with the 1011Ω resistor), which is much higher than background levels of 0.2 pA (about 0.02 V signal). The average value of 30 times $^7Li/^6Li$ ratios in the samples were calculated and finally expressed as permille deviations (δ^7Li) from the average value of L-SVEC standards of before and after sample analyses.

The uncertainty of the δ^7Li value is better than ±0.3 ‰, as estimated from its long-term reproducibility, +8.26 ± 0.46 ‰ (2σ, n = 24), from July 2011 to March 2012 using in-house lithium standard (Kanto Chemical Co.). This replicate δ^7Li value agreed well with the value of +8.28 ± 0.39 ‰ (2σ, n = 47) reported by Nishio et al. (2010) within the analytical uncertainty of ±0.3 ‰. δ^7Li value for the proposed seawater standard IRMM BCR-403 was +30.9 ‰, which agreed approximately with previously

reported values of +31.0 ± 0.5 ‰ (2σ, n = 30, Millot et al. 2004) and +31.3 ‰ (Nishio et al. 2010).

2.3.2. Strontium isotopic measurement

The $^{87}Sr/^{86}Sr$ ratios were measured by TIMS with Sr-loaded single tungsten filaments. Before isotopic measurements, 0.1 M TAMAPURE-AA-100-grade HNO_3 was added into purified strontium residual for dilution into about 160 μg g^{-1} Sr content in the sample solution. The solution samples were loaded on single tungsten filaments together with a tantalum activator solution (Birck, 1986). The Sr-loaded filaments were set up into TIMS. Finally, the $^{87}Sr/^{86}Sr$ ratios were measured by adjusting the current of evaporation filament manually.

The uncertainty of the $^{87}Sr/^{86}Sr$ ratio is better than ±0.000007, as estimated from the long-term reproducibility, 0.7102596 ± 0.0000095 (2σ, n = 13) from July 2011 to March 2012 of the NIST SRM 987 standard (80 ng Sr). This replicate value agreed approximately with the value of 0.7102507 ± 0.0000066 (2σ, n = 36) reported by Nishio et al (2010) within the analytical uncertainty.

Chapter 3

Lithium and strontium isotopic systematics in playas in Nevada, USA: constraints on the origin of lithium

3.1. Abstract

Highly concentrated lithium resources are often formed in salt crusts and playas by repetition of water evaporation and inspissation. Lithium-rich brine in playas is a major raw material for lithium production. Recently, lithium isotopic ratios (δ^7Li) have been identified as a tool for investigating water–rock interactions. Thus, to constrain the origin of lithium in playas by the use of its isotopes, I conducted the leaching experiments on various lacustrine sediments and evaporite deposit samples collected from playas in Nevada, USA. I determined lithium and strontium isotopic ratios and contents and trace element contents of the leachate, estimated the initial δ^7Li values in the water flowing into the playas, and examined the origin of lithium in playas by comparison with δ^7Li values of the possible sources.

In samples from the playas, δ^7Li values show some variations, reflecting differences both in isotopic fractionation during mineral formation and in initial δ^7Li value in water flowing into each playa. However, all δ^7Li values in this study are much lower than those in river water and groundwater samples from around the world, but they are close to those of volcanic rocks. Considering the temperature dependence of lithium isotopic fractionation between solid and fluid, these results indicate that the lithium concentrated in playas in Nevada was supplied mainly through high-temperature water–rock interaction associated with local hydrothermal activity and not directly by low-temperature weathering of surface materials. This study, which is the first to report lithium isotopic compositions in playas, demonstrates that δ^7Li may be a useful tracer for determining the origin of lithium and evaluating its accumulation processes in playas.

3.2. Introduction

Lithium is an industrially useful element with extremely low reduction potential. Lithium compounds are used in many ways, such as in heat-resistant glass products, ceramics, the aluminum industry, lubricants, and medical products (Garrett 2004). At present, one of the most important lithium products is secondary lithium-ion batteries used in electronics, especially mobile phones and notebook computers. The mining production of lithium has increased rapidly: in 2011, worldwide production was 34,000 tonnes, about five times the amount in 1995 (U.S. Geological Survey [USGS] 1996, 2012). The future demand for lithium is expected to increase rapidly as demand for environmentally friendly hybrid and electric automobiles grows (Vikstrom et al. 2013).

There are two types of lithium resources: (1) lithium pegmatite, which is rich in different lithium minerals such as lepidolite, petalite, and spodumene (Garrett 2004), and (2) brine deposits, especially those in salt flats and playas. The latter has recently become dominant as a raw material for lithium production because the costs of processing and production are relatively low (USGS 2012). The worldwide reserves of lithium and identified lithium resources were estimated to be 13 and 34 million tonnes, respectively (USGS 2012). In arid regions, lithium resources form in playas by evaporative enrichment (Jones and Deocampo 2003). As a result of the rising consumption of lithium carbonate, lithium-rich brine in salt flats and playas is now exploited worldwide.

In recent years, lithium isotopes is attracted a great deal of attention as a powerful tool for investigating water–rock interactions. The leaching of lithium from rocks is strongly temperature dependent; however, even at low temperature, the aqueous solubility of lithium is very large. Thi is the reason for its high content in brines (You et al. 1996; James et al. 2003). Another important characteristic of lithium is that it is

easily incorporated into clay minerals due to replacement of Mg^{2+} and Fe^{2+} in the layer silicates (Stoffynegli and Mackenzie 1984).

In this study, to constrain the origin of lithium in playas by the use of its isotopes, I performed two leaching experiments and analyzed lithium contents and isotopic ratios of leachate from lacustrine sediments and evaporite deposit samples collected from playas in Nevada, USA, as a representative of onshore lithium ore deposits. This is the first report of lithium isotopic compositions of lacustrine sediments and evaporite deposits from playas.

3.3. Materials and Methods

3.3.1. Sample descriptions and geological settings

Basin-and-range topography is extensively developed in the western USA as a result of early Miocene faulting (Fig. 3-1a; Diles and Gans 1995). Numerous playas, consisting of flat clay beds and precipitated salts, have formed in the basins.

My collaborator collected nine samples of lacustrine sediments and evaporite deposits from four playas encrusted with precipitated salts (Fig. 3-1b). Brine pumped from the Silver Peak playa has been exploited for lithium since 1964 by the Foote Mineral Company (Davis et al. 1986). Production of lithium carbonate from the Clayton Valley brine field, which includes Silver Peak, by Chemetall Foote Corporation began in 1967 and continues to the present. Alkali Lake is a mining property of Lomiko Metals Inc. The other two studied playas, Fish Lake and Columbus Salt Marsh, have yet to be explored for their lithium resource.

The compositions of the samples varied, but they consisted mainly of clay mud, salts, and sand (volcanic rock fragments). In the Clayton Valley area, alternating deposits of

lacustrine sediments and salt beds and lithium-rich brines formed during the Pleistocene (Munk et al. 2011), with the lithium-rich brines occurring in aquifers (Davis et al. 1986). Hectorite found in the Clayton Valley playa sediments contains 350–1,171 ppm Li (Kunasz 1974). The lithium contents of volcanic rocks in the area are an order of magnitude lower than those in brine and clay minerals (Davis et al. 1986; Price et al. 2000; Munk et al. 2011).

Two hypotheses have been proposed to explain the high lithium contents of brine and clays: (1) long-term chemical weathering of rocks in the surrounding region provided lithium to the surface waters that flowed into the Clayton Valley basin, and (2) hydrothermal activity associated with local volcanism contributed the lithium (Kunasz 1974; Davis et al. 1986). At present, there is insufficient evidence to support either hypothesis.
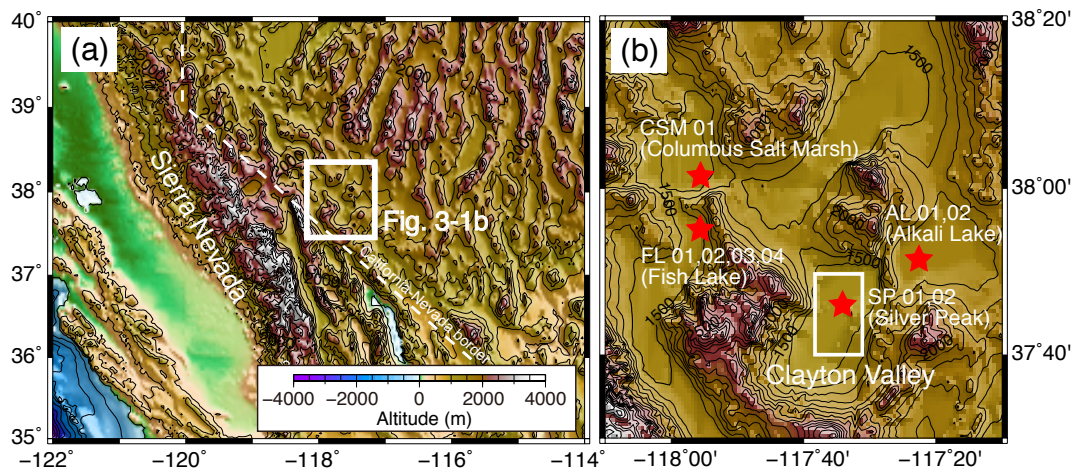
Fig. 3-1 (a) Map showing the topography of the study area and the surrounding region. Basin-and-range topography characterizes the region east of the Sierra Nevada. (b) Locations of the playas and sampling points (*red stars*). The sample numbers for each site are also shown. Clayton Valley is the only lithium brine source currently mined in North America.

3.3.2. Sample preparations and experiments

I examined the mineral composition of samples by X-ray diffraction analysis. To determine the most appropriate method for estimating the initial values of the lithium isotopic ratio in the water flowing into the playas, I conducted two leaching experiments. The leaching experiments would also reveal the main mineralogical phases containing lithium and the effect of leaching on the lithium isotopic ratios of the leachate. The following chemical procedures were performed in a clean laboratory (cleanliness level better than class 1,000) at the Kochi Core Center (KCC), JAMSTEC, Japan.

The experiment 1 was performed using each of the nine samples, but a lithium isotope analysis of the leachate from only one sample, FL01, was performed. This leaching experiment consisted of two steps. In the first step, the samples were dried overnight at room temperature (~25 °C). Then, 10 mL of Milli-Q water was added to 100 mg of the solid sample and the mixture was shaken manually before centrifugation for 30 min with 3,000 rpm to separate the solids from the leaching solution. The supernatant was then passed through a 0.2-μm PTFE syringe filter. In the second step, the residual solids were dried overnight at around 25°C, then shaken manually in 10 mL of 2 wt% ultrapure HNO_3. This mixture was then centrifuged for 30 min with 3,000 rpm, and the supernatant was filtered through a 0.2-μm PTFE syringe filter.

In the experiment 2, 10 mL of 2 wt% ultrapure HNO_3 was added to 100 mg unconsolidated samples, and the mixture was shaken manually, and then centrifuged for 30 min with 3,000 rpm. The resulting supernatant was filtered as in the experiment 1.

3.3.3. Analytical procedure

The contents of Na, Mg, K, Ca, and Fe in the solutions derived from the experiments 1 and 2 were determined with an inductively coupled plasma atomic emission spectrograph (ICP-AES, Optima 4300 DV, PerkinElmer) at KCC, using a ×100 dilution

(for Mg, K, Ca, Fe) or a ×1000 dilution (for Na) of the sample solution. The contents of Li and Sr were determined with a quadrupole inductively coupled plasma mass spectrometer (ICP-MS, ELAN-DRC II, PerkinElmer) at KCC, using a ×100 dilution of the sample containing an internal indium standard. The uncertainties of all measurements were better than ±3 %, as reported by Nishio et al. (2010), who estimated the uncertainty from the reproducibility (2 RSD) of a standard solution.

Lithium and strontium isotopic ratios were measured at KCC with a multi-collector ICP-MS (MC-ICP-MS, Neptune, Thermo Sci. Co.) and a thermal ionization mass spectrometer (TIMS, Triton, Thermo Sci. Co.), respectively, after two-step column separation. The column separation and mass spectrometry procedures were described in Chapter 2 in detail.

3.4. Results and discussion

3.4.1. Experimental procedure for estimating the origin of lithium in playas

The mineral composition of the samples was determined by X-ray diffraction analysis. Clay-rich samples (samples FL01, FL03, SP01, and SP02) are composed of illite and small amounts of halite, calcite and quartz. Salt-rich sample FL02 is composed of halite and a small amount of thenardite; sample FL04 is composed predominantly of thenardite. Sand-rich samples from Alkali Lake (samples AL01 and AL02) are composed of zeolite, quartz, and calcite; the sample from Columbia Salt Marsh (sample CSM91) is composed of zeolite, quartz, and halite.

In the first step of the experiment 1, almost half of the total amount of lithium was eluted from the samples with Milli-Q water (Table 3-1 and Fig. 3-2). Most of the sodium in salt-rich samples was also leached, because halite and thenardite easily

dissolve even in neutral pH water. In contrast, several elements such as magnesium and iron remained in the solid phase (Table 3-1 and Fig. 3-2). In the second step, extraction with HNO_3 transferred the rest of the lithium into solution. A substantial amount of calcium was also eluted form calcite, as well as magnesium and iron from the clay minerals (Table 3-1 and Fig. 3-2). These results indicate that the lithium extracted during the first step was mainly incorporated in halite, and that the lithium extracted during the second step had been mainly incorporated into clay minerals. In fact, a large amount of lithium in the halite-containing samples was eluted with neutral H_2O (e.g., samples FL01, FL02, FL03, SP01, and SP02, Table 3-1 and Fig. 3-2), whereas a large amount of lithium was leached from clay-rich samples by HNO_3 (e.g., samples FL01, FL03, SP01, and SP02, Table 3-1 and Fig. 3-2). In contrast, thenardite and calcite appear to contain less lithium (e.g., samples FL04, AL01, and AL02, Table 3-1 and Fig. 3-2). δ^7Li differed by 9 ‰ between the solutions obtained in the first and second steps of the experiment 1 (sample FL01, Table 3-1), suggesting the preferential uptake of ^6Li via formation of Li-, Mg-, and Fe-bearing clay minerals (Chan et al. 1992; Misra and Froelich 2012).

After the leaching experiment 1, only a small amount of solid residue was left. This residue was probably composed mainly of silicate minerals from basement rocks (e.g., volcanic tuff, granite, and rhyolite; Munk et al. 2011) with low lithium contents. The lithium content of the sample residuals was probably low (less than 22 ppm; Munk et al. 2011). In fact, the lithium contents of salt-rich and clay-rich samples were much higher than those of basement rocks in this region (less than 22 ppm; Munk et al. 2011) and sandy samples of volcanic origin (Table 3-1 and Fig. 3-2). These results suggest that the lithium eluted into the solution by the two steps of the leaching experiment 1 was mostly derived from the water flowing into the playas in the past. Even though the leaching experiment 2 consisted of only one step, extraction with HNO_3, the results

were similar to the estimated lithium contents by summing the results from the two steps of the leaching experiment 1 (Table 3-1 and 3-2). Therefore, I conclude that the solution obtained after leaching in the experiment 2 is representative of the original lithium deposited in the playas in the past in terms of lithium isotopic compositions.
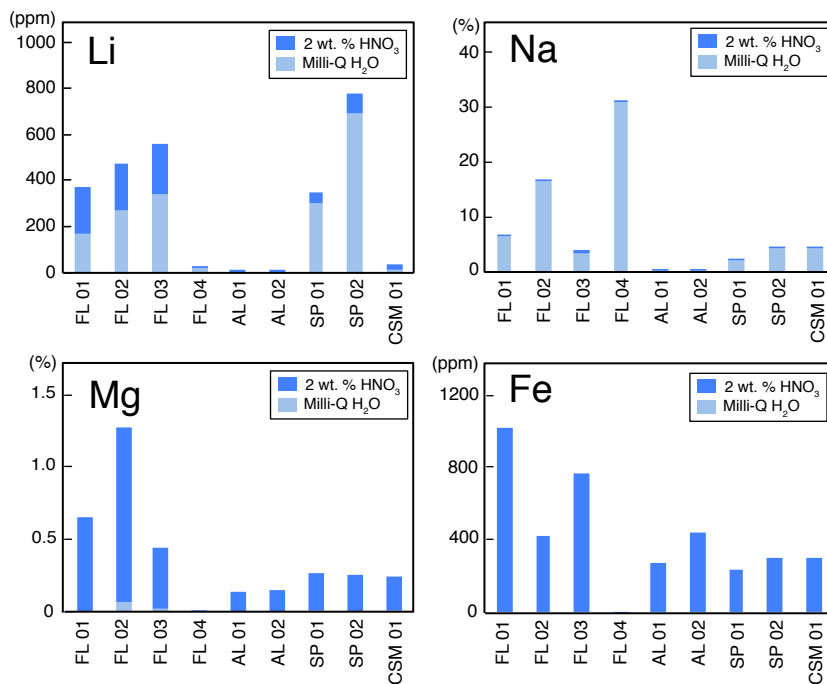

Fig. 3-2 Contents of Li, Na, Mg, and Fe in the solutions after each step of the leaching experiment 1 (see Table 3-1). The contents were calculated from the contents in the leaching solutions in each phase and dilution rates of the samples. Details of the leaching procedures are described in the text.

Table 3-1 Lithium and strontium isotopic compositions and chemical compositions obtained by the leaching experiment 1 for samples from playas in Nevada, USA. Li isotopic compositions were determined by MC-ICP-MS. Li and Sr contents were determined by ICP-MS. Na, Mg, K, Ca, and Fe contents were determined by ICP-AES. The final contents of the samples were calculated from the sample weights and dilution factors

Sample name	Sample description	Sampling point	$\delta^7 Li$ (‰)	Li (ppm)	Sr (ppm)	Na (%)	Mg (%)	K (%)	Ca (%)	Fe (ppm)
By Milli-Q H$_2$O										
FL01	Clay rich		9.3	171	12	6.33	<0.01	0.62	<0.01	n.d.
FL02	Salt rich	Fish Lake	—	269	30	16.50	0.07	0.74	1.41	n.d.
FL03	Clay rich		—	339	24	3.40	0.02	1.02	0.01	n.d.
FL04	Salt rich		—	21	15	30.96	<0.01	0.12	1.59	n.d.
AL01	Sand rich	Alkali Lake	—	1	1	0.33	<0.01	0.06	1.10	n.d.
AL02	Sand rich		—	1	1	0.39	<0.01	0.09	1.45	n.d.
SP01	Clay rich	Silver Peak	—	306	83	2.10	<0.01	0.85	0.19	n.d.
SP02	Clay rich		—	695	209	4.44	<0.01	1.47	0.05	n.d.
CSM01	Sand rich	Columbia Salt Marsh	—	11	60	4.26	0.01	0.18	2.00	n.d.
By 2 wt% ultrapure HNO$_3$										
FL01	Clay rich		0.3	203	882	0.50	0.65	0.39	1.99	1,020
FL02	Salt rich	Fish Lake	—	207	1,704	0.43	1.20	0.21	1.93	424
FL03	Clay rich		—	220	1,213	0.49	0.42	0.64	2.43	763
FL04	Salt rich		—	6	12	0.22	0.01	0.07	0.02	n.d.
AL01	Sand rich	Alkali Lake	—	10	181	0.25	0.14	0.19	3.62	268
AL02	Sand rich		—	10	203	0.24	0.15	0.22	3.86	435
SP01	Clay rich	Silver Peak	—	47	146	0.13	0.26	0.24	1.86	234
SP02	Clay rich		—	80	158	0.17	0.25	0.26	1.83	294
CSM01	Sand rich	Columbia Salt Marsh	—	27	46	0.20	0.23	0.16	0.63	300

Table 3-2 Lithium and strontium isotopic compositions and chemical compositions obtained by the leaching experiment 2 for samples from playas in Nevada, USA. Li and Sr isotopic compositions were determined by MC-ICP-MS and TIMS, respectively. Li and Sr contents were determined by ICP-MS. Na, Mg, K, Ca, and Fe contents were determined by ICP-AES. The final contents of samples were calculated from the sample weights and dilution factors

Sample name	Sample description	Sampling point	$\delta^7 Li$ (‰)	$^{87}Sr/^{86}Sr$	Li (ppm)	Sr (ppm)	Na (%)	Mg (%)	K (%)	Ca (%)	Fe (ppm)
FL01	Clay rich		1.4	0.711608	594	902	4.87	1.01	1.06	1.23	3,506
FL02	Salt rich	Fish Lake	7.4	0.711884	693	1,583	16.83	1.33	1.07	0.89	1,977
FL03	Clay rich		- 1.0	0.711599	637	1,192	3.63	1.09	0.73	1.55	3,007
FL04	Salt rich		4.5	0.711675	102	112	21.76	0.09	0.83	n.d.	199
AL01	Sand rich	Alkali Lake	3.1	0.709893	49	191	0.87	0.31	0.59	2.16	2,119
AL02	Sand rich		4.6	0.709903	59	250	1.35	0.32	1.02	2.88	2,566
SP01	Clay rich	Silver Peak	7.9	0.710148	344	418	2.82	0.46	1.23	1.36	1,044
SP02	Clay rich		7.5	0.710149	1,020	554	3.55	0.65	2.31	2.39	1,562
CSM01	Sand rich	Columbia Salt Marsh	2.0	0.710572	69	130	3.58	0.43	0.47	0.76	1,554

n.d. not determined

3.4.2. Origin of lithium in playas

Possible sources of lithium in playas include (1) fossil seawater, (2) river water, (3) saline groundwater of local meteoric origin, and (4) continental hydrothermal fluids (Jones and Deocampo 2003).

The lithium content and δ^7Li value of seawater is on average 0.18 ppm and $+31.0 \pm 0.5$ ‰ (2σ), respectively (Millot et al. 2004; Tomascak 2004). Because the residence time of lithium in the ocean is very long (~1.2 Ma), lithium in the open ocean reservoir is isotopically homogeneous (Tomascak 2004; Misra and Froelich 2012). On the basis of an analysis of planktonic foraminifera, Misra and Froelich (2012) reported that the δ^7Li value of seawater has ranged from $+22$ to $+31$ ‰ during the past 60 Ma. These δ^7Li values are very high compared with those found in this study (-1 to $+8$ ‰, Table 3-3 and Fig. 3-3). Moreover, the ^{87}Sr/^{86}Sr values determined in this study (range, 0.709893 to 0.711884; mean, 0.710826 ± 0.001696, 2σ) differ from those of both submarine hydrothermal fluids (mean, 0.7025; Davis et al. 2003) and seawater (mean, 0.70917; Veizer 1989), but are consistent with those of continental waters (range, mainly from 0.702 to 0.720; Banner 2004). Taken together, these results indicate that the lithium and strontium in the playas are of continental origin.

Although kinetic effects leading to lithium isotope fractionation have not been reported in laboratory experiments (Tomascak 2004), Δ^7Li$_{solid-fluid}$ fractionation depends on temperature: Δ^7Li$_{solid-fluid}$ = $-4.61(1,000/T[K]) + 2.48$ (Wunder et al. 2006); Δ^7Li$_{solid-fluid}$ = $-7,847/T + 8.093$ (Millot et al. 2010a). As a result, Δ^7Li$_{solid-fluid}$ fractionation is negatively correlated with temperature (Wunder et al. 2006; Millot et al. 2010a). Moreover, because ^{6}Li is preferentially incorporated into the solid phase, δ^7Li values of solutions must be higher than those of rocks (Yamaji et al. 2001). Therefore, the higher the solid-fluid interaction temperature is, the smaller the isotopic differences between solid and fluid will be, although more lithium enters into solution at higher

temperatures.

The dissolved lithium content of river waters from around the world ranges from 0.010 to 23 ppb (flow-weighted mean, 1.8 ppb) and δ^7Li ranges from +6 to +43 ‰ (average, +23 ‰) (Huh et al. 1998; Gaillardet et al. 2003; Misra and Froelich 2012) (Table 3-3). Most dissolved lithium in river water (>90 %) is derived from silicate rocks (Kisakurek et al. 2005; Millot et al. 2010b), and δ^7Li values are significantly heavier than those of the upper continental crust because of high fractionation during low-temperature chemical weathering (Huh et al. 1998; Kisakurek et al. 2005; Millot et al. 2010b). Similarly, the lithium content of saline groundwater, which is common in arid to semi-arid regions, ranges from 0.01 to 16 ppm and δ^7Li ranges from +7 to +30.6 ‰ because water–rock interactions in aquifers occur at low temperature (Tomascak 2004).

Continental hot spring waters are highly enriched in lithium (from 0.3 to 10 ppm), and δ^7Li values are relatively low (+1.0 to +17.1 ‰) (Falkner et al. 1997; Tomascak 2004) because of small isotopic fractionation at high temperatures. Water–rock interactions at 350 °C result in an isotopic difference of only about 5 ‰ between the solid and the fluid (Chan et al. 1993; Wunder et al. 2006; Millot et al. 2010a) and salt crystallization causes little isotopic fractionation (Tomascak et al. 2003), which is consistent with the approximately 5 ‰ difference between the samples in this study and plausible host rocks, such as volcanic rocks collected from the eastern Sierra Nevada (Yosemite National Park, Long Valley area, and Mono Basin, about 100 to 200 km west of the study region: 0 to +4 ‰; Tomascak et al. 2003) and of upper continental crust (–5 to +5 ‰; Teng et al. 2004, Fig. 3-3). In contrast, water–rock interaction associated with chemical weathering at 25 °C results in an isotopic difference of about 19 ‰ between solid and fluid (Millot et al. 2010a), which is too large to account for the δ^7Li values in this study (Fig. 3-3).

From the lithium isotopic results, I thus infer that the lithium in the playas was supplied mainly by continental hydrothermal fluids resulting from local geothermal activity. In contrast, it is thought that lithium in Andean salars, where abundant lithium resources have been identified in brines, originate from the alteration of volcanic rocks, especially ignimbrites because of their rapid alteration and weathering (Risacher and Fritz 2009). This hypothesis was derived from the fact that there was no relationship between lithium content and temperature of dilute springs and ground waters and that there was no significant difference between lithium abundance in waters derived from meteoric and hydrothermal alteration in this region (Risacher and Fritz 2009). However, these are insufficient evidence because the contents of lithium have been modified by evaporation and enrichment. My results suggest that information on the lithium isotopic composition would allow to ascertain the origin of the lithium resources in the playas and salt crusts of the Andes and elsewhere.
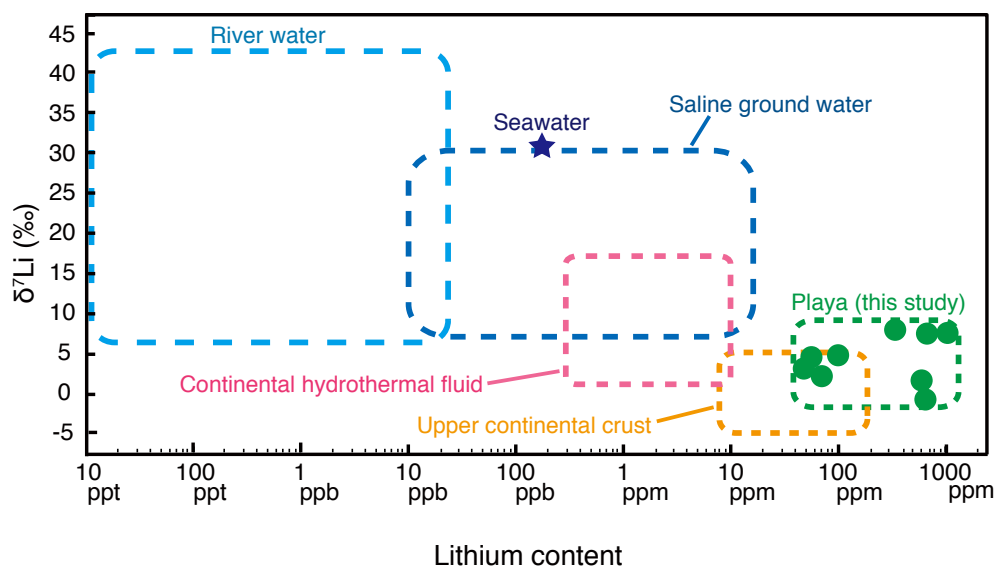

Fig. 3-3 Comparison of Li isotopic compositions (δ^7Li) with the logarithm of the lithium contents of samples in this study (*green circles*) and for various geological reservoirs (*dotted lines*). Details are given in Table 3-3.

Table 3-3 Average lithium contents and ranges, and Li isotopic compositions in various geological reservoirs and in this study

Reservoir	δ^7Li (‰)		Li (ppb or ppm)		Reference
	Average	Range	Average	Range	
River water	+23	+6 to +43	1.8 ppb [a]	0.0010–23 ppb	Huh et al. (1998), Gaillardet et al. (2003), Misra and Froelich (2012)
Saline groundwater	—[b]	+7 to +31	—[b]	0.01–16 ppm	Tomascak (2004)
Seawater	+31.0 ± 0.5 (2σ)	—[c]	180 ppb	—[c]	Millot et al. (2004), Tomascak (2004), Misra and Froelich (2012)
Continental thermal fluid	—[b]	+1 to +17 [d]	—[b]	0.3–10 ppm [d]	Tomascak (2004; excluding data from Falkner et al. 1997)
Upper continental crust	0 ± 2 (1σ)	−5 to +5	35 ± 11 ppm (2σ)	8–187 ppm	Teng et al. (2004)
Playa [e]	+4.2 ± 3.1 (1σ)	−1 to +8	400 ± 350 ppm (1σ)	50–1,020 ppm	This study

[a] Flow-weighted mean value

[b] No data

[c] Homogeneous in the open ocean

[d] Recalculated by excluding the data for dilute hot spring waters from Falkner et al. (1997)

[e] From the results of the leaching experiment 2, shown in Table 3-2

3.4.3. Variation of lithium contents and lithium isotope compositions among samples

The lithium contents and δ^7Li values in this study (Table 3-2) show some variation, reflecting differences in the mineralogical composition among samples (Fig. 3-4a). The leaching experiment 1 revealed that most lithium was incorporated in halite and clay minerals and that thenardite and calcite contained less lithium. This result agrees well with the lithium contents in the samples (Table 3-2).

The variation in δ^7Li values probably reflects differences in isotopic fractionation during each mineral formation. Approximately 16 ‰ difference between secondary clays and seawater has been observed in marine sediment and altered oceanic crust (Chen et al. 1992; Misra and Froelich 2012). In contrast, relatively small (calcite, 2–8 ‰; Tomascak et al. 2003, Marriott et al. 2004a, 2004b) or very small (halite, <1 ‰; Tomascak et al. 2003) isotopic fractionation during salt crystallization between mineral and growth solution has been reported, although the chemistry of the growth solution might affect the isotope composition of the precipitated mineral. Thus, isotopic differences between lithium incorporated in halite and that incorporated into clay minerals could mainly cause the variation in δ^7Li values among the samples, as shown by the results of the leaching experiment 1 (sample FL01). In fact, in samples from Fish Lake, δ^7Li values are higher in salt-rich samples (samples FL02 and FL04, blue squares) than in clay-rich samples (samples FL01 and FL03, red squares, Fig. 3-4a). The thenardite-rich sample FL04 with lower δ^7Li values than the halite-dominant sample FL02 suggests that isotopic fractionation (≈ 3‰, Table 3-2) between thenardite and growth solution might have occurred during crystallization. Differences in the relative proportion of each mineralogical phase among samples could also cause isotopic variation; sample FL01 with a relatively high proportion of salt has higher δ^7Li values than sample FL03 (Table 3-2).

Differences in initial δ^7Li value in the water flowing into each playa should also

affect the δ^7Li values in the samples. ^{87}Sr/^{86}Sr values are relatively uniform in samples from the same playa regardless of mineral composition (Fig. 3-4b). The variation in ^{87}Sr/^{86}Sr values is probably due to subtle differences in host rock characteristics in each playa because the strontium isotopic composition is controlled by the age and composition of host rocks (McDermott and Hawkesworth 1990). Although further studies on the lithium isotopic composition of probable host rock from each playa would be required in order to better understand the variation in δ^7Li values, the initial δ^7Li value in water flowing into each playa is likely slightly different. In fact, all clay-rich samples from Silver Peak have higher δ^7Li values than those from Fish Lake (Table 3-2 and Fig. 3-4b).
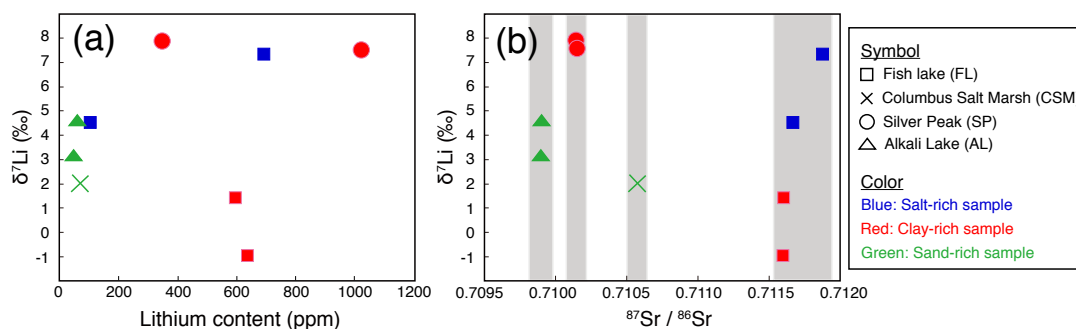
Fig. 3-4 Scatter plots of the lithium isotopic composition (δ^7Li) against (a) lithium contents and (b) the strontium isotopic composition (^{87}Sr/^{86}Sr) of samples, according to sample composition and playa. The *vertical gray bars* in part (b) show the range of strontium isotopic variation in each playa. Details are given in Table 3-2.

3.4.4. A possible scenario for the evolution of lithium in playas

I propose that high-temperature water–rock interaction produced a lithium-enriched hydrothermal solution with low δ^7Li, with some variations in each playa as the result of effective leaching of lithium from different continental rocks (Fig. 3-5). The dissolved lithium remained in solution even at low temperature because lithium is a highly

fluid-mobile element (You et al. 1996; James et al. 2003). The lithium-rich fluids flowed into the playas, then evaporated in the arid climate (Fig. 3-5). Complete evaporation left lacustrine sediments and evaporite deposits on the surfaces of the playas (Fig. 3-5). Most of the lithium was incorporated into clay minerals or halite. The observed variation in the lithium isotopic composition in samples from the playas is mainly attributable to both the preferential uptake of ^{6}Li by clay minerals and little isotopic fractionation during salt crystallization (Chan et al. 1992; Tomascak et al 2003; Misra and Froelich 2012).

The lithium isotopic ratio is thus a good tracer for reconstructing lithium concentration processes in playas. In future works, spatial and stratigraphic investigations are required to clarify the mechanisms of lithium accumulation in playas.
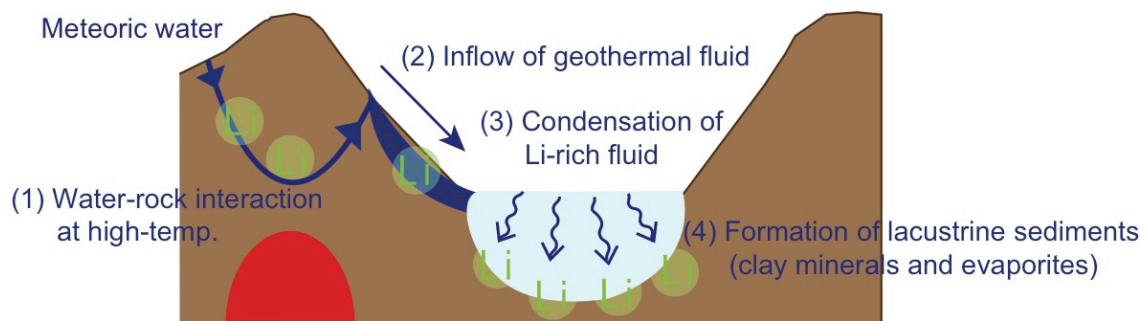

Fig. 3-5 A possible scenario for the evolution of lithium in playas. Details of each process are described in the text.

3.5. Conclusion

To constrain the origin of lithium in playas, I conducted two leaching experiments and determined lithium contents and isotopic ratios of the leachate from samples of lacustrine sediments and evaporite deposits from playas in Nevada, USA. These results suggest that most lithium is incorporated into clay minerals and in halite. Considering the δ^7Li values of the possible sources and temperature dependence of lithium isotopic fractionation between solid and aqueous fluid, the lithium concentrated in playas in this region was supplied mainly by lithium-enriched hydrothermal fluids due to high-temperature water-rock interaction and not directly by low-temperature weathering processes. Minor variation in δ^7Li values of samples is caused by differences both in isotopic fractionation during mineral formation and in initial δ^7Li composition of the water flowing into each playa.

This study reports lithium isotopic compositions in playas for the first time. My study demonstrated that lithium isotopic patterns were preserved in evaporite deposits because most lithium has remained in the playa systems and little isotopic fractionation of lithium was expected to occur during evaporative enrichment. These results suggest that δ^7Li can be a powerful tool for unraveling the origin of lithium and for reconstructing its accumulation processes in playas. Hence, it would be possible to apply lithium isotope studies in other similar environments around the world, especially in regions such as South America, where abundant lithium resources have been identified but the origin of the lithium is poorly understood.

Chapter 4

Lithium isotopic composition of submarine vent fluids from arc and back-arc hydrothermal systems at western Pacific

4.1. Abstract

Submarine hydrothermal systems significant contribute to heat and elemental fluxes to the ocean. Vent fluid geochemistry in mid-ocean-ridge (MOR) hydrothermal systems were well-studied, while studies on vent fluid geochemistry in arc and back-arc systems were insufficient, especially in terms of lithium. To reveal control factors on lithium in arc and back-arc hydrothermal systems, I determined Li contents and its isotopic compositions of 11 vent fluids collected from 5 submarine arc/back-arc hydrothermal systems in the western Pacific.

Based on mass balance calculation, Li in vent fluids are dominated by seawater-rock (seawater-sediment) interaction in sediment-starved (sediment-hosted) hydrothermal systems in arc and back-arc basins. Li contents in vent fluids is also influenced by phase-separated processes, by temperature-related portioning of rock Li into fluid phase, and by host rocks. In contrast, Li isotopic composition in vent fluids may be affected by isotopic fractionation during incongruent mineral dissolution and by host rocks, but not by phase-separated processes. These results demonstrate that lithium is a useful tracer for investigating hydrothermal circulation processes such as a phase separation process and seawater-rock/seawater-sediment interaction under the seafloor not only in MOR but also in arc and back-arc settings.

The global lithium flux and its isotopic compositions from submarine hydrothermal systems to the ocean were re-evaluated using the data of this study, were different from previously estimated values, indicating that arc and back-arc hydrothermal systems are not negligible compared to MOR sites in terms of lithium. Therefore, studies on lithium in arc/back-arc hydrothermal systems are necessary for better understanding the role of submarine hydrothermal systems in global lithium cycles on the earth's surface.

4.2. Introduction

   Submarine hydrothermal system is a fluid circulatory mechanism under the seafloor. Once seawater sinks into seafloor through cracks of the oceanic crust, seawater is heated by a magma reservoir and it rises due to the lower density. Then hydrothermal fluid erupts at the seafloor surface and hydrothermal vents are formed. During this process, cold, oxygenated, and metal-depleted seawater changes into hot, anoxic, and metal-enriched vent fluid by interactions between oceanic crust and seawater at high temperature. When hot vent fluids encounter cold seawater, almost all of metal elements precipitate as sulfides and ore deposits are generated on the seafloor.

   A number of submarine hydrothermal systems have been discovered along spreading center in the Pacific, Atlantic, and Indian Oceans (Fig. 4-1). Among submarine hydrothermal systems all over the world, geochemistry of hydrothermal vent fluids at mid-ocean-ridge (MOR) sites have been well studied. The chemical compositions of vent fluids at MOR sites such as EPR21ºN are unique (e.g. Gamo 1995), indicating that MOR hydrothermal sites are typical systems controlled by seawater-basalt (seawater-MORB) interactions at high-temperature. In contrast, various geological settings and host rocks (not only basalt) have been reported in arc and back-arc hydrothermal sites, which may cause some variations in chemical compositions compared to MOR sites (e.g. Gamo 1995). Similarly, in terms of lithium, studies on the control factor of lithium in arc and back-arc hydrothermal systems are insufficient compared to MOR sites.
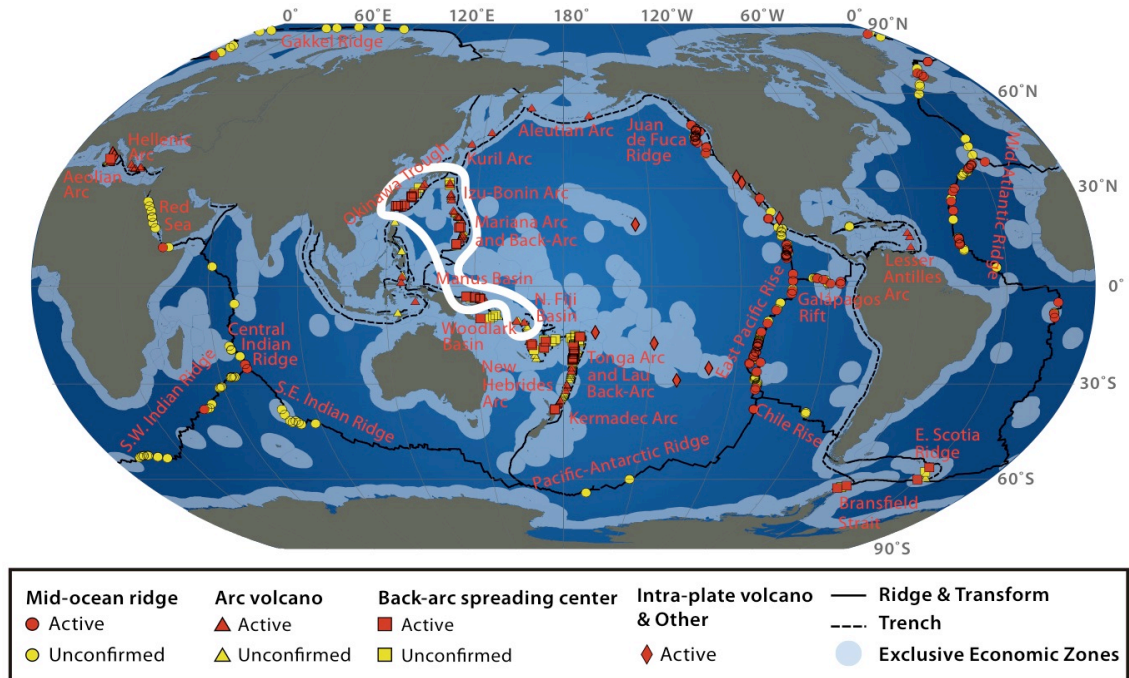
Fig. 4-1 Global distribution of hydrothermal vent fields (from interridge vents database: http://www.interridge.org/irvents/maps). Locations of the sampling hydrothermal sites are surrounded with *white line*.

Phase separation in hydrothermal systems, which causes much variations in chemical compositions of vent fluids, has also been studied at MOR sites such as the Axial Seamount Hydrothermal Emissions Study (ASHES) and Main Endeavour Field (MEF) of the Juan de Fuca Ridge (e.g. Butterfield et al. 1990; Gamo 1995; Foustoukos et al. 2004). Moreover, it is known that sediments greatly influence chemical compositions of vent fluids in sediment-hosted hydrothermal systems at MOR sites such as the Escanaba Trough and Guaymas Basin (e.g. Chan et al 1994; Gamo 1995). However, no study has reported lithium isotopic compositions of phase-separated and sediment-hosted vent fluids in arc and back-arc hydrothermal systems except for the only study at the Abyss vent in the Okinawa Trough (Scholz et al. 2010).

Considering the significant difference of lithium contents and its isotopes between seawater (0.026 mmol/kg, +31.0 ‰; Millot et al. 2004) and MORB (0.94 mmol/kg,

+3.7 ‰; Gale et al. 2013, Tomascak et al. 2008), lithium is expected to be a good tracer in submarine hydrothermal systems during water-rock interactions at high temperature. In this study, I determine lithium contents and its isotopic ratios together with other chemical compositions of 11 vent fluids from 5 sites, the sediment-starved Manus Basin (Vienna Woods, PACMANUS), Izu-Bonin Arc (Suiyo Seamount), Mariana Trough (Alice Springs, Forecast Vent), North Fiji Basin (White Lady, Kaiyo, LHOS), and sediment-hosted Okinawa Trough (JADE, Minami-Ensei, CLAM) in arc and back-arc hydrothermal systems in the western Pacific. By the use of lithium contents and its isotopes, I discuss the control factor and behavior of lithium in hydrothermal fluids during high-temperature water-rock interaction in (1) sediment-starved hydrothermal systems with various host rocks, (2) phase-separated hydrothermal systems, and (3) sediment-hosted hydrothermal systems.

Submarine hydrothermal system is also important for considering global elemental fluxes to the ocean. However, it is unclear whether elemental fluxes from arc and back-arc hydrothermal systems to the oceans are significant compared with those of MOR hydrothermal systems (Shikazono 2003). According to the data from various previous studies on lithium contents and its isotopes of vent fluids and river waters, Misra and Froelich (2012) estimated that lithium flux from hydrothermal vent fluids to the ocean (13×10^9 moles/year) is comparable that from rivers (10×10^9 moles/year) and that the mean value of their isotopic composition is +8.3 ‰ and +23 ‰, respectively. However, estimated lithium flux from hydrothermal systems were based on average lithium contents from mainly MOR sites (Edmond 1979, 1982; Vom Damm et al. 1985; Chan and Edmond 1988; Vom Damm 1990; Chan et al. 1993, 1994; Foustoukos et al. 2004), and the lithium isotopic composition from hydrothermal systems were based on the values at 7 sites, EPR 21ºN, EPR 11ºN - 13ºN, MAR 23ºN, Mariana Trough, Escanaba Trough, Guaymas Basin, and Juan de Fuca Ridge (Chan et al. 1993, 1994;

Foustoukos et al. 2004). Hence, the estimated lithium isotopic composition from whole hydrothermal systems did not contain data from arc and back-arc hydrothermal systems except for the Mariana Trough. This is because lithium isotopic compositions from arc and back-arc vent fluids have yet to be measured (Chan et al. 1994; Scholz et al. 2010). Therefore, another purpose of this study is to re-evaluate hydrothermal lithium fluxes and isotopic compositions to the oceans by determining lithium contents and its isotopic compositions in some vent fluids with various geological settings as a representative of arc and back-arc hydrothermal systems.

4.3. Materials and methods

4.3.1. Geological settings

The vent fluid samples of this study were mainly supplied by Professor Toshitaka Gamo of the Atmosphere and Ocean Research Institute (AORI), The University of Tokyo, and Associate Professor Junichiro Ishibashi of Kyusyu University. The sampling locations are shown in Fig. 4-2. Geological settings and site characteristics (host rock, water depth, location, temperature, and pH) are listed in Table 4-1. Detailed geological information on each site is summarized by Ensong (2013).

The hydrothermal vents in this study have various site characteristics such as geological settings (arc and back-arc), host rocks (basalt and dacite), water depth (from 710 to 3600 m), temperature (from 202 to approx. 400 ℃), and pH (from 2.7 to 5.3) (Table 4-1). Therefore, in this study, I compare lithium contents and its isotopes in vent fluids with such site characteristics in order to determine the control factor and behavior of lithium in hydrothermal fluids.

44
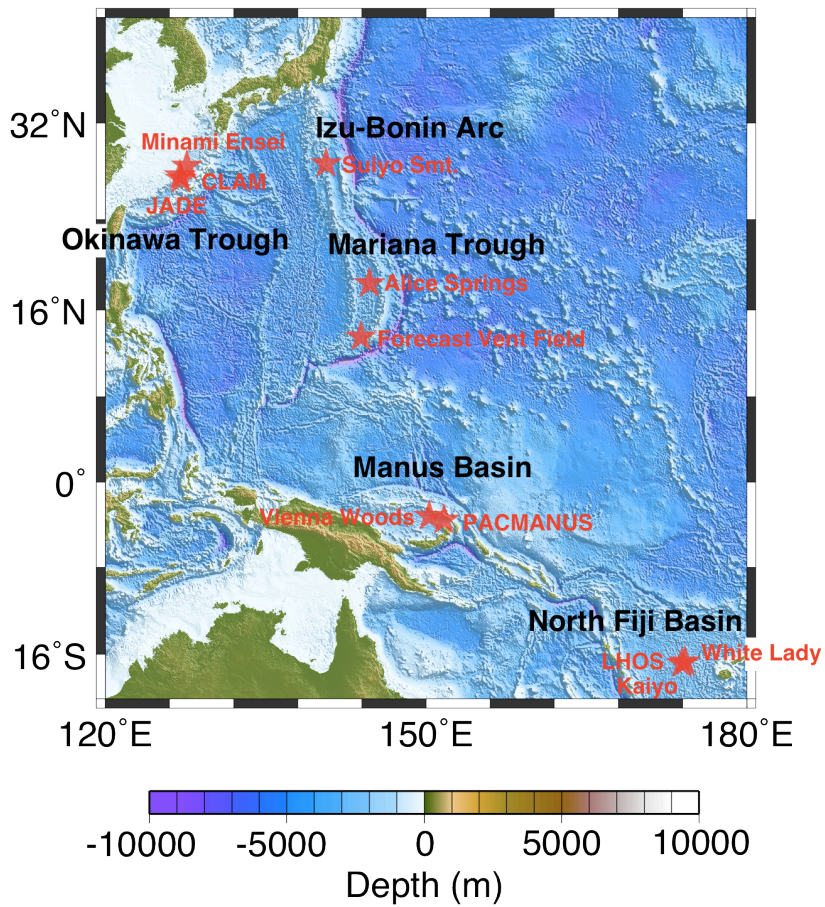
Fig. 4-2 Locations of the sampling sites of submarine hydrothemal vent fluids in this study (*red stars*). These fluids samples were selected from vent fluid archives collected mainly by Prof. Gamo (AORI, The University of Tokyo) and Associate Prof. Ishibashi (Kyusyu University) about 20 years ago. Geological setting and characteristic of each site are listed in Table 4-1.

Table 4-1 Geological settings and site characteristics at submarine hydrothermal site

Site	Manus Basin [1]		Izu-Bonin [2]	Mariana Trough [2]		North Fiji Basin [3]			Okinawa Trough [4]		
	Vienna Woods	PACMAN US	Suiyo Seamount	Alice Springs	Forecast Vent	White Lady	Kaiyo	LHOS	JADE	Minami-Ensei	CLAM
Type	Back-arc	Back-arc	Arc	Back-arc	Arc	Back-arc	Back-arc	Back-arc	Back-arc	Back-arc	Back-arc
Sediment-	starved	starved	starved	starved	starved	starved	starved	starved	hosted	hosted	hosted
Host rock	Basalt	Dacite	Dacite	Basalt	Basalt	Basalt	Basalt	Basalt	Dacite	—	Basalt
Depth (m)	2500	1650 - 1700	1380	3600	1490	1970	2000	2000	1340	710	1390
Location (Latitude)	3°10'S	3°44'S	28°34'N	18°13'N	13°24'N	16°59'S	16°59'S	16°59'S	27°16'N	28°23'N	27°33'N
Location (Logitude)	150°17'E	151°40'E	140°39'E	144°42'E	143°55'E	173°55'E	173°55'E	173°55'E	127°04'E	127°38'E	126°58'E
Temperature (℃)	285 - 300	260	296 -311	280	202	350 - 400	291	291	320	267 - 278	220
pH at 25℃	4.5	2.7 -3.1	3.7	3.9	—	4.7	4.7	4.7	4.7	4.9 -5.1	5.3

[1] Gamo et al. 1996
[2] Gamo et al. 1997
[3] Ishibashi et al. 1994
[4] Chiba et al. 1997

4.3.2. Analytical procedure

Some chemical compositions in fluid samples were already measured and summarized by previous studies (e.g. Gamo et al. 1995). However, to check the alteration of the samples during long-term storage (≈20 years), major and trace element contents of the samples were measured by ICP-AES at National Institute of Advanced Industrial Science and Technology (AIST) and ICP-MS at KCC, JAMSTEC, respectively. The uncertainties of all measurements were better than ±3 %, as reported by Nishio et al. (2010), who estimated the uncertainty from the reproducibility (2 RSD) of a standard solution. The samples whose major element concentrations were different from previous data were not used in this study. Then, two or three samples from each site, whose Mg contents range from seawater value (53.3 mmol/kg) to 0 mmol/kg, were selected for determining the original lithium contents and isotopic values of vent fluids. The Li isotope and Sr isotope measurements were conducted by MC-ICP-MS and TIMS at KCC, JAMSTEC, respectively, after two-step column separation. Detailed analytical procedures on lithium and strontium isotope measurements are described in Chapter 2.

4.4. Results

The results of Li and Sr contents, δ^7Li and ^{87}Sr/^{86}Sr values of fluid samples from each vent fluid are listed in Table 4-2. Mg contents in original hydrothermal fluids are expected to be 0 by the formation of Mg-bearing altered minerals such as smectite and chlorite during water-rock interactions (Bischoff and Dickson, 1975; Seyfried and Bischoff, 1979). Thus, Mg contents in the fluid samples are considered as a mixture of original vent fluids and seawater. Therefore, Li and Sr contents of the end member fluids can be calculated by extrapolating Mg contents to 0 (Fig. 4-3, Table 4-3).

The δ^7Li and ^{87}Sr/^{86}Sr in the end member fluids can also be estimated by mass balance calculations:

$$[\delta^7\text{Li}]_{sample} \times [\text{Li}]_{sample} = R \times [\delta^7\text{Li}]_{hydrothermal} \times [\text{Li}]_{hydrothermal} + (1-R) \times [\delta^7\text{Li}]_{SW} \times [\text{Li}]_{SW}$$
$$\cdots(1)$$

$$[\text{Li}]_{sample} = R \times [\text{Li}]_{hydrothermal} + (1-R) \times [\text{Li}]_{SW} \quad \cdots(2)$$

where R means the mixing ratio of hydrothermal fluid. Thus,

$$[\delta^7\text{Li}]_{sample} = \alpha \, / \, [\text{Li}]_{sample} + \beta \quad \cdots(3)$$

$$\alpha = [\text{Li}]_{hydrothermal} \times [\text{Li}]_{SW} \times ([\delta^7\text{Li}]_{SW} - [\delta^7\text{Li}]_{hydrothermal}) \, / \, ([\text{Li}]_{hydrothermal} - [\text{Li}]_{SW})$$
$$\cdots(4)$$

$$\beta = ([\delta^7\text{Li}]_{hydrothermal} \times [\text{Li}]_{hydrothermal} - [\delta^7\text{Li}]_{SW} \times [\text{Li}]_{SW}) \, / \, ([\text{Li}]_{hydrothermal} - [\text{Li}]_{SW})$$
$$\cdots(5)$$

These formulas demonstrate that δ^7Li value bears a linear relationship to 1/Li. By the use of this linear relationship, δ^7Li values in end member fluids can be calculated by Li content in the end members and δ^7Li values in fluid samples (Fig. 4-3, Table 4-3). Sr contents and ^{87}Sr/^{86}Sr in the end member fluids can be calculated by the same method as that of Li contents and δ^7Li (Fig. 4-3, Table 4-3).

Table 4-2 Li and Sr contents, δ^7Li and ^{87}Sr/^{86}Sr values of hydrothermal samples from each vent fluid

Site		Sample	Mg [1] (mmol/kg)	Li (μmol/kg)	δ^7Li (‰)	Sr (μmol/kg)	^{87}Sr/^{86}Sr
Manus Basin	Vienna Woods	303-TS1	46.3	153	8.3	115	0.707972
		307-1	20.3	677	4.4	187	0.705315
		307-2	2.5	1105	4.7	256	0.704465
	PACMANUS	301-8	21.7	784	6.1	114	0.706625
		304-1	42.0	208	8	88	0.708495
Izu-Bonin	Suiyo Seamount	D630-3	17.7	509	7.6	270	0.704718
		D631-2	0.8	721	7.1	307	0.704011
		D631-6	3.7	708	7.3	295	0.704099
Mariana Trough	Alice Springs	D154-2	0.9	880	4.4	84	0.703737
		D154-5	1.0	965	4.3	94	0.703774
	Forecast Vent	D182-4	43.2	75	12.2	101	0.707897
		D187-2	25.3	193	6.6	147	0.705794
North Fiji Basin	White Lady	IST5-2	8.6	197	5.4	42	0.706405
		IST6-1	25.7	127	7.7	66	0.708164
	Kaiyo	D80-3	31.5	142	8.9	79	0.708273
		D80-4	8.5	356	5.9	60	0.705690
	LHOS	D93-3	24.4	219	6.8	77	0.707443
		D93-4	33.5	140	8.1	80	0.708195
Okinawa Trough	JADE	D423-3	1.0	3802	2.5	180	0.708920
		D423-5	45.2	425	3.9	100	0.709152
	Minami-Ensei	D621-5	27.2	2726	1.7	90	0.708892
		D622-1	4.9	5514	1.9	247	0.710024
		D622-2	1.4	5817	1.3	252	0.710070
	CLAM	D426-6	39.5	1261	1.9	74	0.709003
		D427-6	33.4	2076	1.8	91	0.708962
	(Seawater)		53.1 [2]	26 [3]	31.0 [3]	90 [4]	0.70916 [4]

[1] Mg contents of vent fluids are all from reference data (Gamo et al. 1996; Gamo et al. 1997; Ishibashi et al. 1994; Chiba et al. 1997)

[2] Turekian 1968

[3] Millot et al. 2004

[4] Palmer and Edmond 1989
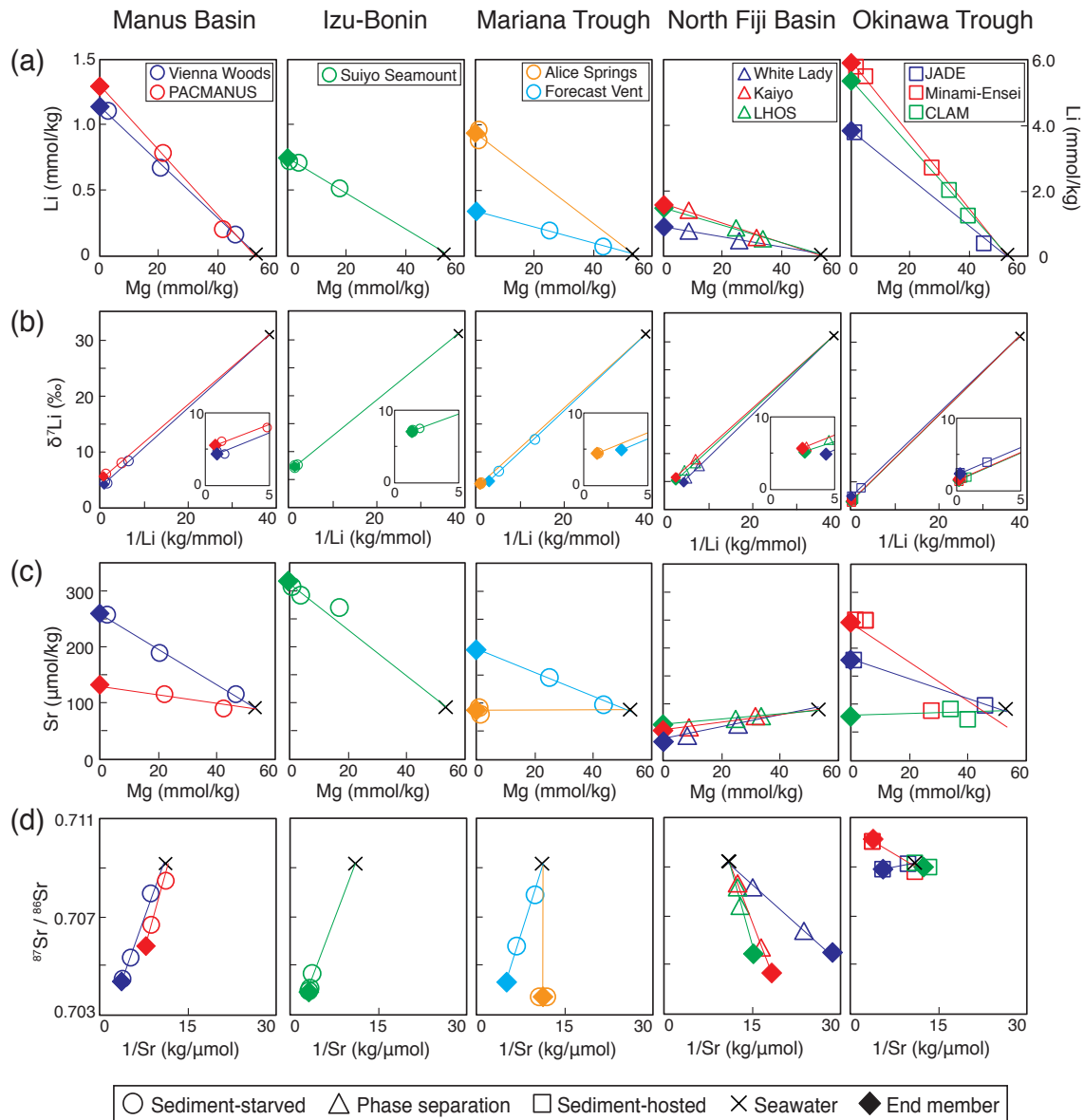
Fig. 4-3 Li and Sr contents, δ⁷Li and ⁸⁷Sr/⁸⁶Sr in the hydrothermal vent fluids samples from each site. Data from samples are shown as open symbols. (a, c) Li (Sr) contents of the samples are plotted with Mg contents. The Li (Sr) end members can be calculated by extrapolating Mg to 0. (b,d) The δ⁷Li (⁸⁷Sr/⁸⁶Sr) values are plotted with 1/Li (1/Sr). The δ⁷Li (⁸⁷Sr/⁸⁶Sr) end members can be calculated by mass balance calculation and the Li (Sr) end members at each site. Details of the calculation for the end member values are described in the text. The data of the end member values are listed in Table 4-3.

Table 4-3 Li and Sr contents, δ^7Li and $^{87}Sr/^{86}Sr$ end members of vent fluids at various arc and back-arc region compared with MOR, geological settings and site characteristics

Site	Manus Basin		Izu-Bonin	Mariana Trough		North Fiji Basin			Okinawa Trough			Vent fluids from MOR	(MORB) [2]	(Seawater)
	Vienna Woods	PACMAN US	Suiyo Seamount	Alice Springs	Forecast Vent	White Lady	Kaiyo	LHOS	JADE	Minami-Ensei	CLAM			
Geological settings														
Type	Back-arc	Back-arc	Arc	Back-arc	Arc	Back-arc	Back-arc	Back-arc	Back-arc	Back-arc	Back-arc			
Sediment-	starved	starved	starved	starved	starved	starved	starved	starved	hosted	hosted	hosted			
Host rock	Basalt	Dacite	Dacite	Basalt	Basalt	Basalt	Basalt	Basalt	Dacite	—	Basalt			
Depth (m)	2500	1650 - 1700	1380	3600	1490	1970	2000	2000	1340	710	1390			
Tempature (℃)	285 - 300	260	296 -311	280	202	350 - 400	291	291	320	267 - 278	220			
pH at 25℃	4.5	2.7 -3.1	3.7	3.9	—	4.7	4.7	4.7	4.7	4.9 -5.1	5.3			
This study														
Li (mmol/Kg)	1.14	1.30	0.75	0.94	0.34	0.23	0.40	0.37	3.86	5.98	5.40			
δ^7Li (‰)	4.3	5.5	7.2	4.3	4.8	4.9	5.7	5.2	2.4	1.6	1.5			
Sr (µmol/kg)	259	130	319	89	198	35	55	65	181	245	79			
$^{87}Sr/^{86}Sr$	0.7044	0.7058	0.7040	0.7037	0.7044	0.7055	0.7047	0.7054	0.7089	0.7101	0.7090			
References														
Li (mmol/Kg)	0.7		0.6	0.59 - 0.83	0.3	0.20 - 0.28			2.5	5.4 - 5.8	3 - 4	0.40 - 1.45 (Average: 0.84 ± 0.26, 1σ)	0.94 ± 0.04	0.03
δ^7Li (‰)			8.6									6.5 - 11.5 (Average: 8.3 ± 1.3, 1σ)	3.7 ± 1.9	31.0
Sr (µmol/kg)			303	72 - 90	165	30 - 43			94	215 - 227			1470 ± 50	90
$^{87}Sr/^{86}Sr$			0.7036 - 0.7038			0.7046			0.7089	0.7100			0.7028 ± 0.0001	0.70916
Reference [1]	1		1	1	1	1			1	1	1	2	3, 4	5, 6

[1] References are below: 1. Gamo (1995), 2. Misra and Froelich (2012), 3. Gale et al. (2013), 4. Tomascak et al. (2008), 5. Millot et al. (2004), 6. Palmer and Edmond (1989)

[2] The global mean values are shown with 2σ uncertainties

The end members of Li and δ^7Li are summarized in Table 4-3 and Fig. 4-4 with reference data from MOR hydrothermal sites. Li and Sr contents and their isotopic values in some vent fluids are almost the same as values from previous studies (Table 4-3). However, there is 4.3 ‰ difference in lithium isotopic composition between this study and previous data from the Alice Springs (Chan et al. 1994).

Lithium in seawater is quite low in content (0.026 mmol/kg) and much high in δ^7Li value (+31.0 ‰), while lithium in MORB is much higher in content (0.94 mmol/kg) and much lower in δ^7Li value (+3.7 ‰). During water-rock interactions at high temperature, it is known that a large amount of lithium is leached from rocks and little isotopic fractionation occurs between fluid and rocks (e.g. You et al. 1996; James et al. 2003; Wunder et al. 2006; Millot et al. 2010). Considering these facts, lithium in hydrothermal fluids is expected to be higher in concentration and lower in isotopic ratios, which are similar values to MORB. In this study, lithium in hydrothermal fluids from arc and back-arc systems follows a similar pattern. However, there are some variations in lithium contents (from 0.23 to 5.98 mmol/kg) and δ^7Li values (from +1.5 to +7.2 ‰) compared to MOR sites (range, from 0.40 to 1.45 mmol/kg and +6.5 to +11.5 ‰: Misra and Froelich 2012). Therefore, I discuss lithium contents and δ^7Li values in vent fluids by dividing into three hydrothermal systems: (1) sediment-starved hydrothermal systems from the Manus Basin, Izu-Bonin Arc, and Mariana Trough, (2) phase-separated hydrothermal systems from the North Fiji Basin, and (3) sediment-hosted hydrothermal systems from the Okinawa Trough.
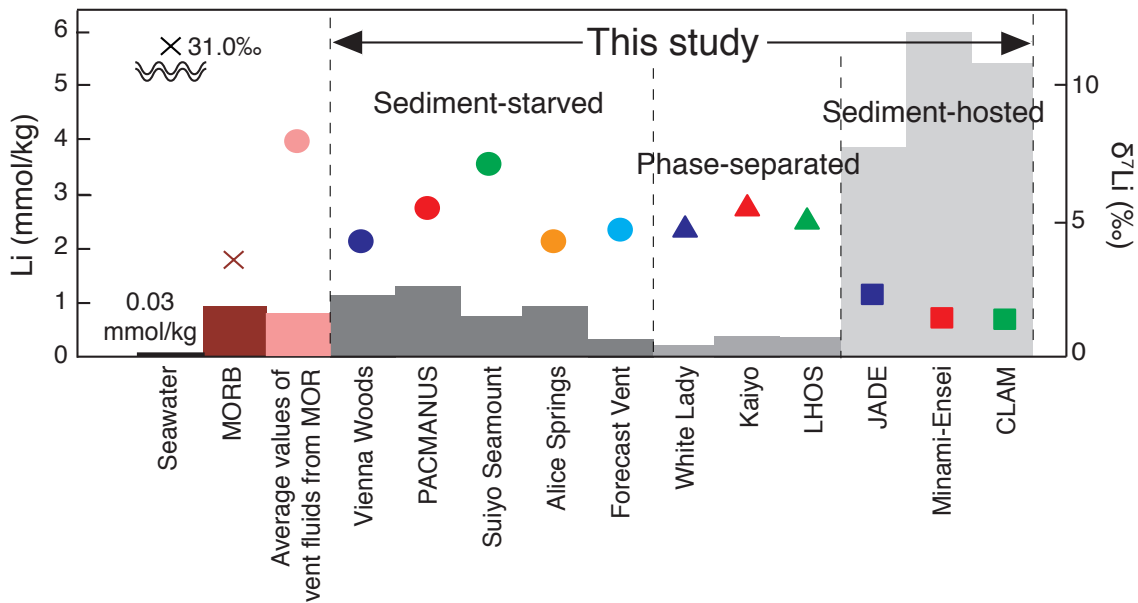
Fig. 4-4 End members of Li contents and δ^7Li of the hydrothermal vent fluids from each site. Li contents are shown as the bar graph; δ^7Li values are plotted. The hydrothemal sites in arc and back-arc systems are classified into three: sediment-straved systems, phase-separated systems, and sediment-hosted systems. The data of the end member values are listed in Table 4-3.

4.5. Discussion

4.5.1. Lithium in hydrothermal systems at Mid-Ocean-Ridge

In MOR hydrothermal systems, the lithium contents and its isotopic compositions in vent fluids are relatively uniform due to typical high-temperature (<350 ºC) seawater-MORB interactions. The unique isotopic compositions of unaltered MORB (+3.7 ± 2.1 ‰, 1σ; Tomascak et al. 2008), temperature-dependent isotopic fractionation during water-rock interactions (4.5 ‰ difference between mineral and fluid at 350 ºC: Millot et al. 2010), and preferential portioning of MORB Li into fluid phase at high temperature (You et al. 1996) should control isotopic homogeneity in MOR vent fluids and the mean δ^7Li of +8.3 ± 1.3 ‰ (1σ) (Misra and Froelich 2012).

At EPR 21ºN in MOR, previous studies on lithium isotopes have been reported the Li contents (mean, 1.07 mmol/kg and range, 0.89−1.42 mmol/kg: Chan et al. 1993) and its isotopic compositions (mean, +7.7 ‰ and range, +6.6 to +10.1 ‰: Chan et al. 1993) (Table 4-3). As a representative of MOR sites, Li content and its isotopic composition in vent fluid from EPR 21ºN are obtained by mass balance calculation in a closed system. In an equilibrium state, the equalities hold as below:

$$[Li]_{rock\text{-}initial} + w/r \, [Li]_{SW} = [Li]_{rock\text{-}altered} + w/r \, [Li]_{hydrothermal} \quad \cdots(6)$$

$$([^7Li/^6Li]_{rock\text{-}initial} \times [Li]_{rock\text{-}initial} + w/r \, [^7Li/^6Li]_{SW} \times [Li]_{SW}) / ([Li]_{rock\text{-}initial} + w/r \, [Li]_{SW}) = ([^7Li/^6Li]_{rock\text{-}altered}$$

$$\times [Li]_{rock\text{-}altered} + w/r \, [^7Li/^6Li]_{hydrothermal} \times [Li]_{hydrothermal}) / ([Li]_{rock\text{-}altered} + w/r \, [Li]_{hydrothermal}) \quad \cdots(7)$$

$$[Li]_{rock\text{-}altered} / [Li]_{hydrothermal} = D \quad \cdots(8)$$

$$[^7Li/^6Li]_{hydrothermal} / [^7Li/^6Li]_{rock\text{-}altered} = \alpha \quad \cdots(9)$$

where w/r, D, and α mean the water/rock mass ratio, distribution coefficient and isotopic fractionation factor between solid and fluid, respectively.

There is 4 mathematical formulae and 7 unknowns: $[Li]_{rock\text{-}altered}$, $[Li]_{hydrothermal}$, $[^7Li/^6Li]_{hydrothermal}$, $[^7Li/^6Li]_{rock\text{-}altered}$, w/r, D, and α. If we presume or refer the value of w/r, D, and α, we can calculate Li contents and its isotopic compositions in hydrothermal vent fluids. At EPR 21ºN, the maximum temperature of hydrothermal fluids is 351 ºC (Chan et al. 1993). Thus, the empirical values for the parameter of D and α at 350 ºC was established as follows: $D = 0.27$; $\alpha = 0.996$ (Magenheim et al. 1995; Chan et al. 2002; Millot 2010). The w/r ratio is also important to constrain the Li behavior in hydrothermal systems. Bowers and Taylor (1985) and Spivack and Edmond (1987) reported that the w/r of hydrothermal fluids from EPR 21ºN is 0.50–0.70 and 0.28–0.66, respectively. If the w/r of 0.62 is adopted for this calculation, the calculated Li content in vent fluid at EPR 21ºN is highly congruent with the observed mean Li content (Table 4-4). However, the calculated δ^7Li value of +5.4 ‰ is 2.3 ‰ lower than the observed δ^7Li value of +7.7 ‰ (Table 4-4 and Fig. 4-5).

Table 4-4 Calculated Li contents and its isotpic compositons in vent fluid from each site based on mass balance calculation

Site	Initial fluid (SW)		Host rock		Vent fluid		Altered rock		Observed vent fluid		Reference[1]
	Li (mmol/kg)	δ^7Li (‰)	Li (mmol/kg)	δ^7Li (‰)	Li (mmol/kg)	δ^7Li (‰)	Li (mmol/kg)	δ^7Li (‰)	Li (mmol/kg)	δ^7Li (‰)	
EPR 21°	0.026	31.0	0.94	3.7	1.07	5.4	0.29	1.4	1.07	7.7	1, 2, 3, 4
Vienna Woods	0.026	31.0	0.98	3.4	0.76	5.3	0.24	0.3	1.14	4.3	1, 5
PACMANUS	0.026	31.0	1.92	4.1	1.44	6.0	0.50	0.0	1.30	5.5	1, 5
CLAM	0.026	31.0	5.04	0	3.84	1.4	1.23	-3.6	3.86	2.4	1, 6

[1] Reference nambers are below: 1. Millot et al (2004), 2. Gale et al (2013), 3. Tomascak et al (2008), 4. Chan et al (1993), 5. Nishio (unpublished), 6. Tang et al. (2004)
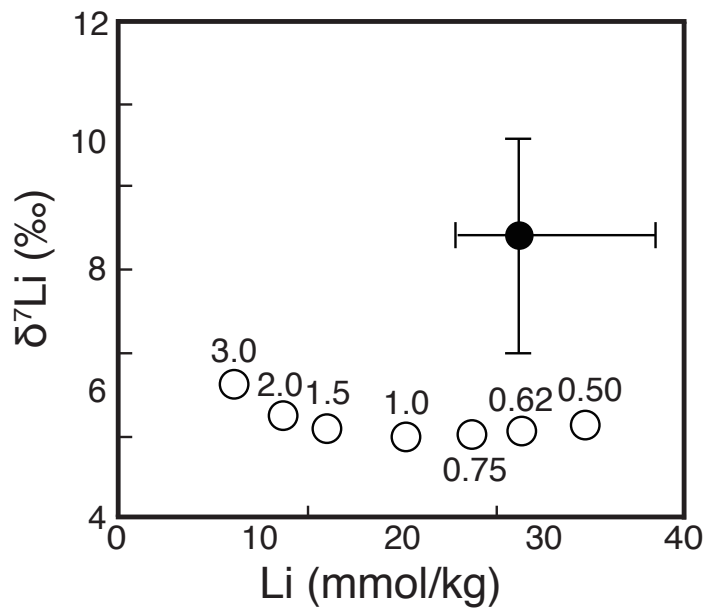

Fig. 4-5   Plots of Li against δ^7Li of the hydrothermal vent fluid end members from EPR 21° as a function of *w/r*. Solid circle means average of observed end member values from vent fluids. The error bars mean range of each vent fluid. Open circles are calculated Li values with the value of *w/r*. The datailed calculation procedure is described in the text.

If the *w/r* varies from 0.50 to 3.0, the calculated Li contents and δ^7Li values in vent fluid change (Fig. 4-5). However, the changes in *w/r* cannot achieve the lowest δ^7Li value in vent fluid (Fig. 4-5). The likely cause of the discrepancy is that the distribution coefficient of Li between alteration phase and fluid depending on temperature is poorly known, especially at relatively high temperature (Foustoukos et al. 2004). The isotopic

fractionation factor strongly depends on mineral species. More accurate knowledge of D and α values would allow more quantitative constraints on w/r. The most likely explanation is isotope fractionation during incongruent mineral dissolution (Pistiner and Henderson, 2003). It is known that isotopically-light Li is subsequently incorporated into secondary clay minerals during high temperature alteration and low temperature weathering (e.g., Chan et al., 1993; James et al., 1999; Huf et al. 2001). Variations in Li contents (range, 0.40 to 1.45 mmol/kg: Misra and Froelich 2012) and δ^7Li (range, +6.5 to +11.5 ‰: Misra and Froelich 2012) in vent fluids may be due to formation and dissolution of secondary minerals in the hydrothermal vent fluids plumbing during being taken preferentially of ^{6}Li by Mg-rich asbestos phase (Chan et al. 2002; German and Von Damm 2003). This phenomenon causes a decrease of ^{6}Li in vent fluids. Hence, The Li contents and δ^7Li values in vent fluids can be changed lower and heavier. In contrast, re-dissolution of these phases in subsequent circulation cycles makes Li contents and δ^7Li values in vent fluids into higher and lighter These explanations are supported by the moderate negative correlation between Li contents and δ^7Li values in vent fluids from various hydrothermal systems (Misra and Froelich 2012).

4.5.2. Sediment-starved hydrothermal systems at arc and back-arc sites

Vent fluids from the Manus Basin, Izu-Bonin, and Mariana Trough (except for the North Fiji Basin) are classified as sediment-starved hydrothermal systems. These hydrothermal sites have various host rock and site characteristics compared to MOR sites. In arc and back-arc hydrothermal systems, the lithium contents of vent fluids (from 0.34 to 1.30 mmol/kg) are the same range as those of MOR vent fluids (from 0.40 to 1.45 mmol/kg: Misra and Froelich 2012), while δ^7Li values (from +4.3 to +7.2 ‰) are lower than those in MOR sites (from +6.5 to +11.5 ‰: Misra and Froelich 2012), except for sediment-hosted MOR sites at the Guaymas Basin and Escanaba Trough

(Table 4-3).

At the Vienna Woods in the Manus Basin, the Li content of 1.14 mmol/kg is similar to those at EPR 21ºN (range, 0.89−1.42 mmol/kg: Chan et al. 1993), while δ^7Li values of +4.3 ‰ is slightly lower than those at EPR 21ºN (range, +6.6 to +10.1 ‰: Chan et al. 1993) (Table 4-3). Other chemical compositions such as K, B and δ^{11}B are similar to those at EPR 21ºN, suggesting that vent fluids from the Vienna Woods show MORB-like properties and Li in vent fluids should be similar to that in other MOR sites (Reeves et al. 2011; Ensong 2013). Other site characteristics in the Vienna Woods such as water depth of the sites, fluid temperature, and pH are the same range as those of MOR sites, indicating that the problem on differences (≈4 ‰) in δ^7Li values of vent fluids between from MOR and from the Vienna Woods still remains.

The δ^7Li values in host rocks from the Vienna Woods were measured by Dr. Yoshiro Nishio of JAMSTEC, and he concluded that there is no differences in Li contents and δ^7Li values between MORB (the mean of 0.94 ± 0.04 mmol/kg and +3.7 ± 1.9 ‰: Gale et al. 2013, Tomascak et al. 2008) and the host rocks from Vienna Woods (the mean of 0.98 mmol/kg and +3.4 ‰, and range from 0.95 to 1.01 mmol/kg and +3.3 to +3.5 ‰) (Nishio, unpublished). The mass balance calculation for estimating Li contents and δ^7Li values in hydrothermal fluids was conducted using the empirical parameters of D and α at 300 ºC, which have been established as follows: D = 0.32, a = 0.995 (Magenheim et al. 1995; Chan et al. 2002; Millot 2010). The w/r ratio is estimated to be 1.0. The result of the calculation shows Li content and isotope values similar to the observed values (Table 4-4). The significantly-small differences in δ^7Li (≈1 ‰) of vent fluids between observed and calculated values can be explained by differences in w/r ratio, temperature-dependent isotopic fractionation derived from uncertainty of observed temperature, and heterogeneity of host rock and vent fluid compositions (Fig. 4-6). Therefore, Li in vent fluid from the Vienna Woods is generated by seawater-basalt

interaction at high temperature in an equilibrium state.
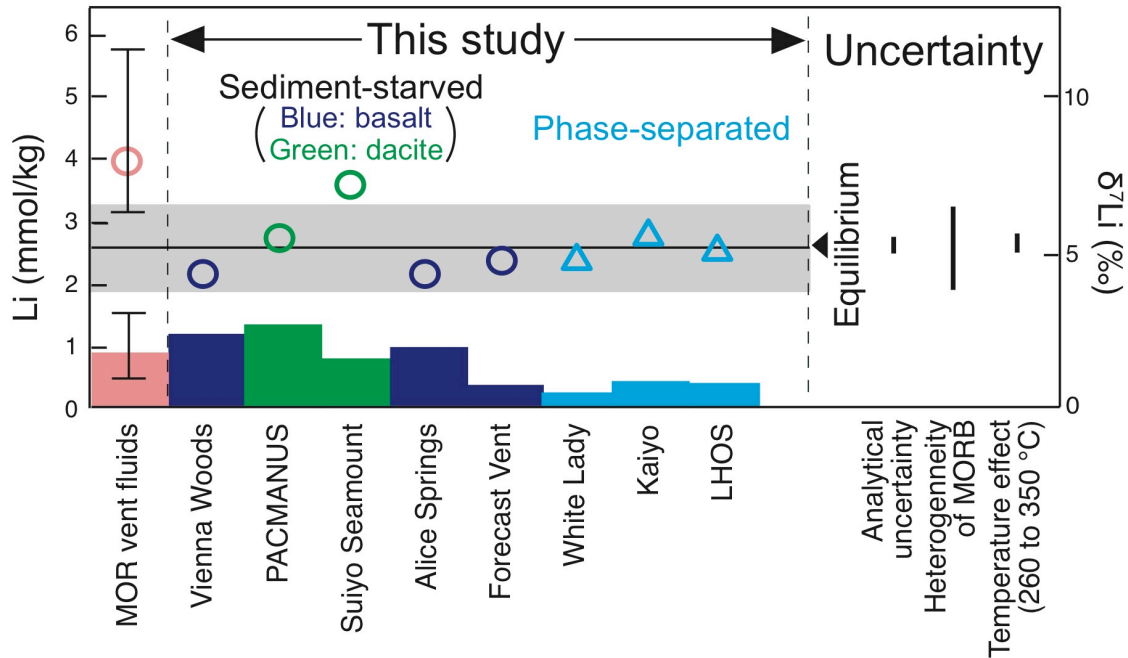
Fig. 4-6　End members of Li contents and δ^7Li of the hydrothermal vent fluids from each sediment-straved site. Li contents are shown as the bar graph; δ^7Li values are plotted. The data of end member values are listed in Table 4-3. The error bars at MOR vent fluids mean the range of obserbed end member values from each vent fluid. The δ^7Li value in equilibrium state shown as black horizontal bar is calculated by the use of the data of Li in seawater, Li in MORB, w/r of 1, intereaction temperature of 350 ºC, α and D at 350 ºC. Black vertical lines on the right side and grey horizontal bars mean isotopic uncertainty of each variable parameter and uncertainty of MORB heterogeneity.

In the Mariana Trough, Li contents and its isotopic compositions in vent fluids are similar to that at the Vienna Woods except for Li content in the Forecast Vent. This result suggests that Li in vent fluids from the Mariana Trough experiences a similar process and Li in host rocks has similar composition with the Vienna Woods. However, it is known that contribution from subducted underneath the Mariana Trough affects some chemical compositions in vent fluids such as B and CO_2, resulting in differences

in $\delta^{11}B$ of vent fluids between from the Vienna Woods and Alice Springs/Forecast Vent (Palmer 1991; Ensong 2013). Moreover, Ensong (2013) reported that differences in $\delta^{11}B$ between the Alice Springs and Forecast Vent can be explained by temperature-dependent $\delta^{11}B_{\text{solid-fluid}}$ fractionation: $\Delta^{11}B_{\text{solid-fluid}} = -10.69 \, (1{,}000/T[K]) +3.88$ (Wunder et al. 2005). In contrast, there is not such a difference in $\delta^{7}Li$, although $\Delta^{7}Li_{\text{solid-fluid}}$ fractionation is negatively correlated with temperature (Wunder et al. 2006; Millot et al. 2010). Based on the equations of $\Delta^{7}Li_{\text{solid-fluid}} = -4.61(1{,}000/T[K]) + 2.48$ (Wunder et al. 2006) and $\Delta^{7}Li_{\text{solid-fluid}} = -7{,}847/T[K] + 8.093$ (Millot et al. 2010), the differences in $\delta^{7}Li$ of vent fluids between the Alice Springs (Temperature, 280 ºC) and Forecast Vent (Temperature, 202 ºC) can be calculated as about 1.4 and 2.3 ‰, respectively. However, the observed differences in $\delta^{7}Li$ of the vent fluids are 0.5 ‰ (Table 4-3). A likely explanation for the B and Li isotopic behavior in the vent fluid is that the slope of temperature-dependent isotopic fractionation on B is sharper than that on Li. Therefore, $\delta^{7}Li$ differences in vent fluids between the Alice Springs and Forecast Vent could not be observed as a function of temperature and slub subducting contribution in this study.

The differences in temperature-related portioning of rock Li into fluid phase (You et al. 1996; James et al. 2003) may be a key factor that controls the lithium contents in the Alice Springs and Forecast Vent. The leaching of Li and B from rocks is strongly temperature dependent. However, the differences in temperature-related portioning of rock B into fluid phase between at 202 ºC and at 280 ºC is small (You et al. 1996; James et al. 2003). In contrast, little Li will be leached from rocks at 202 ºC; most Li will be leached from rocks at 280 ºC (You et al. 1996; James et al. 2003). Moreover, Sr will be leached from rocks at low temperature; Sr will be removed from fluid and into solid phase at high temperature (You et al. 1996; James et al. 2003). These factors can explain the differences in Li, B, and Sr contents between the Alice Springs and Forecast

Vent.

At the PACMANUS and Suiyo Seamount, the Li contents of vent fluids are similar to other sediment-starved hydrothermal sites, while δ^7Li are slightly high values compared to other sites. Dr. Yoshiro Nishio of JAMSTEC analyzed Li contents and δ^7Li in dacite host rocks at the PACMANUS, and reported that Li contents (mean, 1.91 mmol/kg and range, 1.80−2.10 mmol/kg) are almost twice as high as MORB (mean, 0.94 mmol/kg: Gale et al. 2013); δ^7Li values (mean, +4.1 ‰ and range, +2.8 to +4.7 ‰) are approximately the same as MORB (mean, +3.7 ‰: Tomascak et al. 2008) (Nishio, unpublished). By the mass balance calculation similar to the Vienna Woods site, Li contents and δ^7Li values in hydrothermal fluids was calculated using empirical parameters of D and α at 260 ºC, which have been established: D = 0.35 and α= 0.994 (Magenheim et al. 1995; Chan et al. 2002; Millot 2010). The w/r ratio was estimated to be 1.0. The result of the calculation shows higher lithium content and heavier isotope value than the calculated values at the Vienna Woods (Table 4-4). Since the observed Li characteristics in vent fluids between the PACMANUS and Vienna Woods show the same pattern (Fig. 4-6), higher and heavier Li at the PACMANUS and Suiyo Seamount may be attribute to dacitic host rocks.

Therefore, further studies on lithium isotopic ratios are required to constrain the control factor on lithium contents and its isotopic compositions in vent fluids from arc back-arc hydrothermal systems because the lower δ^7Li in vent fluids from arc and back-arc sites than those from MOR sites is still unsolved.

4.5.3. Phase-separated hydrothermal systems at arc and back-arc sites

Phase separation has been occurred under the seafloor in the North Fiji Basin hydrothermal systems. In phase-separated hydrothermal systems, Cl concentration is a good indicator for the experience of phase separation of vent fluids among the variety of

chemical compositions between saline brine and vapor-rich fluid (e.g. Butterfield et al. 1990). Thus, I compare Cl contents in vent fluids to Li contents and Li isotopic compositions (Fig. 4-7).

The lithium contents in vent fluids from the White Lady, Kaiyo, and LHOS in the North Fiji Basin range from 0.23 to 0.40 mmol/kg, quite lower than those in other arc and back-arc hydrothermal fluids (Table 4-3). To compare with other phase-separated hydrothermal systems from MOR sites, vent fluids from ASHES and MEF of the Juan de Fuca Ridge in the eastern Pacific are also illustrated in Fig. 4-7 (Butterfield et al. 1990; Foustoukos et al. 2004). Especially, the Inferno site of the ASHES vents (624 mmol/kg) is higher Cl concentration than seawater (541 mmol/kg) and is known as a Cl-enriched site (Butterfield et al. 1990). The vent fluids which contain Cl similar to seawater (418−550 mmol/kg) are identified as Cl-normal; the fluids whose Cl concentrations are much lower than seawater (32−267 mmol/kg) are identified as Cl-depleted. There is a positive linear correlation between Li and Cl (Fig. 4-7), indicating that phase separation process cause depletion of Li in vapor and enriched in brine when Cl contents are depleted in vapor and enriched in brine, respectively. Moreover, the positive linear correlation also suggests that reduction tendency of Li is similar to that of Cl during phase separation process.

Lithium isotopic composition of the North Fiji Basin vent fluids ranges from + 4.9 to +5.7 ‰, which is close to the values in other vents fluids from arc and back-arc hydrothermal sites (Table 4-3). The phase-separated vents fluids from the MEF, whose Cl contents ranges widely from 32 to 426 mmol/kg, have same δ^7Li signature as those from arc and back-arc hydrothermal sites. These results indicate that δ^7Li values in vapor-rich vent fluids fall within the same range of values both as those in Cl-normal vent fluids from MEF (Foustoukos et al. 2004) and in other vent fluids from MOR sites (e.g. Misra and Froelich 2012) (Fig. 4-7). These characteristics are consistent with the

Li isotopic results of hydrothermal experiments conducted at 431−447 ºC and 322-397 bars. These temperature and pressure are within the supercritical two-phase condition of seawater (Berndt et al. 1996). These results revealed that the isotopic fractionation factor between vapor and brine ($\alpha_{vapor-brine}$) is near unity. Therefore, phase separation can not cause lithium isotopic fractionation. δ^7Li in the vent fluids from the North Fiji Basin are dominated by fluid-rock interaction in subseafloor reaction zone like other arc and back-arc sediment-starved hydrothermal systems.
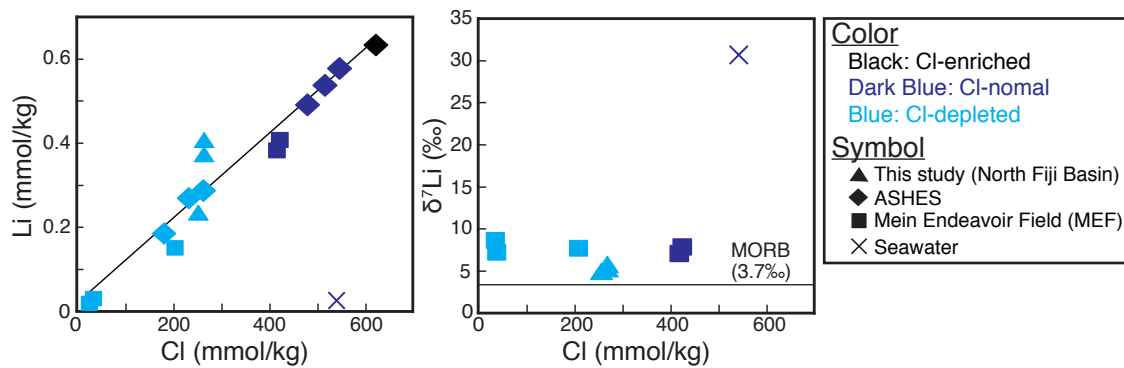

Fig. 4-7 Scatter plots of Cl contents against (a) Li contents and (b) the lithium isotopic composition (δ^7Li) of vent fluid end members, according to phase-separated conditions and hydrothemal fields. Details are described in the text.

4.5.4. Sediment-hosted hydrothermal systems at arc and back-arc sites

Significantly high Li contents (3.86 to 5.98 mmol/kg) and low δ^7Li (+1.5 to +2.4 ‰) are obtained in the vent fluids in sediment-hosted hydrothermal systems, in the Okinawa Trough (Table 4-3, Fig. 4-4). Compared to sediment-starved hydrothermal systems in arc and back-arc sites, Li contents are higher five times and δ^7Li is lower by 2 to 5 ‰ (Table 4-3, Fig. 4-4). Ensong (2013) reported a similar tendency in B (significantly high B contents and low $\delta^{11}B$ values in vent fluids). In fact, high B contents and low $\delta^{11}B$ values were reported from the marine sediments in the Okinawa Trough by Ishikawa and Nakamura (1993). Based on the calculation, the estimated data of B by

seawater-sediment interactions are consistent with the measurement data, suggesting that vent fluids from Okinawa Trough hydrothermal systems underwent water-sediment interactions after water-rock interactions (Ensong 2013). High CH_4, H_2S and NH_4 contents derived from degradation of organic matter in marine sediments also supported the water-sediment reaction (Gamo 1995).

Li contents of marine sediments in the Okinawa Trough were also reported as 6.72−11.66 mmol/kg. These values are sevenfold higher than in MORB and two-hundredfold higher than in seawater (Ishikawa and Nakamura, 1993). However, no δ^7Li data of marine sediments on the Okinawa Trough is obtained. Chan et al. (2006) reported δ^7Li values in various marine sediments from all over the world, indicating that there are some variations in δ^7Li (−4.3 to +14.5 ‰), which reflect sediment type, provenance and diagenetic process. The sediments of the Okinawa Trough is mainly originated from the Eurasian continent, indicating that the δ^7Li in the sediments of the Okinawa Trough can be light because detrital sediments show lighter value (−1.5 to +5.0 ‰); especially clay-rich ediments from mature continental crust have much lighter values (Chan et al. 2006). Moreover, Li in continental crust are enriched (average, 5.0 ± 1.6 mmol/kg, 2σ) and isotopically-light (average, 0 ±2 ‰, 1σ) compared to those in MORB (Teng et al. 2004) (Fig. 4-8). Therefore, the characteristics of Li in vent fluids from the sediment-hosted Okinawa Trough are mainly attributable to water-sediment interactions.
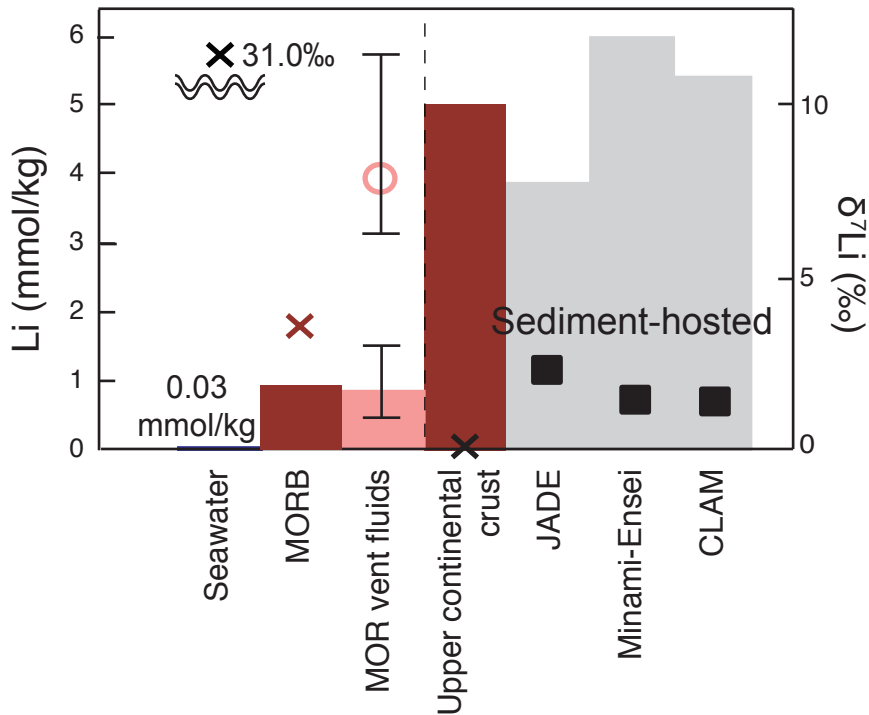
Fig. 4-8   End members of Li contents and δ^7Li of the hydrothermal vent fluids from each sediment-hosted site. Li contents are shown as the bar graph; δ^7Li values are plotted. The data of end member values are listed in Table 4-3.

In fact, mass balance calculation in closed system also support water-sediment interactions. The Li contents and δ^7Li values of the mean upper continental crust were assumed for marine sediments in this region. The distribution coefficient (*D*) of 0.32 and isotopic fractionation factor (α) of 0.995 at 300 ºC were used (Magenheim et al. 1995; Chan et al. 2002; Millot 2010). The *water/sediment* ratio was assumed to be 1. The calculated Li contents and its isotopic value in vent fluid from the JADE site are 3.84 mmol/kg and +1.4 ‰, respectively (Table 4-4). These calculated values are almost consistent with the measured end member values of 3.86 mmol/kg and +2.4 ‰ (Table 4-4). Moreover, the calculated δ^7Li value in sediments with hydrothermal alteration is very low value of -3.6 ‰ (Table 4-4), which is consistent with the lightest isotopic composition (-4.3 ‰) observed in hydrothermally-reached sediments in the Guaymas

Basin. Moreover, the Minami-Ensei and CLAM sites are covered with thicker sediments compared to the JADE site (Shitashima et al. 1994), which is consistent with the data that Li contents and δ^7Li values in the Minami-Ensei (5.98 mmol/kg and +1.6 ‰) and CLAM (5.40 mmol/kg and +1.5 ‰) sites are higher and lower than those in the JADE site (3.86 mmol/kg and +2.4 ‰), respectively (Table 4-3, Fig. 4-8).

Vent fluids from the Okinawa Trough have higher Li contents (3.86 to 5.98 mmol/kg) and lower δ^7Li (+1.5 to +2.4 ‰) relative to those from the Guymas Basin (0.63 to 1.08 mmol/kg, +2.6 to +10.3 ‰) and the Escanaba Trough (1.29 mmol/kg, +6.6 to +8.1 ‰), which are sediment-hosted hydrothermal systems at MOR sites. Ensong (2013) also reported a similar tendency in B. Differences in geological conditions between back-arc and MOR may affect Li in sediment-hosted hydrothermal systems as is the case with Li in sediment-starved and in phase-separated hydrothermal systems at arc and back-arc sites as described above.

Therefore, these results demonstrate that Li contents and its isotopic compositions are a useful tracer for investigating water-sediment interaction processes in subseafloor hydrothermal systems.

4.5.5. Re-evaluation of global lithium flux and its isotopic compositions in hydrothermal systems to the ocean

Misra and Froelich (2012) estimated average Li contents (0.84 mmol/kg) from vent fluids to the ocean and its isotopic composition (+8.3 ‰) by compiling the data from MOR hydrothermal sites (Edmond 1979, 1982; Vom Damm et al. 1985; Chan and Edmond 1988; Vom Damm 1990; Chan et al. 1993, 1994; Foustoukos et al. 2004). However, this study revealed that Li contents in sediment-hosted hydrothermal vent fluids are significantly higher than other reported values in MOR vent fluids (Table 4-3) and that Li isotopic compositions in vent fluids from arc and back-arc hydrothermal

systems show approximately 3 ‰ lower than those in MOR sites. Considering these facts, the average Li contents and its isotopic composition in hydrothermal vent fluids should be re-calculated.

The calculated average Li content from arc and back-arc sites is approximately 1.88 mmol/kg, if hydrothermal water flux of each vent is equal. Hence, I could calculate weighted mean δ^7Li of 2.7 ‰ from arc and back-arc hydrothermal sites by considering Li content from each site. However, the ratio of total water flux from arc and back-arc hydrothermal systems to that from MOR systems is unknown. I would therefore roughly estimate total water flux from arc and back-arc hydrothermal systems.

In modern back-arc hydrothermal systems, the eruption rate of volcanic rocks is estimated to be 0.25×10^{15} g/year (Fujii and Nakamura 1979). The circulated water flux from back-arc hydrothermal systems can be calculated to be $2.5-12.5\times10^{15}$ g/year by considering the ratio of circulated seawater to volcanic rocks, which is estimated to be 10 to 50 (Shikazono 1993, 2003). In contrast, Elderfield and Schultz (1996) reported hydrothermal water flux of $1.5-4.5\times10^{16}$ g/year from MOR systems based on some simulation such as the heat flux from oceanic crusts, mass balance calculation using Mg concentration and Sr isotopes, and so on. Therefore, the ratio of total water flux from arc and back-arc hydrothermal systems to that from MOR systems can be calculated to be 1:1.2 – 1:18. If we adopt mean hydrothermal water flux value of 7.5×10^{15} g/year (back-arc) and 3.0×10^{16} g/year (MOR), the ratio can be calculated to be 1:4. When we adopt this ratio, the average Li content and weighted mean δ^7Li from total hydrothermal sites are estimated to be 1.05 mmol/kg and +6.3 ‰, respectively. These values were differ by approximately 0.21 mmol/kg and 2.0 ‰ from total values estimated previously. This study indicate that arc and back-arc hydrothermal systems are not negligible for calculation of total Li flux and its isotopic composition from submarine hydrothermal systems, although there are some presumptions for the calculation. More studies on

66

lithium isotopes in vent fluids would be required to determine accurate Li flux and its isotopic composition from submarine hydrothermal systems. This would lead to better understanding of Li contribution in submarine hydrothermal systems to global lithium cycles.

4.6. Conclusion

In this chapter, I determined Li contents and its isotopic compositions of vent fluids collected from submarine hydrothermal systems of arc and back-arc in the western Pacific. The Li in vent fluids was discussed by dividing three hydrothermal systems into (1) sediment-starved hydrothermal systems, (2) phase-separated hydrothermal systems, and (3) sediment-hosted hydrothermal systems. Main conclusions of each site are as follows:

(1) In sediment-starved hydrothermal systems, calculated Li contents and its isotopic compositions based on the mass balance calculation are almost consistent with the observed compositions, suggesting that Li in vent fluids are dominated by seawater-rock interactions. Li contents in vent fluids are also controlled by temperature-related portioning of rock Li into fluid phase and by host rocsk. In contrast, small differences in lithium isotopic composition in vent fluids may be caused by host rocks and isotopic fractionation during incongruent mineral dissolution. Especially, such kinetic isotope effect is strongly affected to MOR sites, while seawater-rock interaction is occurred in equilibrium state at arc and back-arc sites.

(2) In phase-separated hydrothermal systems, Li contents in vent fluids are correlated to Cl contents, indicating the phase separation process influences Li contents in phase-separated fluids. In contrast, lithium isotopic fractionation can not occur during the phase separation process.

(3) In sediment-hosted hydrothermal systems, calculated Li contents and its isotopic compositions based on the mass balance calculation using possible marine sediments are consistent with the observed compositions, suggesting that significantly high Li contents and low δ^7Li in vent fluids are caused by seawater-sediment interactions.

Differences ($\approx$3 ‰) in δ^7Li values in vent fluids between MOR and arc/back-arc hydrothermal systems were observed. Then, I re-evaluated the average Li content and its isotopic composition from whole hydrothermal based on some assumptions of hydrothermal water flux. The estimated values of 1.05 mmol/kg and +6.3 ‰ were different from previously estimated values only from MOR sites, indicating that arc and back-arc hydrothermal systems are not negligible compared to MOR sites in terms of lithium.

This study demonstrated that lithium is a useful tracer for investigating hydrothermal circulation and seawater-rock/seawater-sediment interaction under the seafloor not only on MOR but also in arc and back-arc settings. Moreover, studies on lithium in arc and back-arc hydrothermal systems are necessary for better understanding the role of submarine hydrothermal systems in global lithium cycles on the earth's surface.

Chapter 5

Controlling factor of lithium contents and its isotopic compositions in river waters

– A case study on Ganges-Brahmaputra-Meghna river systems –

5.1. Abstract

Terrestrial river water greatly influences on ocean lithium chemistry and the global lithium cycles. Lithium isotopes in river systems are recognized as a proxy for silicate weathering because of large isotopic fractionation during weathering in rivers. However, there are few detailed studies for controlling factors on lithium contents and its isotopic compositions during flowing-down processes by comparing individual river systems with different geological settings and in wet/dry seasons. Thus, I and collaborators conducted extensive field surveys in Bangladesh and determined various chemical compositions including Li and Sr isotopes in water samples from the Ganges-Brahmaputra-Meghna river systems, one of the major rivers in the world.

In the Ganges and Brahmaputra rivers, the riverine Li is likely to be derived from silicate weathering, while Sr is strongly controlled by carbonate weathering. In the Ganges and Brahmaputra rivers, the large variations in Li contents and its isotopic compositions relative to variations in Sr during flowing down are mainly caused by incongruent weathering, which changes dissolved Li to lower and isotopically heavier values. In contrast, the relatively-small Meghna river is very influenced by ground water with slightly-light δ^7Li values, which cause dissolved δ^7Li lighter but Li content change little. The differences in Li flux and its isotopic composition in each river between dry and wet seasons could be explained by changes in drainage basin areas and in residence time of the river. This study proposed that the behavior on Li during flowing down and seasonal variation on Li should be considered when the global lithium flux and its isotopic compositions from river systems to the ocean are estimated.

5.2. Introduction

Terrestrial river water greatly influences on the global material cycles. Active chemical weathering occurs in river regions by the reaction of terrestrial rocks and water, consuming atmospheric CO_2 and transporting dissolved and suspended materials into the ocean through rivers. Therefore, it is important to clarify the role of river water in the earth surface environment for understanding global material cycles and climate changes associated with atmospheric CO_2 level variations.

It is well established that changes in rates of weathering have the potential to change atmospheric CO_2 level on timescales of longer than ~one million years. The increase in $^{87}Sr/^{86}Sr$ of seawater during the Cenozoic has been linked to enhanced weathering due to initiation of the Himalayan orogeny together with the global cooling (e.g. Raymo and Ruddiman 1992). However, strontium isotopes are not a good tracer of silicate weathering because the strontium in Himalaya is mainly derived from carbonate weathering, which causes no reduction of atmospheric CO_2 because of sedimentation of biogenic carbonate in marine environments (Jacobson and Blum, 2000). Therefore, it is important to find a new proxy for silicate weathering.

It is known that most dissolved lithium in river water (>90 %) is derived from weathering of silicate rocks (Kisakurek et al. 2005). Moreover, a large lithium isotopic fractionation can occur during silicate weathering, which is evidenced by a large isotopic difference (≈23 ‰) between average isotopic composition of river water (+23 ‰) and that of the upper continental crust (0 ‰). In recent years, therefore, lithium contents and its isotopes are identified as a proxy for silicate weathering.

Previous studies reported lithium isotopes together with some elemental isotopes such as magnesium and uranium in river waters with various geological settings in the world for validating lithium isotopes as a silicate weathering proxy (Hathorne and

James, 2006; Huh et al. 1998, 2001, 2004; Kisakurek et al. 2005; Liu et al. 2012; Liu et al. 2011, 2013; Millot et al. 2010; Pistiner and Henderson 2003; Pogge von Strandmann et al. 2010; Teng et al. 2010; Tipper et al. 2012; Vigier et al. 2009; Wimpenny et al. 2010; Yoon 2010). Especially, most of the studies dealt with comparison of riverine δ^7Li among the rivers with different geology in drainage basins (e.g. Huh et al. 1998, 2001), comparison of dissolved δ^7Li with suspended δ^7Li in the river (e.g. Kisakurek et al. 2005), and weathering experiment in the laboratory (e.g. Pistiner and Henderson 2003). However, systematic and extensive studies in major rivers are now limited. Especially, few studies focused on changes in lithium contents and isotopic compositions during flowing down in association with differences in basement lithologies and seasons (dry and wet). These insights are necessary for considering lithium flux from the river to the ocean and its influence.

In this study, I and co-workers conducted extensive field surveys and collected river and ground waters from Ganges-Brahmaputra-Meghna river systems in wet and dry seasons. I measured isotopic and chemical compositions in the water samples to discuss what controls dissolved lithium in the river systems. Moreover, the role of rivers to the global lithium cycles in earth surface environments are discussed.

5.3. Materials and Methods

5.3.1. Geological settings

Three major rivers (the Ganges, Brahmaputra, and Meghna rivers) were investigated in this study (Fig. 5-1, 5-2, and 5-3). The Ganges and Brahmaputra rivers originate from the high Himalayas (Fig. 5-1). Regional metamorphism with limestones and coexisting silicate rocks occurs in this area, which influences a dissolved load in the river by

weathering. The Ganges river flows southeastward across India and Bangladesh, while the Brahmaputra river flows eastward in China, southwestward in India, southward in Bangladesh, and finally meets the Ganges river at the central part of Bangladesh (Fig. 5-1). In contrast, the Meghna river originates from a hilly region of eastern India (Fig. 5-1). The Meghna river, formed by merger of the Surma and the Kusiyara rivers, flows southwestward in Bangladesh, and finally meets the Ganges river at a point south of Dhaka (Fig. 5-2). This river water flows through the Himalayan alluvium region in the lowland, which influences a dissolved load in this river (Fig. 5-2). The combined river water discharges into the Bay of Bengal.

The total lengths of the Ganges, Brahmaputra, Meghna rivers are 2,645 km, 2,840 km, and 930 km, respectively (Parua 2010). The drainage basin area of the Ganges and Brahmaputra is 1.03×10^6 km^2 and 6.51×10^5 km^2, respectively (Parua 2010). The mean annual river flow of the Ganges under the Hardinge Bridge (near the location G-3) is 1.14×10^4 m^3/s, while the flood-swollen river flow in the wet season is about 5.5×10^4 m^3/s (Webster et al. 2010). The mean annual river flow of the Brahmaputra is 2.01×10^4 m^3/s, while the flood-swollen river flow in the wet season is about 6.4×10^4 m^3/s (Webster et al. 2010). In contrast, the Meghna river has much smaller flow than the Ganges and Brahmaputra rivers: the average annual river flow of the river is 3.51×10^3 m^3/s, while the flood-swollen river flow in the wet season is about 1.22×10^4 m^3/s (Paura 2010).

Only two lithium isotopic studies were conducted in this area. One targeted upstream tributaries of the Ganges in the central and eastern Nepal near Himalaya and reported the δ^7Li values of +10.2 to +25.0 ‰ (Kisakurek et al. 2005). The other surveyed three sites in the upstream and the middle stream of the Ganges in India, and middle stream of the Brahmaputra in India, and reported the δ^7Li values of +11.4, +23.1, and +20.0 ‰, respectively (Huh et al. 1998) (Fig. 5-1).

73
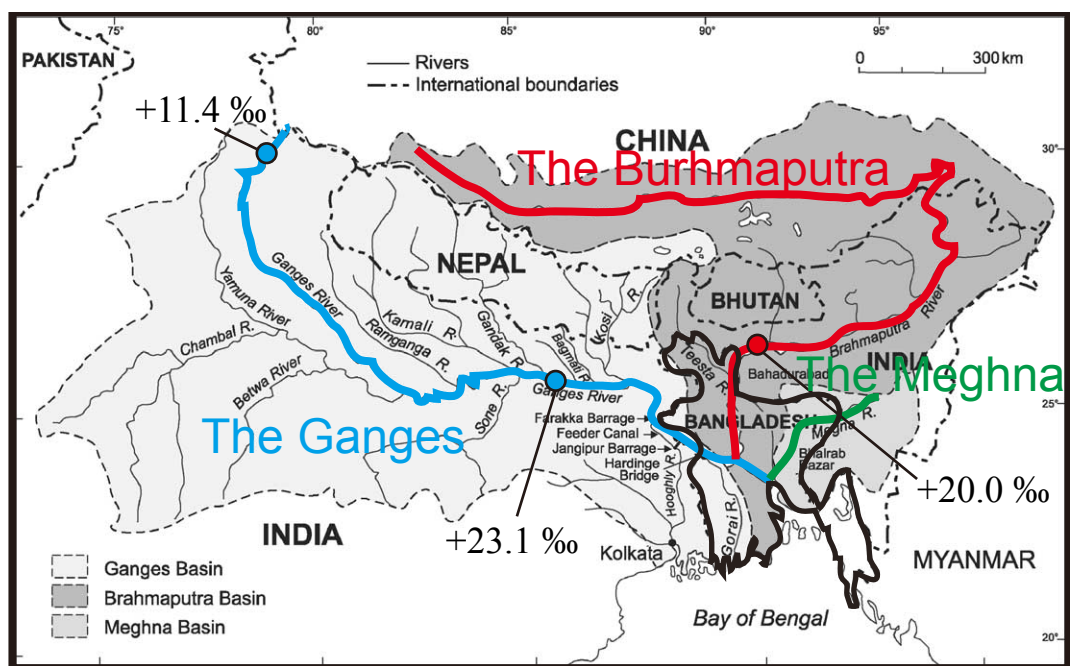
Fig. 5-1 Locations of the Ganges, Brahmaputra, and Meghna rivers and these drainage basin (modified from Mirza 2001). Water sampling was conducted in Bangladesh enclosed by a black lines. The δ^7Li values in the maps are previously reported values by Huh et al. (1998).
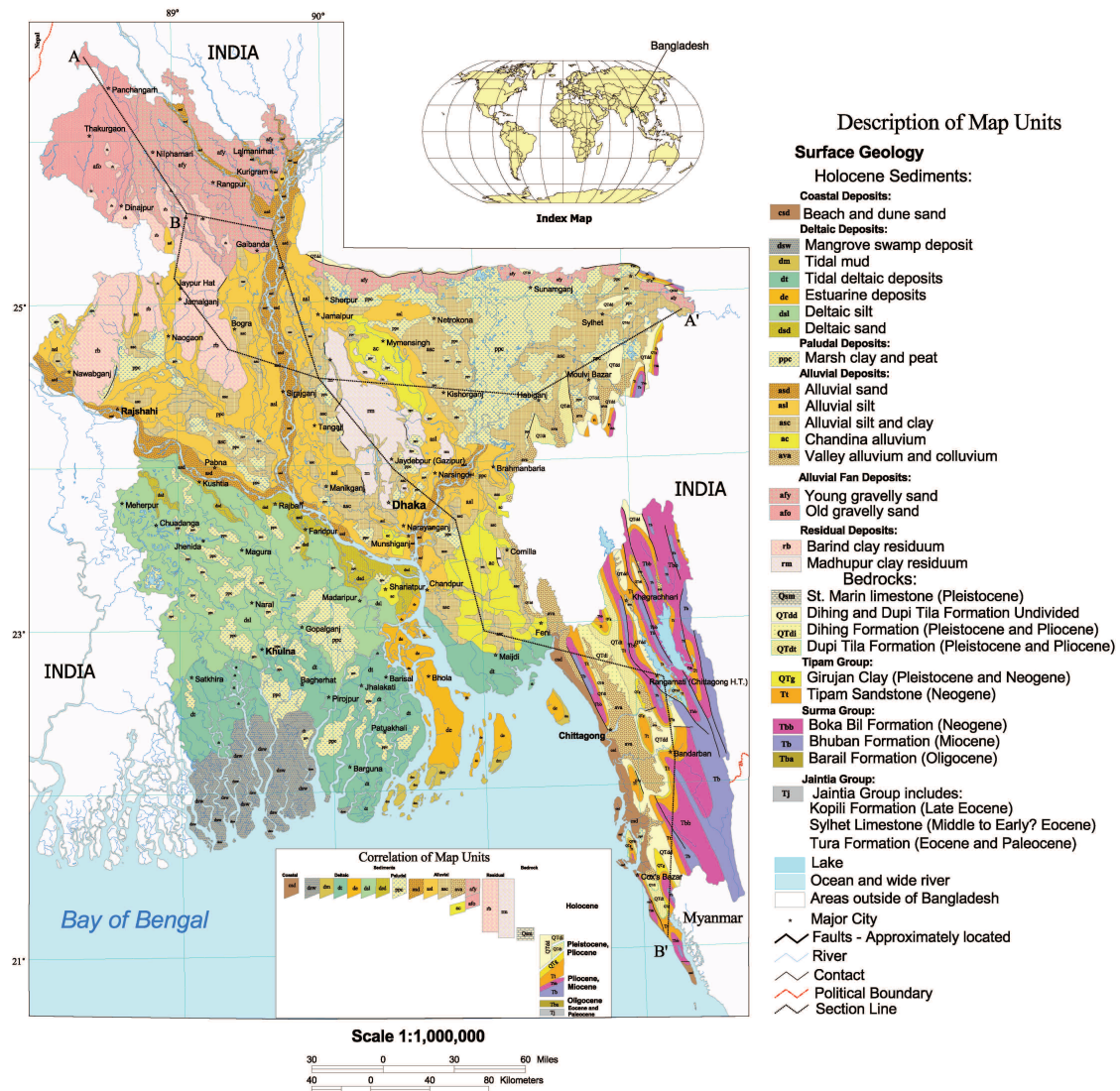
Fig. 5-2 Geological map of Bangladesh prepared by Geological survey of Bangladesh. Original data can be download (http://www.psb.gov.bd/english/images/files/BANG_GEO.pdf).

5.3.2. Sample descriptions

I and collaborator conducted two sampling surveys during the dry and wet seasons in Bangladesh in order to evaluate seasonal variations in chemical compositions of the river water. The first survey I joined (11-18 January 2011) was conducted in the dry season, and the second survey (5-9 September 2011) was in the rainy season. The river water samples were collected at three stations in the Ganges (Locations G-1, G-2, and

G-3) and the Brahmaputra (Locations B-1, B-2, and B-3) both from the upper stream to lower stream in Bangladesh (Fig. 5-3). In the Meghna and its upper tributaries (the Surma and Kusiyara rivers), river water samples were taken at four sampling sites in Bangladesh before the river meets the Ganges: one river water sample from the Surma (Location S-1), one from the Kusiyara (Location K-1), and two from the main stream of the Meghna (Locations M-1 and M-2) (Fig. 5-3). The water samples of the Ganges were also collected at the sites downstream of where the Ganges meets the Brahmaputra (location GB-1) and furthermore meets the Meghna river (location GBM-1) (Fig. 5-3). Each river water sample was taken from the center of the river by the ships. Moreover, the ground waters were collected from wells near Dhaka (locations GR-1, GR-2, GR-3, and GR-4) (Fig. 5-3). The river water samples from location G-3, B-3, M-2, GB-1, and GBM-1 were collected both in the dry and wet seasons.

Outdoor analysis was conducted for pH measurements. The pH was finally corrected at the state of 25 °C. The water samples were filtered through a 0.45-μm acetate membrane filters and were divided into HNO_3-washed polypropylene bottles for laboratory analyses.
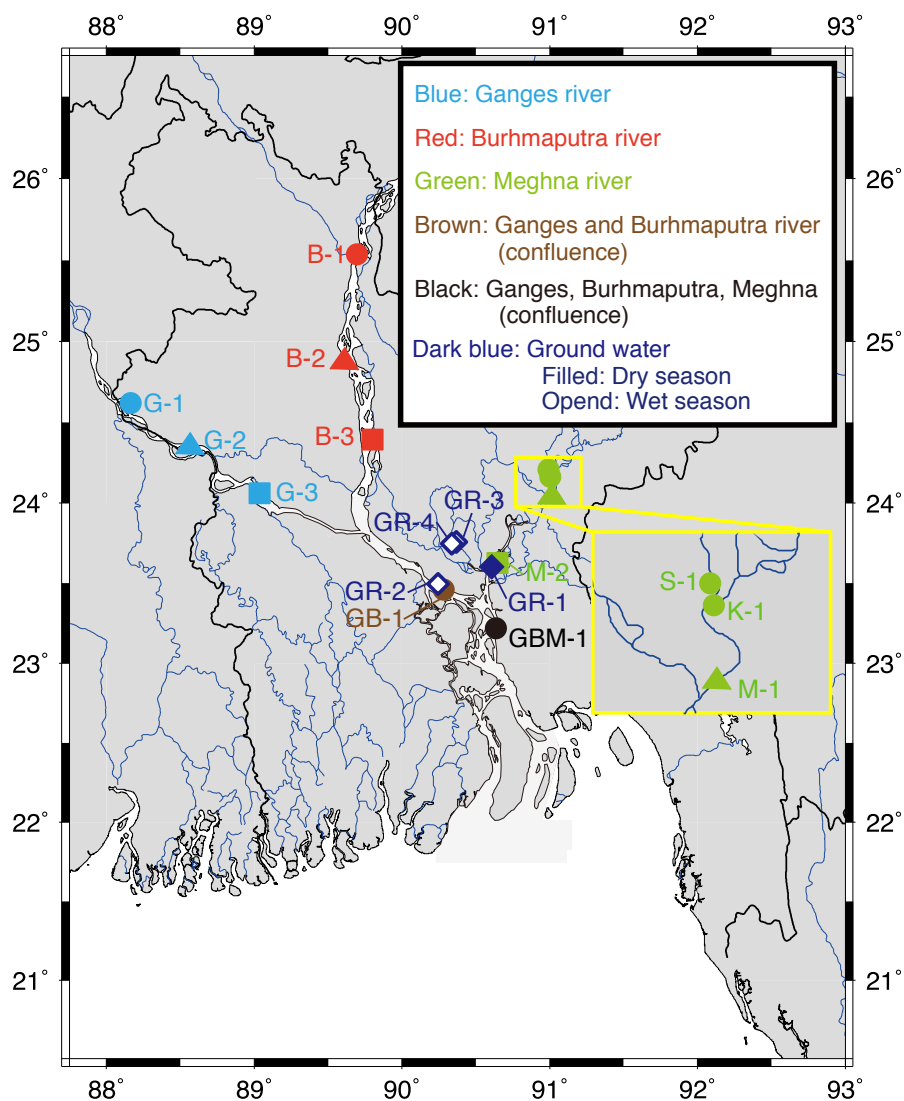
Fig. 5-3 Locations of the sampling points of river and ground waters. Detailed sample descriptions are listed in Table 5-1. The river water samples from location G-3, B-3, M-2, GB-1, and GBM-1 were collected both in the dry and in wet seasons.

5.3.3. Analytical procedures

Major and trace element contents of the samples were measured by ICP-AES and ICP-MS at KCC, JAMSTEC, except for Na, K, Ca, and Cl contents that were determined by Ion Chromatography (IC) at KCC, JAMSTEC (Table 5-1). The uncertainties of all measurements were better than ±3 %, as reported by Nishio et al. (2010), who estimated the uncertainty from the reproducibility (2 RSD) of a standard

solution. The Li and Sr isotope measurements were conducted by MC-ICP-MS and TIMS at KCC, JAMSTEC, respectively, after two-step column separation. Detailed analytical procedures on the isotope measurements are described in Chapter 2. The total alkalinity of the water samples was conducted by Mr. Manaka of AORI, The University of Tokyo.

5.4. Results

The isotopic and chemical compositions of river and ground water samples collected from the Ganges, Brahmaputra, and Meghna river systems in Bangladesh are listed in Table 5-1. The major cation contents in the samples are shown as a ternary diagram (Fig. 5-4), indicating that the major cation content of the dissolved load is distinct for each lithology. The Ganges and Brahmaputra rivers have high concentration of Ca (Table 5-1, Fig. 5-4), which is derived from carbonates, and low concentration of Na + K (Table 5-1, Fig. 5-4), which is mainly derived from silicate minerals such as feldspars and muscovite. In contrast, the Meghna river and ground water have relatively high Na + K, but lower Ca compared to the Ganges and Brahmaputra rivers (Table 5-1, Fig. 5-4). These water samples contain low Mg (Table 5-1, Fig. 5-4), which is derived from dolomite.
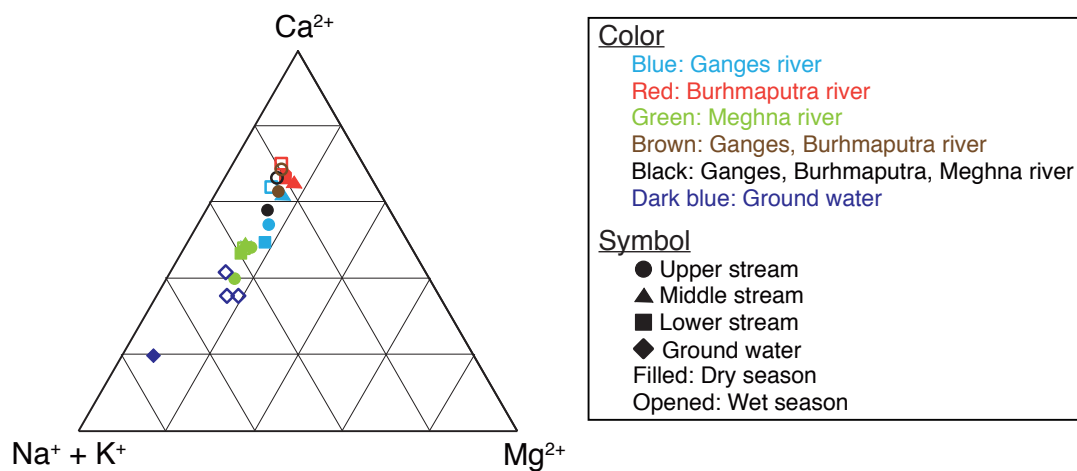
Fig. 5-4 Ternary diagram showing the major cation compositions of river and ground waters. Na, Mg, Ca, and K contents in the water samples are shown in Table 5-1. The sampling locations of water samples are shown in Fig. 5-2. The symbols and their colors in this figure conrrespnd with those in Fig. 5-3.

In the dry season, the Sr contents of river water samples in the Ganges and Brahmaputra rivers were higher than the global mean value of 78 ppb (Palmer and Edmond 1989), while those in the Meghna river has lower contents (Table 5-1). The $^{87}Sr/^{86}Sr$ values in the Ganges, Brahmaputra, and Meghna rivers have heavier than the global average value of 0.7119 (Palmer and Edmond 1989) (Table 5-1). The Sr of river water show high and heavy values in the Ganges, Brahmaputra, and Meghna rivers in this order (Table 5-1).

The Li contents and its isotopic compositions of the river water samples in Ganges and Brahmaputra rivers in the dry season were higher than the global mean value of 1.8 ppb (Gaillardet et al. 2003) and heavier than the flow-weighted mean value of +23 ‰ (Huh et al. 1998; Misra and Froelich 2012), while those in Meghna river were lower and heavier than the global averages (Table 5-1, Fig. 5-5).

In the wet seasons, Li and Sr contents and Li isotopic compositions of all river water samples are lower and lighter than those in the dry seasons (Table 5-1, Fig. 5-5).

However, the $^{87}Sr/^{86}Sr$ in the Meghna river shows a value almost similar to that in the dry season, while those in the Ganges and Brahmaputra rivers show lighter values (Table 5-1). The ground waters in Bangladesh show high Li contents with slightly low δ^7Li values (Table 5-1, Fig. 5-5).
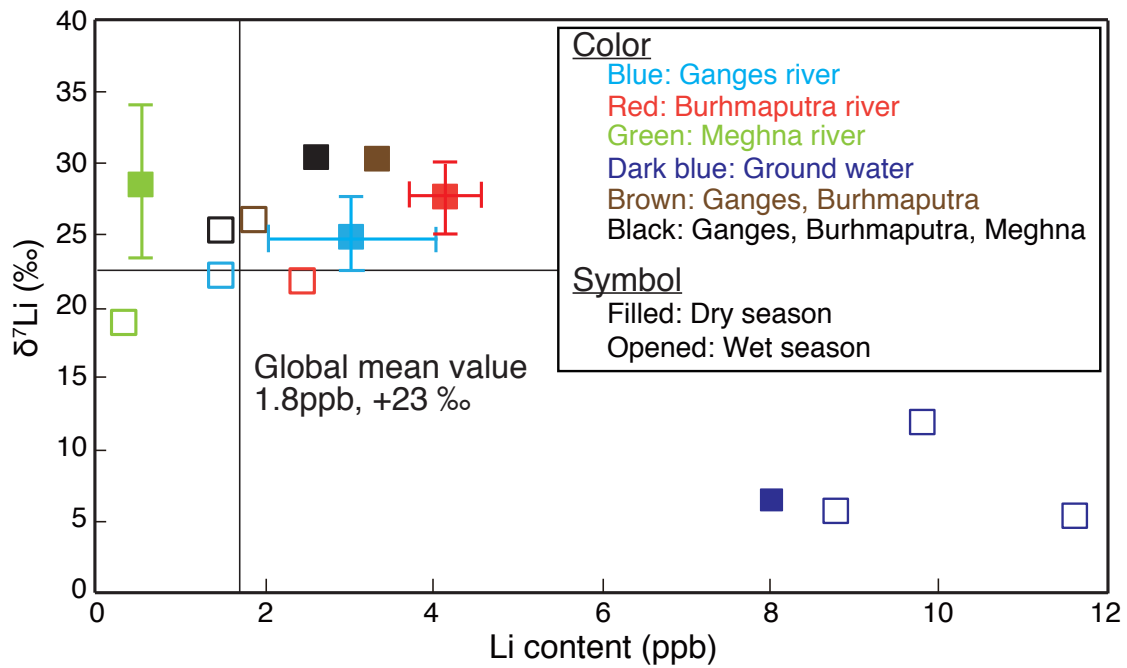

Fig. 5-5 Scatter plots of Li contents against δ^7Li of river and ground waters. The error bars mean the range of values from each sampling point in the river. The Li contents and their isotopic compositions are shown in Table 5-1.

Table 5-1 Isotopic and chemical compositions of river and groud water samples collected from Ganges, Brahmaptra, and Meghna river systems in Bangladesh. Li and Sr isotopic compositions were determined by MC-ICP-MS and TIMS, respectively. Li, Sr, and As contents were determined by ICP-MS. Mg and Si contents were determined by ICP-AES. Na, K, Ca and Cl contnets were determined by IC. pH and Total Alkalinity were reported by Manaka et al. (in preparation).

Sample ID	Sampling season	Sample description	pH	Total Alkalinity (μmol kg^{-1})	δ^{7}Li (‰)	^{87}Sr/^{86}Sr	Li (ppb)	Na (ppm)	Mg (ppm)	Si (ppm)	Cl (ppm)	K (ppm)	Ca (ppm)	As (ppb)	Sr (ppb)
Ganges river															
G-1	dry		8.23	3128	23.1	0.728633	4.0	16.5	11.0	4.0	10.3	4.1	38.7	2.9	177
G-2	dry		8.36	3037	27.6	0.728716	2.0	11.3	10.5	3.5	7.2	4.2	44.3	2.1	154
G-3	dry		8.52	2897	24.3	0.728691	3.0	15.7	10.4	2.5	10.3	4.0	30.4	2.3	148
	wet		8.06	1875	22.5	0.725690	1.4	6.7	5.1	4.3	3.0	3.6	27.8	1.9	99
Brahmaputra river															
B-1	dry		7.91	1675	25.4	0.719358	4.6	4.9	5.0	5.1	1.2	2.3	25.7	1.0	95
B-2	dry		8.13	1709	28.0	0.720028	4.1	4.8	6.3	5.3	1.2	2.3	25.8	0.9	95
B-3	dry		7.88	1717	29.8	0.720696	3.7	4.9	5.0	5.2	1.3	2.4	25.3	1.3	94
	wet		8.01	1088	22.2	0.718672	2.4	2.7	3.0	4.5	0.7	2.4	19.1	1.1	67
Meghna river and its upper tributaries															
S-1	dry	Surma River	7.67	928	34.2	0.715658	0.6	7.4	3.3	7.4	2.9	2.2	8.7	1.8	54
K-1	dry	Kusiyara River	7.41	826	28.7	0.715529	0.4	5.3	2.8	3.4	2.1	1.4	9.0	0.7	48
M-1	dry		7.48	834	28.3	0.715722	0.5	5.4	2.5	3.7	2.1	1.4	8.8	1.2	47
M-2	dry		7.44	809	23.8	0.716214	0.5	5.9	2.5	4.5	3.1	1.5	8.9	1.5	44
	wet		7.40	374	19.1	0.716367	0.3	2.4	1.2	3.6	1.0	1.0	4.3	1.3	22
Ganges and Brahmaputra river (confluence)															
GB-1	dry		8.09	1979	30.4	0.722851	3.3	7.2	5.9	4.3	3.0	2.7	27.6	1.2	105
	wet		8.12	1161	26.5	0.720782	1.8	3.2	3.0	3.9	1.1	2.5	19.1	1.4	70
Ganges, Brahmaputra and Meghna river (confluence)															
GBM-1	dry		8.03	1682	30.5	0.721214	2.6	8.5	5.5	4.9	4.3	2.5	23.1	1.6	90
	wet		7.92	1228	25.7	0.722127	1.4	3.9	3.1	3.9	1.5	2.6	19.2	1.6	68
Groud water															
GR-1	dry	Approx. 100 m deep	7.67	3360	6.4	0.714767	8.0	72.4	6.9	25.8	55.7	1.1	20.2	0.8	139
GR-2	wet	Approx. 150 m deep	7.21	4480	11.6	0.718198	9.8	58.6	20.9	26.0	85.8	4.1	46.2	2.5	348
GR-3	wet	Approx. 80 m deep	6.56	3645	5.1	0.717962	11.6	30.2	8.8	35.3	3.7	2.0	29.6	0.4	204
GR-4	wet	Approx. 260 m deep	6.99	3758	5.3	0.716154	8.8	29.0	12.8	38.3	3.7	2.5	24.3	0.7	197

5.5. Discussion

5.5.1. Estimate for dominant controlling factors of dissolved Li and Sr contents and $^{87}Sr/^{86}Sr$ in river water

The Ca/Mg ratios against Mg in the samples are plotted in Fig. 5-5. The Ca/Mg ratios in rivers would depend on Ca and Mg supplied from various sources such as carbonates, silicates, and evaporites, and on the behavior of Ca and Mg in the rivers. Fig. 5-6 shows decrease in Ca/Mg ratios with increase in Mg, which indicates a contribution of dolomite weathering to Ca and Mg. Singh et al. (2005) suggested that low Ca/Mg ratios can result from silicate/dolomite weathering and high Ca/Mg ratio from calcite weathering. The Ca/Mg ratios in river water are high in Brahmaputra, Ganges, and Meghna rivers in that order (Fig. 5-6), suggesting the significance of contribution from calcite weathering. The Li contents in river water are also high in Brahmaputra, Ganges, and Meghna rivers in this order (Table 5-1, Fig. 5-5). This similar pattern between Ca/Mg ratios and Li contents in river water demonstrates that riverine Li is derived from dissolution of fine-grained silicates released from carbonate matrix because the concentrations of Li in the carbonate-dominated catchments are high (Kisakurek et al. 2005). This hypothesis is supported by the facts that the Li concentration in marine carbonate (>1 ppm) is generally much lower than that in silicate rocks (average, 35 ppm) of the upper continental crust (Tang et al. 2004) and that a weathering rate in carbonate is at least several times higher than that in silicate rocks (Einsele 1992). Moreover, the dissolved Li contents are not correlated with Ca contents and total alkalinity and correlated weakly with Si contents (Fig. 5-7). Therefore, dissolved Li in river water is likely to reflect the rate of silicate weathering.
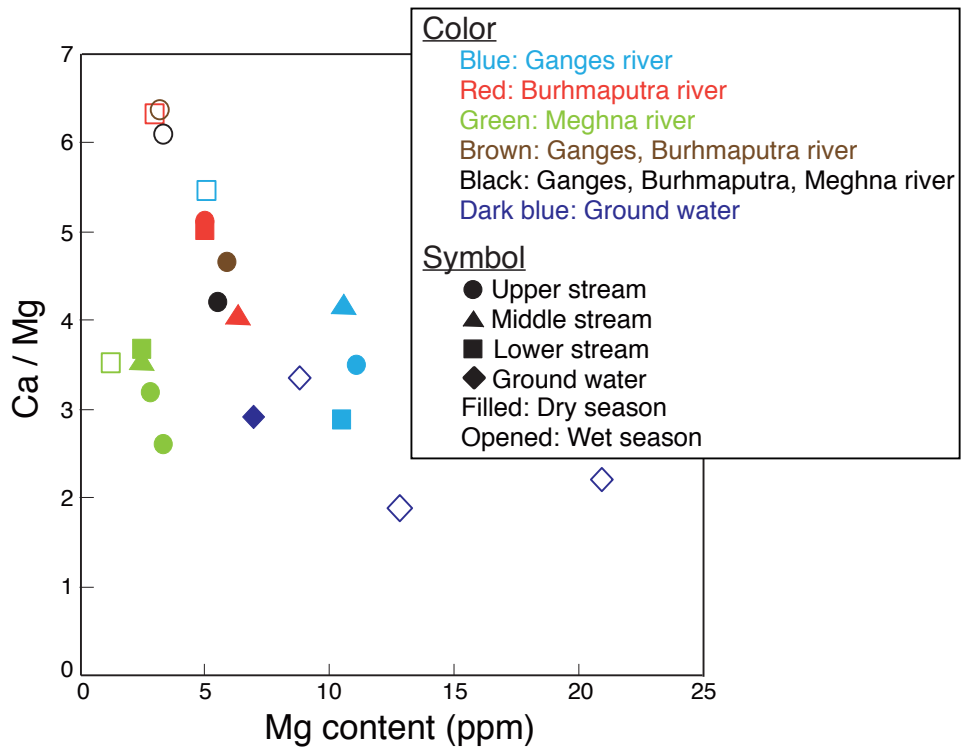
Fig. 5-6 Plots of Ca/Mg ratios against Mg contents showing the major cation composition of river and ground waters. Ca and Mg contents in the water samples are shown in Table 5-1. The sampling locations of water samples are shown in Fig. 5-3. The symbols and their colors in this figure correspond with those in Fig. 5-3.
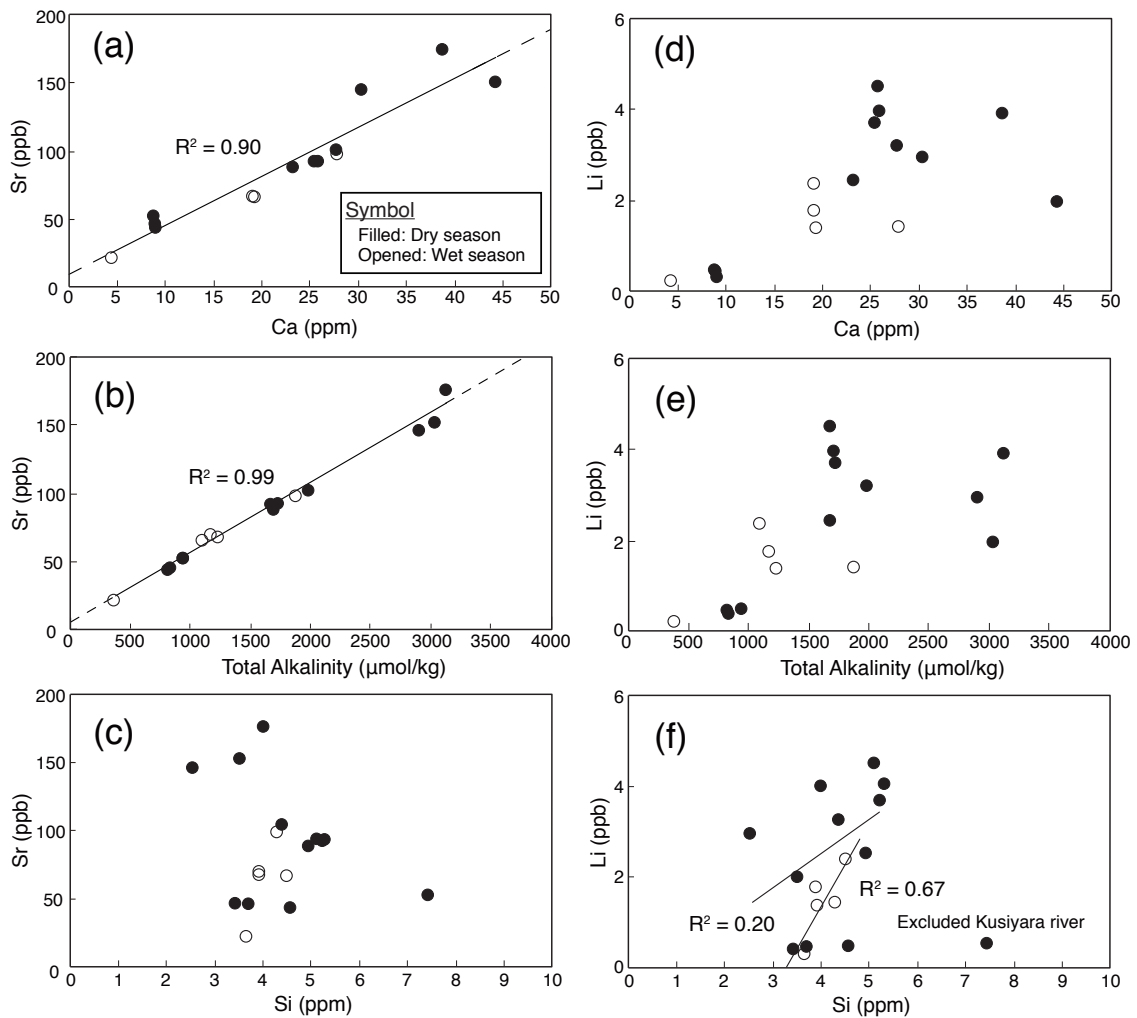
Fig. 5-7 Plots of Sr contents against (a) Ca contents, (b) Total Alkalinity, and (c) Si contents, and plots of Li contents against (d) Ca contents, (e) Total Alkalinity, and (f) Si contents of river water samples both in the dry (*Filled circle*) and wet seasons (*open circle*). Total alkalinity and elemental compositions in river water are shown in Table 5-1. The symbols and their colors in this figure correspond with those in Fig. 5-3.

In contrast, the strong correlation between Sr contents and Ca contents (total alkalinity) suggests that the dissolved Sr contents in river water can reflect carbonate weathering (Fig. 5-7). Jacobson et al. (2002) pointed that carbonate dissolution provides more than 90 % of the weathering-derived Ca and Sr in the river water. Moreover, higher $^{87}Sr/^{86}Sr$ values in the Ganges and Brahmaputra rivers (Table 5-1) than the global average value (0.7119; Palmer and Edmond 1989) reflect the significantly high $^{87}Sr/^{86}Sr$

values in bed rocks consisted of silicate rocks (from 0.77 to 1.2) with disseminated calcite (from 0.79 to 0.93) and metasedimentary carbonate (from 0.72 to 0.82) in the upper Ganges and Brahmaputra watershed within the Himalaya of the northern Pakistan (Jacobson et al. 2002). The liner relationship between Sr contents and $^{87}Sr/^{86}Sr$ values in dissolved load (Fig. 5-8) supports that Sr in river water reflects weathering of carbonate with high $^{87}Sr/^{86}Sr$. In the wet season, the dilution effect derived from floodplain area in lowland is likely to cause decreases of both $^{87}Sr/^{86}Sr$ values in the Ganges and Brahmaputra rivers and Sr contents in the Ganges, Brahmaputra, and Meghna rivers compared to the dry season (Fig. 5-8), despite an increase of Sr fluxes from these rivers estimated by the changes of the river runoff between the dry and wet seasons (river flow in dry season is about 3 to 5 times greater than that in wet season).
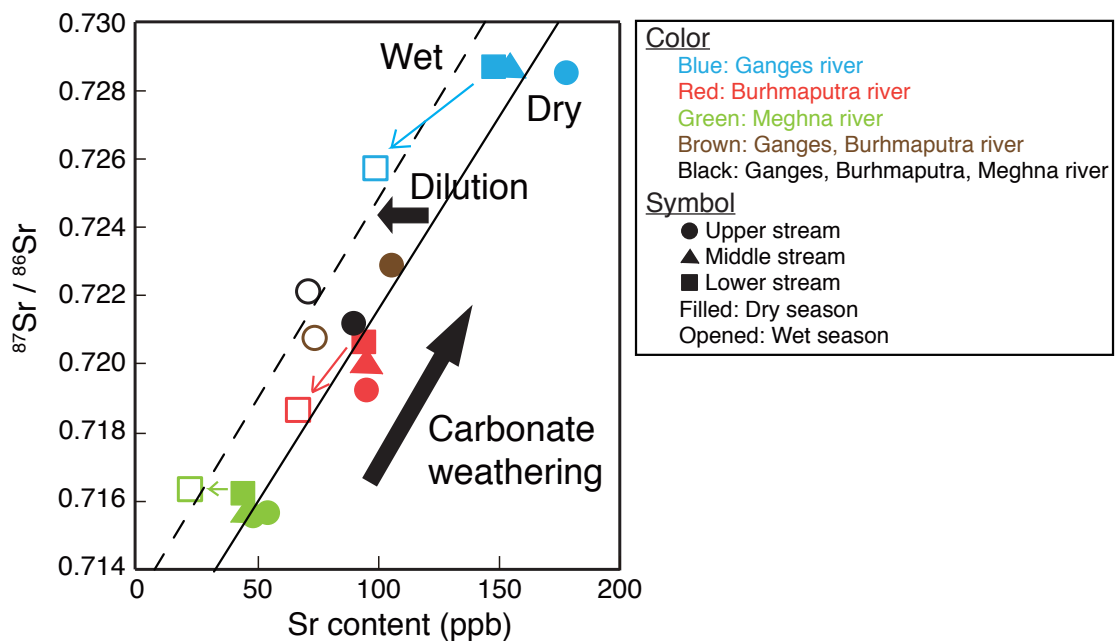
Fig. 5-8 Plots of Sr contents against $^{87}Sr/^{86}Sr$ of river waters. The Sr contents and $^{87}Sr/^{86}Sr$ values are shown in Table 5-1. The symbols and their colors in this figure correspond with those in Fig. 5-3.

As mentioned above, Li in river water is likely to be derived from silicate weathering while Sr is from carbonate weathering. However, there are large variations in Li contents and δ^7Li compared to Sr contents and ^{87}Sr/^{86}Sr of dissolved load in each river system (Fig. 5-9). These results indicate that Li in river water does not reflect basement geology at upper stream of the river, unlike ^{87}Sr/^{86}Sr.
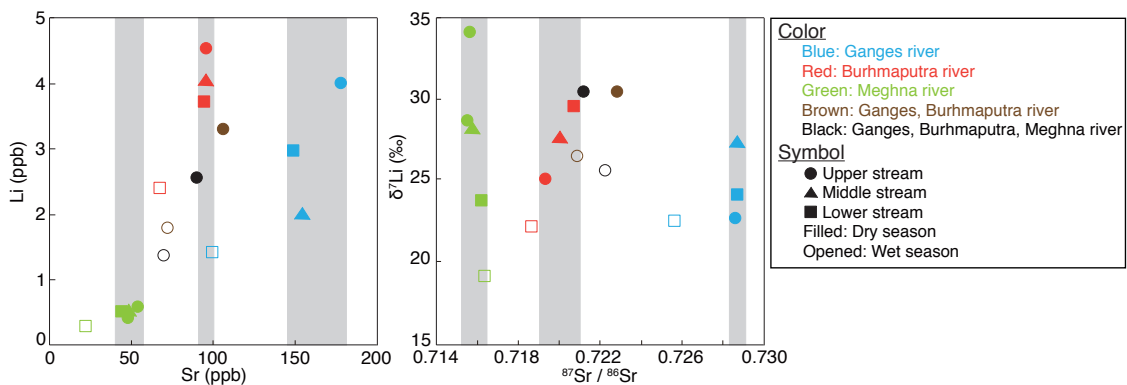

Fig. 5-9 Plots of (a) Sr contents against Li contents, and (b) ^{87}Sr/^{86}Sr against δ^7Li of river and ground waters. The vertical gray bars show the range of sample composition in each river. The elemental and isotopic compositions are shown in Table 5-1. The symbols and their colors in this figure correspond with those in Fig. 5-3.

5.5.2. Estimate for a controlloing factor of dissolved Li in river water

The plots of Li contents against its isotopic composition of river and ground water both in the dry and wet seasons are shown in Fig. 5-10. This figure shows that there are large changes in dissolved Li in river waters and liner relationship between Li contents and δ^7Li values in the Ganges, Brahmaputra, and Meghna river systems.
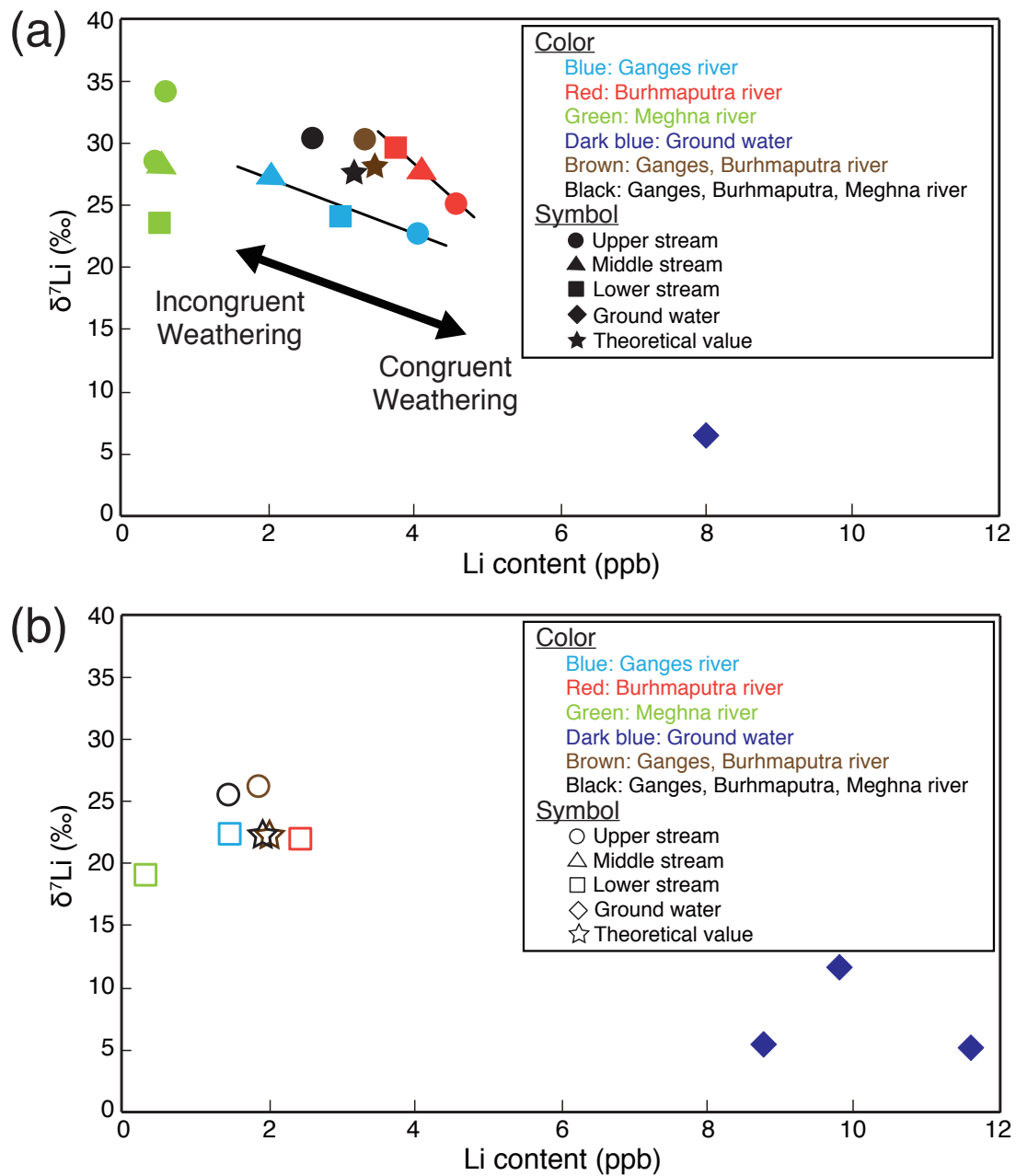
Fig. 5-10 Scatter plots of Li contents against δ⁷Li of river and ground waters in (a) dry season and (b) wet season. The theoretical values in the Ganges combined with the Brahmaputra (*blown*) and Meghna (*black*) were calculated by the use of river flow, Li content, and its isotopic composition in each river. The Li contents and its isotopic compositions are shown in Table 5-1. The symbols and their colors in this figure correspond with those in Fig. 5-3.

There are some possible factors that change dissolved Li compositions. Since dissolved Li exists only as monovalent cation and Li is not the essential elements for living matter, the biological effect and the changes in redox status in the river during flowing down are negligible. The contribution of rainwater to the dissolved Li is expected to be also negligible, although the rainwater of the Gange-Brahmaputra-Meghna drainage basin has not been analyzed for Li. This is because Li concentrations in snow samples reported in the Alps are 4.5 to 6.7 ppt (Bensimon et al. 2000), which are several orders lower than river and ground waters in this study. Moreover, it is not necessary to consider the mixing of tributaries to the main stream. Therefore, the possible factors to change dissolved Li compositions are likely to be weathering in the river and mixing of ground water.

There is two types of weathering processes: incongruent weathering and congruent weathering (e.g., Huh et al. 2001; Pistiner and Henderson, 2003; Misra and Froelich 2012). Incongruent weathering is the formation of secondary clays bearing Li during weathering. The preferential uptake of ^{6}Li into secondary alumino silicate clay minerals and oxides that formed in the river (Misra and Froelich 2012) makes riverine Li decrease and isotopically lighter. In contrast, congruent weathering is complete dissolution of secondary minerals, which makes riverine Li increase and isotopically heavier. In Ganges and Brahmaputra rivers, Li contents and δ^7Li in river water become lower and heavier from the upper to lower stream except for the lower stream of the Brahmaputra (Fig. 5-10). This result suggests that incongruent weathering occurs in the river and ^{6}Li are incorporated into secondary minerals during flowing down. This is because that Li partition coefficients between secondary minerals and fluid (D $_{mineral\,/\,fluid}$) are <1 below 50 °C (Berger et al. 1998). Therefore, δ^7Li in river water is dominated by fractionation between solution and secondary minerals during silicate weathering and reflect degree of silicate weathering (silicate weathering intensity) (e.g., Kisakurek

88

et al. 2005).

In contrast, the Meghna river shows a different tendency. The dissolved Li in the Meghna river becomes isotopically lighter from the upper to lower stream (Fig. 5-10 and 5-11). The δ^7Li values in lower stream can be achieved by mixing of ground water if the mixing ratio of ground water collected from near lower stream of the Meghna is estimated of 1.7 % (Fig. 5-11). By the use of conservative components during flowing down process such as Cl and Na contents in the river water, mixing ratio of ground water can be calculated as 1.8 % and 0.8 %, respectively. Therefore, the Meghna river much smaller than the Ganges and Brahmaputra rivers is easily influenced by ground water with slightly light δ^7Li values.
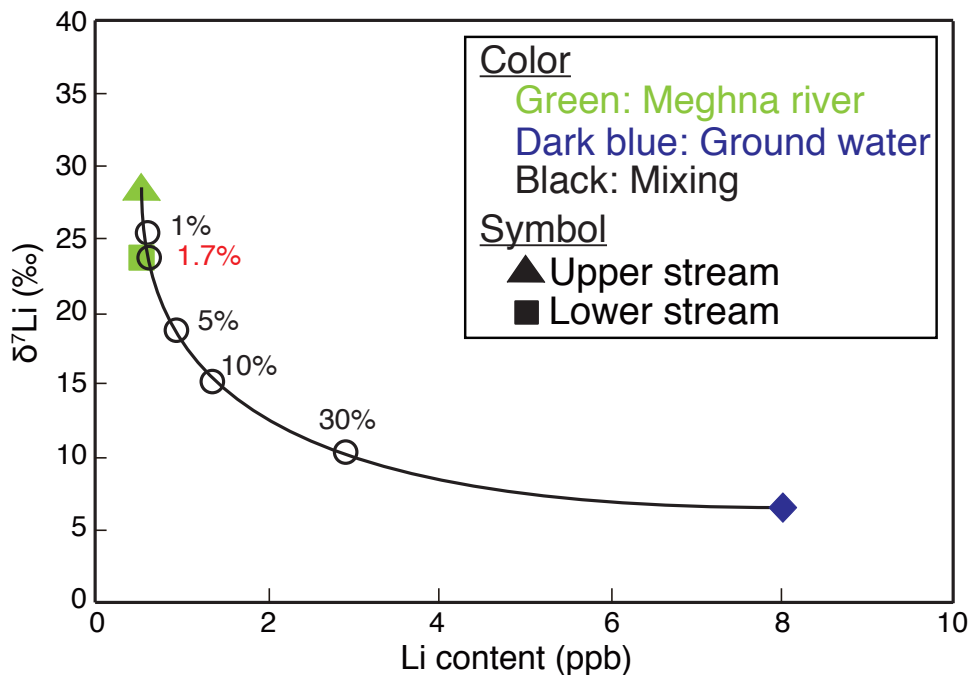
Fig. 5-11 Scatter plots of Li contents against δ^7Li of Meghna river and ground water from near lower stream of Meghna river. Black curve indicates the mixing line with the value of mixing ratio of ground water.

In the lower stream of the Ganges combined with the Brahmaputra (location GB-1 shown as blown in Fig. 5-10) and Meghna (location GBM-1 shown as black in Fig. 5-10), I calculated theoretical values by the use of river flow, Li content, and its isotopic composition in each river. The observed Li in each river is lower and isotopically-heavier than the theoretical values (Fig. 5-10), indicating that incongruent weathering continuously occurs in the river during flowing down. In the wet season, riverine Li reflects a similar trend (Fig. 5-10), although Li contents and its isotopic composition are lower and lighter than those in the dry season. Moreover, reported δ^7Li values in upper stream of the Ganges and Braphmaputra rivers is higher that those in study region in Bangladesh (Fig. 5-1). These results suggest that incongruent weathering has been continuously occurred in from head to mouth of the rivers during flowing down in both seasons.

The Li fluxes in the dissolved load can be estimated by the use of river flow both in the dry and wet seasons (Fig. 5-12). All Li flux from the rivers in the wet season is much higher than that in the dry season (Fig. 5-12). This phenomenon is probably caused by changes in drainage basin areas and flow velocity (residence time of the river). The drainage basin will expands in the wet season, which causes an increase of the erosion rate and suspended materials in river. Weathering of silicates will be more intense due to elevated temperature and higher runoff in the wet season (Kisakurek et al. 2005). However, short residence time of the river in rainy season reduce the interaction between dissolved and suspended matters, resulting in keeping low δ^7Li values in river water. Hence, dissolved Li flux will increase and isotopically-light compared to dry season (Fig. 5-12).
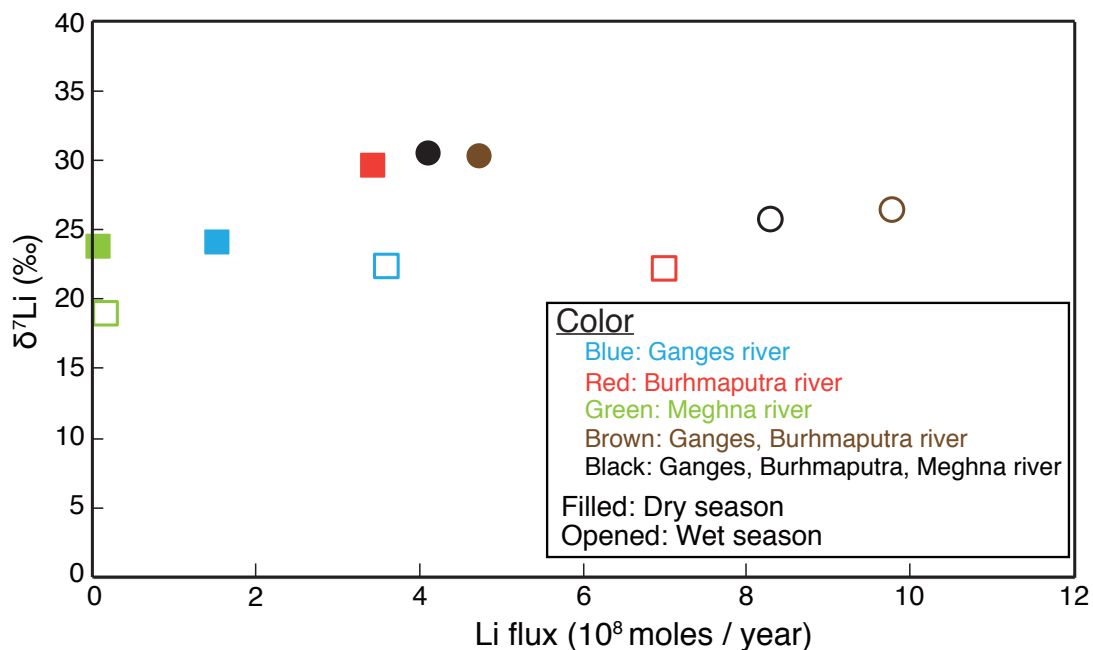
Fig. 5-12 Plots of dissolved Li flux from the rivers against δ^7Li of the river water in both seasons. The dissolved Li fluxes from the rivers were calculated by the use of annual river flow in the dry season and flood-swollen river flow in the wet season. The Li isotopic compositions are shown in Table 5-1. The symbols and their colors in this figure correspond with those in Fig. 5-3.

Misra and Froelich (2012) estimated dissolved Li flux from rivers to the ocean (10×10^9 moles/year) and an average of their isotopic compositions, +23 ‰, which greatly influences ocean lithium chemistry. In the Gange-Brahmaputra-Meghna river systems, the dissolved Li fluxes in the nearest part of exit to the ocean can be estimated of 4.1×10^8 and 8.2×10^8 moles/year in the dry and wet seasons, respectively. It is known that only about one-fifth of Li is carried in the dissolved load (Misra and Froelich 2012). Thus, the total Li fluxes in Bangladesh river system can be estimated to be 2.1×10^9 and 4.1×10^9 moles/year in the dry and wet seasons, respectively. If the wet and dry season is same time period during throughout the year, the Gange-Brahmaputra-Meghna river systems account for 6.2 % of total riverine dissolved Li flux all over the world.

This study demonstrates that large changes in Li contents and its isotopic

compositions occur by incongruent weathering in the river during flowing down. Previous studies evaluated global Li flux and its isotopic composition by compiling the river data that were sampled at various points from the upper to lower stream in rivers (Huh et al. 1998; Misra and Froelich, 2012). Therefore, Li flux and its isotopic composition from river to the oceans should be evaluated by considering behavior on Li in each river system during flowing down.

5.6. Conclusion

To reveal the dominant controlling factors on riverine Li during flowing down, I and collaborators conducted extensive field surveys to collect water samples in the dry and wet seasons from Ganges-Brahmaputra-Meghna river systems, one of the major river systems in the world. The river water from upper to lower part of the Ganges, Brahmaputra, and Meghna rivers and ground waters were analyzed for various chemical composition and Li and Sr isotopic ratios.

The riverine Li in the Ganges and Brahmaputra rivers are likely to be derived from silicate weathering while Sr is from carbonate weathering. There were large variations in Li contents and its isotopic compositions compared to Sr during flowing down. In the Ganges and Brahmaputra rivers, changes in dissolved Li to lower and isotopically heavier values from the upper to lower stream indicates that incongruent weathering occurs in the rivers. In contrast, the ground water cause the riverine Li isotopically-light in the relatively-small Meghna river. The differences in Li flux and its isotopic composition in each river between the dry and wet seasons may be explained by changes in drainage basin areas and flow velocity. These results indicate that further studies on Li isotopes in dissolved and suspended phase and its interaction must be

required to ascertain the process to change Li in the river water during flowing down. However, this study suggests that the behavior on Li during flowing down and seasonal variation in Li should be considered when the global lithium flux and its isotopic compositions from river systems to the ocean are estimated.

Summary of conclusions

In this thesis, I investigated lithium isotope ratios in the three earth surface reservoirs that take important roles in global lithium cycles in earth surface environment. First, I referred to the general introduction and objectives in this thesis as described in the "Preface" section. The analytical procedure of lithium isotopic measurements is also summarized in the following chapter. Then, I discuss three subjects about lithium isotope geochemistry.

To constrain the origin of lithium in onshore lithium ore deposits, I applied lithium isotope geochemistry to evaporites and lacustrine sediments from playas in Nevada, USA. This is the fist study that applies lithium isotopes to samples from playas. These results demonstrated that lithium isotope ratios can be a useful tracer for determining the origin of lithium and evaluating its accumulation processes in playas.

I applied lithium isotope geochemistry to submarine vent fluids from arc and back-arc hydrothermal systems in the western Pacific. These results demonstrated that lithium contents and its isotopic compositions in vent fluids are useful tracers for investigating hydrothermal circulation processes such as phase separation process and seawater-rock/seawater-sediment interactions under the seafloor not only on MOR but also in arc and back-arc sites. Moreover, this study proposed that lithium flux and its isotopic compositions from arc and back-arc sites are not negligible for the global lithium flux and its isotopic compositions from whole submarine hydrothermal systems to the ocean.

Finally, I applied lithium isotope geochemistry to river and ground waters from the Ganges-Brahmaputra-Meghna river systems, the major river systems in the world. These results demonstrated that the large changes in Li contents and its isotopic compositions in river water during flowing down are mainly controlled by incongruent

weathering and mixing of ground water. This study proposed that the behavior on lithium during flowing down process and seasonal variations should be considered for estimating accurate global lithium flux and its isotopic compositions from river systems to the ocean.

Since lithium isotope ratios in various earth surface materials could have been measured, lithium isotopic studies have played an important role for investigating various geochemical and geological processes such as chemical weathering on the earth's surface and material cycles in subduction zones. In this thesis, I showed that it could also be useful for resource geology such as the genesis of lithium ore deposits in playas. Further studies will enable to develop resource exploration methods and assess resource potential by the isotopes. Moreover, lithium isotopic ratio is also a useful tracer for investigating geological and geochemical processes in submarine hydrothermal systems and river systems. The global lithium flux and its isotopic compositions from these systems to the ocean are important for ocean lithium chemistry and global lithium cycles. Further studies will enable to estimate accurate lithium flux and its isotopic compositions by considering controlling factors and the behavior on lithium in these systems.

Acknowledgements

References

Chapter 1

Araoka, D., M. Inoue, A. Suzuki, Y. Yokoyama, R. L. Edwards, H. Cheng, H. Matsuzaki, H. Kan, N. Shikazono, and H. Kawahata (2010), Historic 1771 Meiwa tsunami confirmed by high-resolution U/Th dating of massive *Porites* coral boulders at Ishigaki Island in the Ryukyus, Japan, *Geochem. Geophys. Geosys.*, *11*, Q06014, doi:10.1029/2009GC002893

Araoka, D., Y. Yokoyama, A. Suzuki, K. Goto, K. Miyagi, K. Miyazawa, H. Matsuzaki, and H. Kawahata (2013), Tsunami recurrence revealed by *Porites* coral boulders in the southern Ryukyu Island, Japan, *Geology*, *41*, 919-922, doi:10.1130/G34415.1

Araoka D., H. Kawahata, T. Takagi, Y. Watanabe, K. Nishimura, and Y. Nishio (in press), Lithium and strontium isotopic systematics in playas in Nevada, USA: constraints on the origin of lithium, *Miner. Depos.*, doi:10.1007/s00126-013-0495-y

Burton K. W., and N. Vigier (2012), Lithium isotopes as tracers in marine and terrestrial environments, In: Baskaran M. (ed), *Advances in isotope geochemistry*, *handbook of environmental isotope geochemistry*, Springer, Berlin, 41-59

Elliott T., A. Jeffcoate, and C. Bouman (2004), The terrestrial Li isotope cycle: light-weight constrains on mantle convection, *Earth Planet. Sci. Lett., 220*, 231-245

Kisakurek B., R. H. James, and N. B. W. Harris (2005), Li and δ^7Li in Himalayan rivers: proxies for silicate weathering? *Earth Planet. Sci. Lett., 237*, 387-401

Lowenstein T. K., and F. Risacher (2009), Closed basin brine evolution and the influence of Ca–Cl inflow waters: Death Valley and Bristol Dry Lake California,

Qaidam Basin, China, and Salar de Atacama, Chile, *Aquat. Geochem., 15*, 71-94

Misra S., and P. N. Froelich (2012), Lithium isotope history of Cenozoic seawater: changes in silicate weathering and reverse weathering, *Science, 335*, 818-823

Risacher F., and B. Fritz (2009), Origin of salts and brine evolution of Bolivian and Chilean salars, *Aquat. Geochem., 15*, 123-157

Risacher F., H. Alonso, and C. Salazar (2003), The origin of brines and salts in Chilean salars: a hydrochemical review, *Earth Sci. Rev., 63*, 249-293

Tang Y. J., H. F. Zhang, and J. F. Ying (2007), Review of the lithium isotope system as a geochemical tracer, *Int. Geol. Rev., 49*, 374-388

Tomascak P. B. (2004), Developments in the understanding and application of lithium isotopes in the earth and planetary sciences, *Rev. Mineral. Geochem., 55*, 153-195

Zack T., P. B. Tomascak, R. L. Rudnick, C. Dalpé, and W. F. McDonough (2003), Extremely light Li in orogenic eclogites: the role of isotope fractionation during dehydration in subducted oceanic crust, *Earth Planet. Sci. Lett., 208*, 279-290

Chapter 2

Birck J. L. (1986), Precision K-Rb-Sr isotopic analysis: application to Rb-Sr chronology, *Chem. Geol., 56*, 73-83

Jeffcoate A. B., T. Elliott, A. Thomas, and C. Bouman (2004), Precise, small sample size determinations of lithium isotopic compositions of geological reference materials and modern seawater by MC-ICP-MS, *Geostandards Geoanal. Res., 28*, 161-172

Millot R., C. Guerrot, and N. Vigier (2004), Accurate and high-precision measurement of lithium isotopes in two reference materials by MC-ICP-MS, *Geostand. Geoanal. Res., 28*, 153-159

Nishio Y., and S. Nakai (2002), Accurate and precise lithium isotopic determinations of igneous rock samples using multi-collector inductively coupled plasma mass spectrometry, *Anal. Chim. Acta, 456*, 271-281

Nishio Y., S. Nakai, J. Yamamoto, H. Sumino, T. Matsumoto, V. S. Prikhod'ko, and S. Arai (2004), Lithium isotopic systematics of the mantle-derived ultramafic xenoliths: implications for EM1 origin, *Earth Planet. Sci. Lett., 217*, 245-261

Nishio Y., K. Okamura, M. Tanimizu, T. Ishikawa, and Y. Sano (2010), Lithium and strontium isotopic systematics of waters around Ontake volcano, Japan: implications for deep-seated fluids and earthquake swarms, *Earth Planet. Sci. Lett., 297*, 567-576

Tomascak P. B., R. W. Carlson, and S. B. Shirey (1999), Accurate and precise determination of Li isotopic compositions by multi-collector sector ICP-MS, *Chem. Geol., 158*, 145-154

Chapter 3

Araoka D., H. Kawahata, T. Takagi, Y. Watanabe, K. Nishimura, and Y. Nishio (in press), Lithium and strontium isotopic systematics in playas in Nevada, USA: constraints on the origin of lithium, *Miner. Depos.*, doi:10.1007/s00126-013-0495-y

Banner J. L. (2004), Radiogenic isotopes: systematics and applications to earth surface processes and chemical stratigraphy, *Earth Sci. Rev.* 65, 141-194

Burton K. W., and N. Vigier (2012), Lithium isotopes as tracers in marine and terrestrial environments, In: Baskaran M. (ed), *Advances in isotope geochemistry*, *handbook of environmental isotope geochemistry*, Springer, Berlin, 41-59

Chan L. H., J. M. Edmond, and G. Thompson (1993), A lithium isotopic study of hot

springs and metabasalts from mid-ocean ridge hydrothermal systems, *J. Geophy. Res., 98*, 9653-9659

Chan L. H., J. M. Edmond, G. Thompson, and K. Gillis (1992), Lithium isotopic composition of submarine basalts: implications for the lithium cycle in the oceans, *Earth Planet. Sci. Lett., 108*, 151-160

Davis A. C., M. J. Bickle, and D. A. H. Gleason (1986), Imbalance in the oceanic strontium budget, *Earth Planet. Sci. Lett., 211*, 173-187

Davis J. R., I. Friedman, and J. D. Gleason (1986), Origin of the lithium-rich brine, Clayton Valley, Nevada, *U. S. Geol. Survey Bull., 1622*, 131-138

Diles J. H., and P. B. Gans (1995), The chronology of Cenozoic volcanism and deformation in the Yerington area, western Basin and Range and Walker Lane, *Geol. Soc. Am. Bull., 107*, 474-486

Falkner K. K., M. Church, C. I. Measures, G. LeBaron, D. Thouron, C. Jeandel, M. C. Stordal, G. A. Gill, R. Mortlock, P. Froelich, and L. H. Chan (1997), Minor and trace element chemistry of Lake Baikal, its tributaries, and surrounding hot springs, *Limnol. Oceanogr., 42*, 329-345

Gaillardet J., J. Viers, B. Dupre (2003), Trace elements in river waters, In: Holland H. D., and K. K. Turekian (eds), *Treatise on geochemistry*, Pergamon, Oxford, *5*, 225-272

Garret D. E. (2004), Handbook of lithium and natural calcium chloride: their deposits, processing, uses and properties, Elsevier, Oxford, 488 p.

Huh Y., L. H. Chan, L. Zhang, and J. M. Edmond (1998), Lithium and its isotopes in major world rivers: implications for weathering and the oceanic budget, *Geochim. Cosmochim. Acta, 62*, 2039-2051

James R. H., D. E. Allen, and Jr W. E. Seyfried (2003), An experimental study of alteration of oceanic crust and terrigenous sediments at moderate temperatures (51

to 350 °C): insights as to chemical processes in near-shore ridge-flank hydrothermal systems, *Geochim. Cosmochim. Acta, 67*, 681-691

Jones B. F., and D. M. Deocampo (2003), Geochemistry of Saline Lakes, In: Holland H. D., and K. K. Turekian (eds), *Treatise on geochemistry*, Pergamon, Oxford, *5*, 393-424

Kisakurek B., R. H. James, and N. B. W. Harris (2005), Li and δ^7Li in Himalayan rivers: proxies for silicate weathering? *Earth Planet. Sci. Lett., 237*, 387-401

Kunasz I. (1974), Lithium occurrence in the brines of Clayton Valley, Esmeralda County, Nevada, *Fourth Symposium on Salt–Northern Ohio Geological Survey*, 57-66

Lowenstein T. K., and F. Risacher (2009), Closed basin brine evolution and the influence of Ca–Cl inflow waters: Death Valley and Bristol Dry Lake California, Qaidam Basin, China, and Salar de Atacama, Chile, *Aquat. Geochem., 15*, 71-94

McDermott F., and C. Hawkesworth (1990), The evolution of strontium isotopes in the upper continental crust, *Nature, 344*, 850-853

Marriott C. S., G. M. Henderson, N. S. Belshaw, and A. W. Tudhope (2004a), Temperature dependence of δ^7Li, δ^{44}Ca and Li/Ca incorporation into calcium carbonate, *Earth Planet. Sci. Lett., 222*, 615-624

Marriott C. S., G. M. Henderson, R. Crompton, M. Staubwasser, and S. Shaw (2004b), Effect of mineralogy, salinity, and temperature on Li/Ca and Li isotope composition of calcium carbonate, *Chem. Geol., 212*, 5-15

Millot R., C. Guerrot, and N. Vigier (2004), Accurate and high-precision measurement of lithium isotopes in two reference materials by MC-ICP-MS, *Geostand. Geoanal. Res., 28*, 153-159

Millot R., B. Scaillet, and B. Sanjuan (2010a), Lithium isotopes in island arc geothermal systems: Guadeloupe, Martinique (French West Indies) and

experimental approach, *Geochim. Cosmochim. Acta, 74*, 1852-1871

Millot R., N. Vigier, and J. Gaillardet (2010b), Behaviour of lithium and its isotopes during weathering in the Mackenzie Basin, Canada, *Geochim. Cosmochim. Acta, 74*, 3897-3912

Misra S., and P. N. Froelich (2012), Lithium isotope history of Cenozoic seawater: changes in silicate weathering and reverse weathering, *Science, 335*, 818-823

Munk L. A., D. Bradley, S. Hynek, and C. P. Chamberlain (2011), Origin and evolution of Li-rich brines at Clayton Valley, Nevada, USA, *Abstract V13B-2602 presented at 2011 Fall Meeting*, AGU, San Francisco, California, 5-9 Dec.

Nishio Y., K. Okamura, M. Tanimizu, T. Ishikawa, and Y. Sano (2010), Lithium and strontium isotopic systematics of waters around Ontake volcano, Japan: implications for deep-seated fluids and earthquake swarms, *Earth Planet. Sci. Lett., 297*, 567-576

Price J. G., P. J. Lechler, M. B. Lear, and T. F. Giles (2000), Possible volcanic sources of lithium in brines in Clayton Valley, Nevada, *Geology and Ore Deposits: The Great Basin and Beyond Proceedings, 1*, 241-248

Risacher F., and B. Fritz (2009), Origin of salts and brine evolution of Bolivian and Chilean salars, *Aquat. Geochem., 15*, 123-157

Risacher F., H. Alonso, and C. Salazar (2003), The origin of brines and salts in Chilean salars: a hydrochemical review, *Earth Sci. Rev., 63*, 249-293

Schmitt A. D., N. Vigier, D. Lemarchand, R. Millot, P. Stille, and F. Chabaux (2012), Processes controlling the stable isotope compositions of Li, B, Mg and Ca in plants, soils and waters: A review, *C. R. Geosci., 344*, 704-722

Stoffynegli P., and F. T. Mackenzie (1984), Mass balance of dissolved lithium in the oceans, *Geochim. Cosmochim. Acta, 48*, 859-872

Teng F. Z., W. F. McDonough, R. L. Rudnick, C. Dalpe, P. B. Tomascak, B. W.

Chappell, and S. Gao (2004), Lithium isotopic composition and concentration of the upper continental crust, *Geochim. Cosmochim. Acta 68*, 4167-4178

Tang Y. J., H. F. Zhang, and J. F. Ying (2007), Review of the lithium isotope system as a geochemical tracer, *Int. Geol. Rev., 49*, 374-388

Tomascak P. B. (2004), Developments in the understanding and application of lithium isotopes in the earth and planetary sciences, *Rev. Mineral. Geochem., 55*, 153-195

Tomascak P. B., N. G. Hemming, and S. R. Hemming (2003), The lithium isotopic composition of waters of the Mono Basin, California, *Geochim. Cosmochim. Acta, 67*, 601611

U.S.G.S. (1996), Mineral commodity summaries 1996, *U.S. Geological Survey*

U.S.G.S. (2012), Mineral commodity summaries 2012, *U.S. Geological Survey*, 198 p.

Veizer J. (1989), Strontium isotopes in seawater through time, *Annu. Rev. Earth. Planet. Sci., 17*, 141-167

Vikstrom H., S. Davidsson, and M. Hook (2013), Lithium availability and future production outlooks, *Appl. Energ., 110*, 252-266

Wunder B., A. Meixner, R. L. Romer, and W. Heinrich (2006), Temperature-dependent isotopic fractionation of lithium between clinopyroxene and high-pressure hydrous fluids, *Contrib. Mineral. Petrol., 238*, 277-290

Yamaji K., Y. Makita, H. Watanabe, A. Sonoda, H. Kanoh, T. Hirotsu, and K. Ooi (2001), Theoretical estimation of lithium isotopic reduced partition function ratio for lithium ions in aqueous solution, *J. Phys. Chem. A, 105*, 602-613

You C. F., P. R. Castillo, J. M. Gieskes, L. H. Chan, and A. J. Spivack (1996), Trace element behavior in hydrothermal experiments: implications for fluid processes at shallow depths in subduction zones, *Earth Planet. Sci. Lett., 140*, 41-52

Chapter 4

Berndt M. E., R. R. Seal II, W. C. Shanks III, and W. E. Seyfried Jr (1996), Hydrogen isotope systematics of phase separation in submarine hydrothermal systems: experimental calibration and theoretical models, *Geochim. Cosmochim. Acta, 60*, 1595-1604

Bischoff J. L., and F. W. Dickson (1975), Seawater-basalt interaction at 200ºC and 500bars: implications for origin of sea-floor heavy-metal deposits and regulation of seawater chemistry, *Earth Planet. Sci. Lett., 25*, 385-397

Bowers T. S., and H. P. Taylor Jr. (1985) An integrated chemical and stable-isotope model of the origin of mid-ocean ridge hot spring systems, *J. Geophys. Res., 90*, 583-606

Butterfield D. A., G. J. Massoth, R. E. McDuff, J. E. Lupton, and M. D. Lilley (1990), Geochemistry of hydrothermal fluids from Axial Seamount Hydrothermal Emissions Study vent field, Juan de Fuca Ridge: subseafloor boiling and subsequent fluid-rock interaction, *J. Geophys. Res., 95*, 12895-12921

Chan L. H., and J. M. Edmond (1988), Variation of lithium isotope composition in the marine environment: A preliminary report, *Geochim. Cosmochim. Acta, 52*, 1711-1717

Chan L. H., J. M. Edmond, and G. Thompson (1993), A lithium isotope study of hot springs and metabasalts from mid-ocean ridge hydrothermal systems, *J. Geophys. Res., 98*, 9653-9659

Chan L. H., J. M. Gieskes, C. F. You, and J. M. Edmond (1994), Lithium isotope geochemistry of sediments and hydrothermal fluids of the Guaymas Basin, Gulf of California, *Geochim. Cosmochim. Acta, 58*, 4443-4454

Chan L. H., J. C. Alt, and D. A. H. Teagle (2002), Lithium and lithium isotope profiles through the upper oceanic crust: a study of seawater–basalt exchange at ODP

Sites 504B and 896A, *Earth Planet. Sci. Lett., 201*, 187-201

Chan L. H., W. P. Leeman, and T. Plank (2006), Lithium isotopic composition of marine sediment, *Geochem. Geophys. Geosys., 7*, Q06005.

Chiba H. (1997), Geochemistry of active hydrothermal systems in Okinawa Trough back arc basin, *JAMSTEC J. Deep-Sea Res. Spec. Vol.: Deep Sea Research in subduction zones, spreading centers and backarc basins*, 63-68

Edmond J. M., C. Measures, R. E. Macduff, L. H. Chan, R. Collier, B. Grant, L. I. Gordon, and J. B. Corliss (1979), Ridge crest hydrothermal activity and the balances of the major and minor elements in the ocean: The Galapagos data, *Earth Planet. Sci. Lett., 46*, 1-18

Edmond J. M., K. L. Von Damm, R. E. McDuff, and C. I. Measures (1982), The chemistry of the hot springs on the East Pacific Rise and their effluent dispersal, *Nature, 297*, 187-191

Elderfield H., and A. Schultz (1996), Mid-ocean ridge hydrothermal fluxes and the chemical composition of the ocean, *Annu. Rev. Earth Planet. Sci., 24*, 191-224.

Ensong H. (2013), Boron content and isotope of vent fluids from seafloor hydrothermal systems, Master Thesis, The University of Tokyo, 49 p.

Foustoukos D. I., R. H. James, M. E. Berndt, and W. E. Seyfried Jr. (2004), Lithium isotopic systematics of hydrothermal vent fluids at the Main Endeavour Field, Northern Juan de Fuca Ridge, *Chem. Geol., 212*, 17-26

Fuji Y., and K. Nakamura (1979), Distribution of volcanic mountain, *Chikyukagaku 7*, Iwanami-kouza, Kazan.

Gamo T. (1995), Wide variation of chemical characteristics of submarine hydrothermal fluids due to secondary modification processes after high temperature water-rock interaction: a review, In: Sakai H., and Y. Nozaki (eds), *Biogeochemical Processes and Ocean Flux in the Western Pacific*, 425-451

Gamo T., K. Okamura, J. L. Charlou, T. Urabe, J. M. Auzende, J. Ishibashi, and K. Shitashima (1996), Chemical exploration of hydrothermal activity in the Manus Basin, Papua New Guinea (ManusFlux Cruise), *JAMSTEC J. Deep Sea Res., 12*, 335-345

Gamo T., U. Tsunogai, J. Ishibashi, H. Masuda, and H. Chiba (1997), Chemical characteristics of hydrothermal fluids from the Mariana Trough, *JAMSTEC J. Deep-Sea Res. Spec. Vol.: Deep Sea Research in subduction zones, spreading centers and backarc basins*, 69-74

Gale A., C. A. Dalton, C. H. Langmuir, Y. Su, J. G. Schilling (2013), The mean composition of ocean ridge basalts, *Geochem. Geophys. Geosyst., 14*, 489-518

German C. E., and K. L. Von Damm (2003), Hydrothermal processes, In: Holland H. D., and K. K. Turekian (eds), *Treatise on geochemistry*, Pergamon, Oxford, *6*, 181-222

Huh Y., L. H. Chan, L. Zhang, and J. M. Edmond (2001), Lithium isotopes as a probe of weathering processes: Orinoco River, *Earth Planet. Sci. Lett., 194*, 189-199

Ishibashi J., D. Grimaud, Y. Nojiri, J. M. Auzende, and T. Urabe (1994), Fluctuation of chemical compositions of the phase-separated hydrothermal fluid from the North Fiji Basin Ridge, *Mar. Geol., 116*, 215-226

Ishikawa T., and E. Nakamura (1993), Boron isotope systematics of marine sediments, *Earth and Planet. Sci. Lett., 117*, 567-580

James R. H., M. D. Rudnicki, and M. R. Palmer (1999), The alkali element and boron geochemistry of the Escanaba Trough sediment-hosted hydrothermal system, *Earth Planet. Sci. Lett. 171*, 157-169

James R. H., D. E. Allen, and Jr W. E. Seyfried (2003), An experimental study of alteration of oceanic crust and terrigenous sediments at moderate temperatures (51 to 350 °C): insights as to chemical processes in near-shore ridge-flank

hydrothermal systems, *Geochim. Cosmochim. Acta, 67*, 681-691

Magenheim A. J., A. J. Spivack, J. C. Alt, G. Bayhurst, L. H. Chan, E. Zuleger, and J. M. Gieskes (1995), Borehole fluid chemistry in hole 504B, leg 137: formation water or in-situ reaction? *Proceedings of the Ocean Drilling Program, Scientific Results*, *137/140*, 141-152

Millot R., C. Guerrot, and N. Vigier (2004), Accurate and high-precision measurement of lithium isotopes in two reference materials by MC-ICP-MS, *Geostand. Geoanal. Res., 28*, 153-159

Millot R., B. Scaillet, and B. Sanjuan (2010), Lithium isotopes in island arc geothermal systems: Guadeloupe, Martinique (French West Indies) and experimental approach, *Geochim. Cosmochim. Acta, 74*, 1852-1871

Misra S., and P. N. Froelich (2012), Lithium isotope history of Cenozoic seawater: changes in silicate weathering and reverse weathering, *Science, 335*, 818-823

Nishio Y., K. Okamura, M. Tanimizu, T. Ishikawa, and Y. Sano (2010), Lithium and strontium isotopic systematics of waters around Ontake volcano, Japan: implications for deep-seated fluids and earthquake swarms, *Earth Planet. Sci. Lett., 297*, 567-576

Palmer M. R. (1991), Boron isotope systematics of hydrothermal fluids and tourmalines: a synthesis, *Chem. Geol., 94*, 111-121

Palmer M. R., J. M. and Edmond (1989), The strontium isotope budget of the modern ocean, *Earth and Planet. Sci. Lett., 92*, 11-26

Pistiner J. S., and G. M. Henderson (2003), Lithium-isotope fractionation during continental weathering processes, *Earth Planet. Sci. Lett., 214*, 327-339

Reeves E. P., J. S. Seewald, P. Saccocia, W. Bach, P. R. Craddock, W. C. Shanks, S. P. Sylva, E. Walsh, T. Pichler, and M. Rosner (2011), Geochemistry of hydrothermal fluids from the PACMANUS, Northeast Pual and Vienna Woods hydrothermal

fields, Manus Basin, Papua New Guinea, *Geochim. Cosmochim. Acta, 75*, 1088-1123

Scholz F., C. Hensen, G. J. D. Lange, M. Haeckel, V. Liebetrau, A. Meixner, A. Reitz, and R. L. Romer (2010), Lithium isotope geochemistry of marine pore waters – Insights from cold seep fluids, *Geochim. Cosmochim. Acta, 74*, 3459-3475

Seyfried W. E., and J. L. Bischoff (1979), Low temperature basalt alteration by seawater: and experimental study at 70ºC and 150ºC, *Geochim. Cosmochim. Acta, 43*, 1937-1947

Shikazono N. (1993), Influence of hydrothermal flux on arsenic geochemical balance of seawater, *Chikyukagaku, 27*, 135-139

Shikazono N. (2003), Geochemical and tectonic evolution of arc-backarc hydrothermal systems: implication for the origin of kuroko and epithermal vein-type mineralizations and the global geochemical cycle, *Developments in Geochemistry*, Elsevier, 478 p.

Spivack A. J., and J. M. Edmond (1987), Boron isotope exchange between seawater and the oceanic crust, *Geochim. Cosmochim. Acta, 51*, 1033-1043

Teng F. Z., W. F. McDonough, R. L. Rudnick, C. Dalpe, P. B. Tomascak, B. W. Chappell, and S. Gao (2004), Lithium isotopic composition and concentration of the upper continental crust, *Geochim. Cosmochim. Acta 68*, 4167-4178

Tomascak P. B., C. H. Langmuir, P. J. Roux, and S. B. Shirey (2008), Lithium isotopes in global mid-ocean ridge basalts, *Geochim. Cosmochim. Acta, 72*, 1626-1637

Turekian K. K. (1968), Oceans, Prentice-Hall, 120 p.

Von Damm K. L. (1990), Seafloor hydrothermal activity: Black smoker chemistry and chimneys, *Annu. Rev. Earth Planet. Sci., 18*, 173-204

Von Damm K. L., J. M. Edmond, B. Grant, C. I. Measures, B. Walden, and R. F. Weiss (1985), Chemistry of submarine hydrothermal solutions at 21°N, East Pacific Rise,

Geochim. Cosmochim. Acta, 49, 2197-2220

Wunder B., A. Meixner, R. L. Romer, R. Wirth, and W. Heinrich (2005), The geochemical cycle of boron: constraints from boron isotope partitioning experiments between mica and fluid, *Lithos, 84*, 206-216

Wunder B., A. Meixner, R. L. Romer, and W. Heinrich (2006), Temperature-dependent isotopic fractionation of lithium between clinopyroxene and high-pressure hydrous fluids, *Contrib. Mineral. Petrol., 238*, 277-290

You C. F., P. R. Castillo, J. M. Gieskes, L. H. Chan, and A. J. Spivack (1996), Trace element behavior in hydrothermal experiments: implications for fluid processes at shallow depths in subduction zones, *Earth Planet. Sci. Lett., 140*, 41-52

Chapter 5

Berger G., J. Schott, and C. Guy (1998), Behaviour of Li, Rb and Cs during basalt glass and olivine dissolution and chlorite, smectite and zeolite precipitation from seawater: experimental investigations and modelization between 50 ºC and 300 ºC, *Chem. Geol. 71*, 297-312

Bensimon M., J. Bourquin, and A. Parriaux (2000), Determination of ultra-trace elements in snow samples by inductively coupled plasma source sector field mass spectrometry using ultrasonic nebulization, *J. Anal. At. Spectrom., 15*, 731-734

Einsele G. (1992), Sedimentary basins: evolution, facies and sediment budget, Splinger, Berlin, 628 p.

Gaillardet J., J. Viers, B. Dupre (2003), Trace elements in river waters, In: Holland H. D., and K. K. Turekian (eds), *Treatise on geochemistry*, Pergamon, Oxford, *5*, 225-272

Hathorne E. C., and R. H. James (2006), Temporal record of lithium in seawater: a

tracer for silicate weathering? *Earth Planet. Sci. Lett., 246*, 393-406

Huh Y., L. H. Chan, L. Zhang, and J. M. Edmond (1998), Lithium and its isotopes in major world rivers: implications for weathering and the oceanic budget, *Geochim. Cosmochim. Acta, 62*, 2039-2051

Huh Y., L. H. Chan, L. Zhang, and J. M. Edmond (2001), Lithium isotopes as a probe of weathering processes: Orinoco River, *Earth Planet. Sci. Lett., 194*, 189-199

Huh Y., L. H. Chan, L. Zhang, and O. A. Chadwick (2004), Behavior of lithium and its isotopes during weathering of Hawaiian basalt, *Geochem. Geophys. Geosys., 5,* Q09002

Jacobson A. D., and J. D. Blum (2000), The Sr/Ca and $^{87}Sr/^{86}Sr$ geochemistry of disseminated calcite in Himalayan silicate rocks from Nanga Parbat: influence on river-water chemistry, *Geology, 28*, 463-466

Jacobson A. D., J. D. Blum, C. P. Chamberlain, M. A. Poage, and V. F. Sloan (2002), Ca/Sr and Sr isotope systematics of a Himalayan glacial chronosequence: carbonate versus silicate weathering rates as a function of landscape surface age, *Geochim. Cosmochim. Acta, 66,* 13-27

Kisakurek B., R. H. James, and N. B. W. Harris (2005), Li and δ^7Li in Himalayan rivers: proxies for silicate weathering? *Earth Planet. Sci. Lett., 237*, 387-401

Liu C. Q., Z. Q. Zhao, Q. Wang, and B. Gao (2012), Isotope compositions of dissolved lithium in the rivers Jinshajiang, Lancangjiang, and Nujiang; implication for weathering in Qinghai-Tibet Plateau, *Appl. Geochem., 26*, S357-S359

Liu X. M., and R. L. Rudnick (2011), Constraints on continental crustal mass loss via chemical weathering using lithium and its isotopes, *Proc. Natl. Acad. Sci. USA, 108*, 20873-20880

Liu X. M., R. L. Rudnick, W. F. McDonough, and M. L. Cummings (2013), Influence of chemical weathering on the composition of the continental crust: Insights from

Li and Nd isotopes in bauxite profiles developed on Columbia River Basalts, *Geochim. Cosmochim. Acta, 115,* 73-91

Millot R., N. Vigier, and J. Gaillardet (2010), Behaviour of lithium and its isotopes during weathering in the Mackenzie Basin, Canada, *Geochim. Cosmochim. Acta, 74*, 3897-3912

Mirza M. M. Q. (2002) Global warming and changes in the probability of occurrence of floods in Bangladesh and implications, *Global Environ. Change, 12*, 127-138

Misra S., and P. N. Froelich (2012), Lithium isotope history of Cenozoic seawater: changes in silicate weathering and reverse weathering, *Science, 335*, 818-823

Nishio Y., K. Okamura, M. Tanimizu, T. Ishikawa, and Y. Sano (2010), Lithium and strontium isotopic systematics of waters around Ontake volcano, Japan: implications for deep-seated fluids and earthquake swarms, *Earth Planet. Sci. Lett., 297*, 567-576

Palmer M. R., J. M. and Edmond (1989), The strontium isotope budget of the modern ocean, *Earth and Planet. Sci. Lett., 92*, 11-26

Parua P. K. (2010), The Ganga: water use in the Indian subcontinent, *Water Science and Technology Library*, Springer, 391 p.

Pistiner J. S., and G. M. Henderson (2003), Lithium-isotope fractionation during continental weathering processes, *Earth Planet. Sci. Lett., 214*, 327-339

Pogge von Strandmann P. A. E., K. W. Burton, R. H. James, P. van Calsteren, S. R. Gislason (2010), Assessing the role of climate on uranium and lithium isotope behaviour in rivers draining a basaltic terrain, *Chem. Geol., 270*, 227-239

Raymo M. E., and W. F. Ruddiman (1992), Tectonic forcing of late Cenozoic climate, *Nature, 359*, 117-122

Singh S. K., M. M. Sarin, and C. F. Lanord (2005), Chemical erosion in the eastern Himalaya: major ion composition of the Brahmaputra and $\delta^{13}C$ of dissolved

inorganic carbon, *Geochim. Cosmochim. Acta, 69*, 3573-3588

Teng F. Z., W. F. McDonough, R. L. Rudnick, C. Dalpe, P. B. Tomascak, B. W. Chappell, and S. Gao (2004), Lithium isotopic composition and concentration of the upper continental crust, *Geochim. Cosmochim. Acta 68*, 4167-4178

Teng F. Z., W. Y. Li, R. L. Rudnick, and L. R. Gardner (2010), Contrasting lithium and magnesium isotope fractionation during continental weathering, *Earth Planet. Sci. Lett., 300,* 63-71

Tipper E. T., D. Calmels, J. Gaillardet, P. Louvat, F. Capmas, B. Dubacq (2012), Positive correlation between Li and Mg isotope ratios in the river waters of the Mackenzie Basin challenges the interpretation of apparent isotopic fractionation during weathering, *Earth Planet. Sci. Lett., 333-334*, 35-45

Vigier N., S. R. Gislason, K. W. Burton, R. Millot, F. Mokadem (2009), The relationship between riverine lithium isotope composition and silicate weathering rates in Iceland, *Earth Planet. Sci. Lett., 287*, 434-441

Webster P. J., Jian J., Hopson T. M., Hoyos C. D., Agudelo P. A., Chang H. R., Curry J. A., Grossman R. L., Palmer T. N., and Subbiah A. R. (2010), Extended-range probabilistic forecasts of Ganges and Brahmaputra floods in Bangladesh, *Bulletin of the American Meteorological Society, 91*, 1493-1514

Wimpenny J., R. H. James, K. W. Burton, A. Gannoun, F. Mokadem, and S. R. Gislason (2010), Glacial effects on weathering processes: new insights from the elemental and lithium isotopic composition of West Greenland rivers, *Earth Planet. Sci. Lett., 290*, 427-437

Yoon J. (2010), Lithium as a silicate weathering proxy: problems and perspectives, *Aquat. Geochem., 16*, 189-206